Exploring the behaviour of coupled feed-forward loops composed of RNA riboregulators and σ-factors in vitro and in silico

Master thesis of	:	B.L. Nathalia (0948510)
Department	:	Biomedical Engineering – Computational Biology
Course code	:	8ZM104
Organisation	:	Eindhoven University of Technology
Graduation committee	:	T.F.A. de Greef – Biomedical Engineering (Computational Biology) P.A.J. Hilbers – Biomedical Engineering (Computational Biology) E. Steur – Mechanical Engineering (Dynamics and Control)
Period	:	05/19 – 08/20

TU/e EINDHOVEN UNIVERSITY OF TECHNOLOGY

ABSTRACT

Living cells contain vast networks of biochemical interactions regulating several processes, including transcription. Within these transcription regulation networks, recurring patterns of interactions between genes have been observed and marked as network motifs. A network motif is a specific pattern of interactions that occurs significantly more within a network than any other arbitrary sequence of interactions. An example of such a network motif is the feed-forward loop, present in genetic circuits of bacteria, yeast, and mammals. The feed-forward loop consists of three genes which together form a motif capable of delaying output gene expression and filtering of non-persistent input signals. It has been shown that within large networks, feed-forward loops might also be coupled at one or two nodes, forming a larger network motif with shared genes. Exploring the behaviour of such network motifs gives insight in how processes in cells are regulated and how incoming signals can possibly be delayed. Here we show how one could implement the coupled feed-forward loop genetic circuit using in vitro transcription-translation (IVTT) and characterise the behaviour of this circuit in vitro and in silico. The input and control elements of the genetic circuit are composed of RNA riboregulators and σ-factors, and functioning of the circuit is measured from eGFP and CFP fluorescence. We demonstrate that the coupled feed-forward loop can be implemented in vitro, and observe that removing the network inputs result in a decrease of fluorophore production of up to 5-fold. Moreover, we show the importance of the control elements, and reveal that shared nodes of the network motif can take over each others function under certain conditions. Furthermore, simulations with an ODE model of the coupled feed-forward loop show which control elements influence time delay and kinetic filtering, and they demonstrate the importance of input order. This work gives an insight in the functioning of a coupled feed-forward loop and demonstrates how to influence its properties.

CONTENTS

1 INTRODUCTION

Synthetic biology is a still emerging discipline in science which combines knowledge from biology and engineering, showing great successes throughout the past decades in different fields of application [1]. Researchers have previously described the field of synthetic biology as the "DESIGNING AND CONSTRUCTING OF BIOLOGICAL MODULES, BIOLOGICAL SYSTEMS, AND BIOLOGICAL MACHINES OR, RE-DESIGN OF EXISTING BIOLOGICAL SYSTEMS FOR USEFUL PURPOSES" [2]. Re-designing of biological systems has for example been done in the construction of a minimal bacterial genome. By knocking out certain genes and investigating the consequences of this, it was discovered that this minimal bacterial genome only exists of 473 genes, involved in crucial processes like transcription and translation [3]. By conducting this research, one gains a better understanding of how a cell functions and which processes are crucial to retain a cell's function. Moreover, by studying and rebuilding of biological modules, one can gain insights in the functioning of these modules in living cells. With this knowledge, one could even redesign such a module and use it for new biotechnological inventions like synthetic genetic networks or complete synthetic cells.

TRANSCRIPTION REGULATION NETWORKS Another way to look at a living cell is by investigating the vast biochemical networks of transcription interactions [4]. This analysis has for example been peformed for the genomic network of *E. coli*, in which the connections within transcriptional regulation networks have been uncovered [5]. It has been discovered that the functioning of a cell is depended on such transcriptional interactions in order to successfully transmit important signals within the cell, ordering movement, growth or cell differentiation [6]. Furthermore, these transcription interactions are also used to transmit signals coming from the outside environment of the cell, through using simple computations, to the inside of the cell [7].

NETWORK MOTIFS During efforts of uncovering networks of transcription interactions, interesting recurring patterns have been discovered within the interaction cascades. At first, such patterns might be spotted randomly throughout a series of interactions. However, when investigated more thoroughly, it can be shown that such patterns occur significantly more often than any other arbitrary sequence of interactions [8]. Using graph theory and computer algorithms, it

is possible to detect such network motifs in larger networks [9] [10] [11].

Network motifs can be found in networks of different origins. For example, network motifs have been detected in World Wide Web networks, food webs and neuron networks [8]. Furthermore, network motifs exist in the transcriptional networks of living organisms. For example, these network motifs have previously been identified in bacteria [8] [12] [13], yeast [8] [14] and different species of animals [15] [16] and plants [17] [18].

One of the simplest network motifs that can be found in many different networks are positive and negative autoregulation. The transcription factor in these motifs, respectively, activates or represses the transcription of its own gene [19] (Figure 1a). An example of a larger network motif is a single-input module (SIM) (Figure 1b). This motif consists of one single regulator X, which regulates, positively or negatively, a set of downstream genes. The regulator X might also regulate its own production. This SIM pattern is used to stimulate or repress a group of genes with a common function. Depending on the activation thresholds of the downstream genes, an increasing concentration of regulator X can induce a specific order of activation in the downstream genes [19]. The SIM network motif has been identified in for example the activation and assembly of flagella in E. Coli [20]. Furthermore, the SIM can be recognised in the arginine biosynthesis pathway, where *ArgR* represses downstream genes encoding for enzymes involved in the synthesis. Absence of arginine leads to subsequent activation of the downstream genes, showing the temporal order typical for SIMs [19]. Other examples of network motifs are the bi-fan and bi-parallel circuits, and the dense overlapping regulon [12] [8] [19].

Other network motifs are also known as functional units and exist within larger (transcription regulation) networks. An example of such a functional unit is the bistable switch. The bistable switch consists of two nodes (X and Y), possibly transcription factors, and two edges. Node X represses node Y and vice versa (Figure 1c). This topology results in a network motif showing toggle switch behaviour, which can be used in cells as a memory unit [21]. Bistable switches have been recognised in human MAPK signaling pathways influencing cell fate decisions and cellular differentiation [22]. Another network motif that includes repressors is the repressilator, consisting of three nodes (X, Y, and Z) and three edges. Node X represses node Y, Y represses Z and Z in its turn represses node X, forming a circuit of interactions (Figure 1d) [23] [24]. This network motif has been designed and constructed synthetically in *E. coli* using three different genes (LacI, tetR, and λ cI) cloned from *E. coli* and λ *phage* [23]. Research from Elowitz and

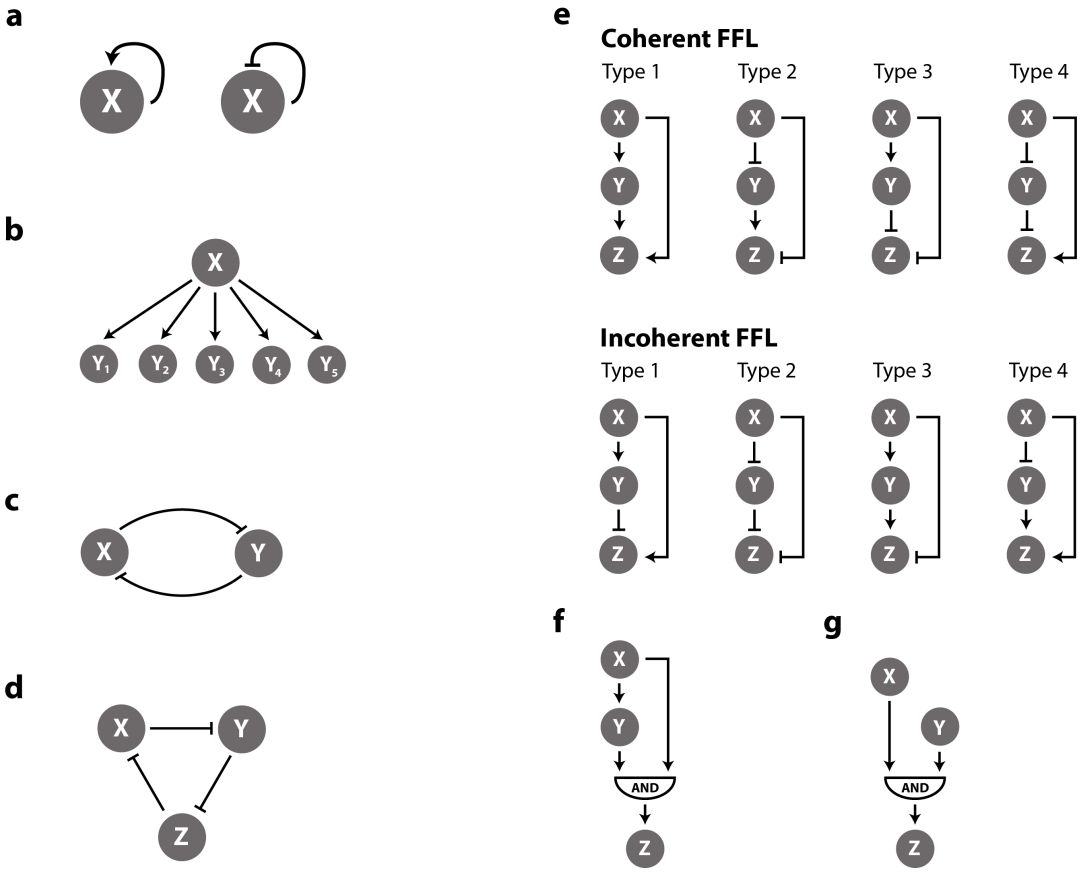

Figure 1: Multiple types of common network motifs:
(a) Autoregulation can be positive or negative. (b) Single-input module (SIM). (c) Bistable switch. (d) Repressilator.
(e) Eight different types of feed-forward loops, classified as either coherent or incoherent.
(f) Coherent feed-forward loop type 1, where production of species Z only starts when both transcription factors X and Y are present.
(g) Control circuit for the coherent feed-forward loop, where the interaction between node X and Y is absent.

Leibler showed that this particular genetic network shows oscillatory behaviour with periods of a few hours and can be used as a synthetical biological clock. Transcription networks involved in for example cell-fate decisions are often comprised of multiple, intertwined simpler network motifs, leading to specific behaviour [19]. Rebuilding and redesigning of such concepts found in nature might give us a better understanding of their function in living organisms and learn us how to construct them ourselves synthetically.

FEED-FORWARD LOOPS Another functional unit that will be focused on more in this project is the feed-forward loop (FFL). The feed-forward loop is a common network motif and has been found in the transcription networks of bacteria (*E. coli*), yeast (*S. cerevisiae*) and

mammals [12] [8] [14] [25]. The feed-forward loop consists of three nodes (X, Y, Z) and three edges. The transcription factor representing node X regulates node Y, after which node Y regulates node Z, together with node X (Figure 1e). This structure can be modelled as an AND-gate like activation of node Z, since both transcription X and Y need to be present in order to fully regulate node Z (Figure 1f). The feed-forward loop can exist in eight different particular structures, in which the interactions between nodes can be either activating or repressing [4] (Figure 1e). The first class of feed-forward loops is the coherent feed-forward loop (cFFL), containing four specific configurations. A feed-forward loop is named coherent if the direct regulation from node X to Z has the same sign as the final regulation from node X, through Y, to Z. Type 1 of the coherent feed-forward loop class is the most abundant form of FFL found in *E. coli* and has the property that all transcription interactions are positive. [4]. The second class of FFLs is the incoherent feed-forward loop, where the signs of both interaction paths are opposite from each other (activating and repressing). Incoherent feed-forward loops have been found to be more present in yeast than in bacteria [4]. Because of the different signs of the interactions, each FFL has a different function and shows different behaviour.

COHERENT FEED-FORWARD LOOP TYPE 1 During this project, we will focus on the construction and behaviour of coherent feed-forward loop type 1 (cFFL1). The AND-gate like behaviour of node Z and the fact that the interaction path from X, through Y, to Z has one more interactions along the way than the direct interaction between node X and Z, leads to some interesting behaviour. When transcription factor X is activated, it can instantaneously interact with species Z. However, species Z is not directly activated because it also needs activation from transcription factor Y. While species X interacts with Z, another pathway is activated from X to Y. This leads to the production of transcription factor Y, which in its turn can complete the activation of species Z. Since the activation from X to Z consists of two paths, and one path takes longer than the other, a time delay arises between the activation of X and the final production of Z [4]. Moreover, it has been shown that cFFL1 works as a persistence detector or noise cancelling element [12]. The interaction from species X, through Y, to Z is delayed via the long arm of the circuit, meaning that it takes a longer time for species Y to reach a sufficient level to activate Z than species X. Therefore, if the input signal X is only transient, the concentration of species Y cannot reach the activation threshold of species Z. If the input signal X is more persistent, the concentration of transcription factor Y can increase to a sufficient level, such that also species Z will be activated. One can compare the time delay behaviour of the cFFL to a control circuit where the interaction between X and Y is absent

(Figure 1g). Models have shown that this circuit shows less time delay in the production of species Z [4]. Furthermore, it has been shown that time delay does not occur in the OFF-step of the cFFL1. When species X is removed from the system, degradation of species Z happens as fast as in the control circuit [4]. This behaviour is different for the other types of feed-forward loops. For example, cFFL type 2 shows delay in species Z production when switching off the circuit. Furthermore, a cFFL1 with an OR-gate instead of an AND-gate at node Z shows delay in the OFF-step of the circuit [4].

The coherent feed-forward loop type 1 has been experimentally studied in *E. coli* by Mangan et al. They investigated the function and behaviour of the L-arabinose utilisation system and compared this FFL to the lactose utilisation control system [4]. It was demonstrated that the arabinose system showed a clear time delay upon activation and no time delay when the system was turned off, compared to the lactose control system. The delay of the system was about 20 minutes, which was shown to be similar to possible false activation by the system inducer cAMP [19].

COUPLED FEED-FORWARD LOOP As was described earlier, network motifs often occur intertwined within more complex networks with a distinct function [19]. Relatively simple and isolated network motifs have been investigated and rebuild in the past, but less research has been done on sets of coupled network motifs and their specific functioning [26]. Gorochowski et al. discussed in how many different ways two feed-forward loops can be coupled and where they are found in complex (transcription regulation) networks. Computer algorithms to determine motif clustering in complex networks were used to discover how and where simple network motifs are clustered and in which way they are coupled to each other. It was found that the coherent feed-forward loop can be coupled in twelve distinct ways. Examples of such couplings include circuits where the input or output nodes are shared between two cFFLs, or where the output node of the first FFL acts as the input or intermediate node of the second FFL. All possible coupled feed-forward loops were discovered in the transcription networks of *E. coli* and *S. cerevisiae*, metabolism cascades of *E. coli* and *A. fulgidus*, or the neural network of *C. elegans*. The coupled feed-forward loops were also discovered in other types of networks, like food webs and file-sharing systems.

In this project we aim to further investigate the functioning and behaviour of variant 4 of the coupled feed-forward loops demonstrated by Gorochowski et al. (Figure 2). We aim to determine what temporal behaviour this circuit shows and whether it is possible to implement it in an in vitro setup. This circuit consists of five nodes and six edges, of which two nodes act as input (X1 and X2) for the system and two

nodes as output (Z1 and Z2) for the system. The two coherent feed-forward loops are coupled at the intermediate node Y. It is yet unknown how this coupled feed-forward loop behaves, but is expected that the time delay in production of both outputs might be different. This hypothesis is constructed as follows. If one activates for example the input node X1 on the left side of the circuit, output Z1 will be produced with a time delay as also happens in a regular cFFL. Simultaneously, product Y of the intermediate node is also produced in the process. When the right side of the coupled feed-forward loop is stimulated at node X2, output Z2 could be produced at a faster rate than its counterpart Z1. This might happen because no extra time is needed to activate node Y since it is already present from the first activation of the circuit at node X1. In this project we want to validate this hypothesis and determine to what extent the time delay in the production of both outputs differs. Furthermore, we are interested in whether it is possible to construct this particular (genetic) circuit in an in vitro system. This gives us more insight in how living cells apply such networks and how this network can be used in the construction of for example a synthetic gene network within a synthetic cell.

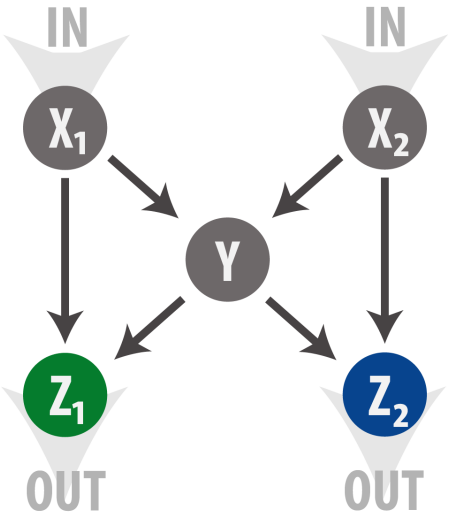

Figure 2: Schematic representation of coupled feed-forward loop topology. The coupled feed-forward loop consists of five nodes, of which two act as input (X1 and X2) and two act as output (Z1 and Z2). The middle node (Y) acts as the connection between the two separate coherent feed-forward loops.

CONSTRUCTION OF THE COUPLED FEED-FORWARD LOOP IN VITRO

If we take a closer look at the topology of the coupled feed-forward loop described before, we can recognise two separate coherent feed-forward loops which are joined at the intermediate node. Therefore, in order to study the coupled feed-forward loop, one first needs to gain more insight in the functioning of the components it is made up

of. Therefore, this project will start with constructing a set of coherent feed-forward loops to study how they behave in vitro. For this we use a platform that is inspired by the 'All *E. coli* TX-TL Toolbox 2.0' from Garamella et al. [27]. To construct the coherent feed-forward loop in vitro, we need to implement control elements into the genetic circuit that together can resemble the function of a cFFL. One of the control elements will regulate transcription of the genetic circuit and will be represented by *E. coli* transcription factors (sigma factors) [27] [28]. The second control element will be represented by a riboregulator (toehold switch), which can regulate the translation of the genes within the genetic circuit [29]. Once the coherent feed-forward loop has been constructed and characterised in vitro, we will couple two distinct cFFL versions to construct one coupled feed-forward loop genetic circuit. We will discuss whether it is feasible to construct such a circuit in vitro and characterise how it behaves.

IN SILICO CHARACTERISATION OF COUPLED FEED-FORWARD LOOP TEMPORAL BEHAVIOUR It takes a considerable amount of time to produce certain species involved in a (coupled) FFL. Since we aim to utilise a genetic circuit to demonstrate the behaviour of the FFL, we also have to take into account the amount of time it costs for processes like transcription and translation to take place. Unfortunately, the TXTL protocol requires to conduct in vitro experiments in batch. Therefore, it is not possible to give the genetic circuit in question time to conduct transcription and translation of the DNA species, before an input signal is fed to the system. This causes the problem that when an input is given to the system, the effect of this on the output of the system cannot be detected accurately because transcriptional and translational processes at multiple levels of the system overlap. Therefore, in order to also characterise the temporal behaviour of the coupled feed-forward loop, we will construct an ODE-model to demonstrate this behaviour [30] [31].

Using these methods, we aim to describe the function of, and reveal the temporal behaviour of the coupled feed-forward loop. Furthermore, we set out to successfully demonstrate an implementation of this genetic circuit in vitro.

Part I

COHERENT FEED-FORWARD LOOP

2

IN VITRO CHARACTERISATION OF THE COHERENT FEED-FORWARD LOOP

In order to successfully implement the coupled feed-forward loop in an in vitro system, it is necessary to first characterise the separate components involved in the system. The coupled feed-forward loop topology consists of two single coherent feed-forward loops, which are coupled at the intermediate node. By using two distinguishable input signals, one can control both sides of the coupled feed-forward loop separately. Furthermore, the outputs of the system need to be distinguishable from each other and components from both sides need not to engage in crosstalk. This means that in order to construct the coupled feed-forward loop, two distinct coherent feed-forward loops need to be available. Therefore, the assembly and characterisation of two distinct coherent feed-forward loops in vitro that can later be used for the assembly of the coupled feed-forward loop will be discussed in this chapter. Moreover, the components that are used to assemble the circuits, the implementation in an in vitro system and the output and behaviour of the circuits will be discussed.

2.1 COHERENT FEED-FORWARD LOOP TOPOLOGY

The coherent feed-forward loop topology consists of three nodes and three edges (Figure 3). The input of this genetic circuit is given through species X, which in its turn activates species Y. Subsequently, species Z is activated through stimulation by both species X and species Y in an AND-gate like fashion. Therefore, species X and species Y will need two distinct ways to stimulate the production of species Z. In the coming sections, an elaboration will be given on how these species are implemented in an in vivo system. In order to regulate transcription of species Z, a set of two different sigma transcription factors will be used. Furthermore, translation of species Y and species Z will be controlled by a riboregulator called a toehold switch.

2.1.1 *In vitro transcription-translation*

The coherent feed-forward loop will be constructed using a genetic circuit. For this project, the in vitro cell-free transcription-translation (TXTL) platform is used to express the components needed to form a FFL circuit. This platform has been tested extensively and has shown to be a versatile method to construct and express genetic circuits in vitro [27] [32] [33]. It is possible to express a genetic circuit in vitro,

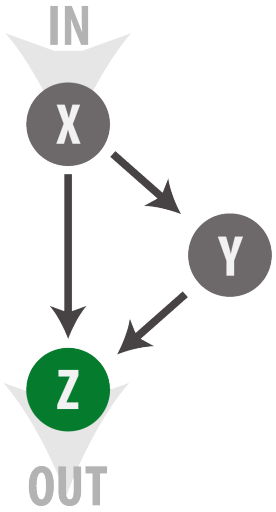

Figure 3: Coherent feed-forward loop topology. Activation of species Z is controlled by an AND-gate, only activated when both species X and Y stimulate the AND-gate.

because the system uses the endogenous components of an *E. coli* crude cytoplasmic extract. This extract contains the natural transcription and translation machinery necessary to execute RNA transcription and protein translation. For example, endogenous *E. coli* RNA polymerase, sigma factor 70 and ribosomes are present in the cytoplasmic extract [27]. The *E. coli* cytoplasmic extract is complemented by an energy mixtures, also containing nucleotides, salts, and tRNAs. Apart from this, one only needs to add the genetic circuit of interest to the mixture in order to start expression of this circuit [27]. One can easily swap in or out certain genes between experiments, which makes the platform very flexible in use.

Furthermore, the In Vitro Transcription-Translation (IVTT) expression of the genetic circuits in this project is realised using linear DNA fragments. The linear DNA fragments added to the IVTT mixture are used instead of circular DNA plasmids. It has been demonstrated that synthetic genetic circuits can be build more easily and rapidly in TXTL systems using linear DNA fragments than using plasmid DNA [34]. Multiple DNA fragments, like promoter regions, gene-coding regions, terminator regions, and the DNA vector can be assembled using Golden Gate Assembly (GGA). The resulting plasmid DNA is then cloned in *E. coli*. Traditional methods would then clone the DNA in vivo in order to produce great amounts of plasmid DNA that can be used for IVTT experiments. Sun et al. use PCR to produce many copies of linear DNA fragments produced in the GGA to be used in IVTT experiments. This in vitro method is faster than the traditional in vivo cloning and therefore, complete genetic circuits can be produced and tested more rapidly [34]. However, a problem that occurs when using linear DNA, is that linear DNA is more prone to degrada-

tion in the *E. coli* cytoplasmic extract than plasmid DNA. In IVTT experiments, linear DNA is mainly degraded by endogenous RecBCD, an exonuclease present in the *E. coli* crude extract. In order to protect linear DNA from exonuclease degradation, one can add GamS to the TXTL reaction mixture [34]. GamS is the truncated version of the protein Gam found in lambda bacteriophages. Gam is a RecBCD inhibitor, and therefore protects linear DNA from being degraded [35] [36].

The protocol for production of these linear DNA fragments and gamS can be found in respectively Section 2.2.

2.1.2 *Sigma factors*

The first control elements of the FFL circuit that are being discussed are sigma factors. Sigma factors can regulate the transcription of genes and can therefore control the activation of the three different species in the circuit. Sigma factors are prokaryotic polypeptide transcription factors that control transcription by binding to RNA polymerase (RNAP), forming a RNAP holoenzyme [37]. When bound to a specific sigma factor, this holoenzyme can recognise sigma factor specific promoter regions. The RNAP complex is directed to, and able to melt the double-stranded DNA near the promoter and bind to the promoter site, initiating transcription [38]. One specific prokaryotic sigma factor variant is sigma factor 70 (σ70), the primary or housekeeping sigma factor [38]. Sigma factor 70 is known as the primary sigma factor because many processes in bacteria, like cell growth, are controlled by the presence of this sigma factor [39]. Sigma factor 70 is already abundantly present in the *E. coli* cytoplasmic extract of the TXTL mixture and can, together with the core RNA polymerase, transcribe DNA species that need no regulation [27].

Another prokaryotic sigma factor that can be used to regulate transcription of the linear DNA fragments is sigma factor 28 (σ28). This sigma factor is not abundantly present in the TXTL mixture and can therefore serve as a specific activator of transcription once produced in IVTT. The σ28-RNAP holoenzyme only binds to σ28 specific promoter regions and will only transcribe the associated genes when σ28 is present. Since both σ70 and σ28 bind to the same pool of core RNAP, transcription of genes regulated by σ70 promoters (P70) or σ28 promoters (P28) can happen at the same time in the same reaction mixture [27] [28]. Therefore, no extra components facilitating transcription are needed besides the core RNAP.

2.1.3 *Toehold switches*

The second control element that will be used to regulate activation of specific species of the FFL circuit is the toehold switch. The toe-

hold switch is a synthetic riboregulator and can regulate gene expression by controlling the translation of mRNA species [29]. A complete and activated toehold switch element consists of a fragment of switch RNA and trigger RNA. The switch works as an AND-gate; if both trigger and switch RNA are present, the gene will be active and able to be translated (Figure 4). If the trigger RNA is not present, the three-dimensional structure of the switch will block translation of the gene. A toehold switch represses gene translation by forming a hairpin around the ribosome binding site (RBS). Base pairing of RNA right before the RBS and after the RBS (where the start codon AUG is situated) creates a hairpin structure, making it unable for ribosomes to bind to the mRNA, thereby repressing translation. Figure 4 shows how domain a* of the trigger RNA can bind to the complementary toehold domain a of the switch RNA. Once the trigger RNA is bound to the toehold domain, hairpin unwinding can be initiated and trigger RNA domain b* binds to domain b of the switch RNA [29].

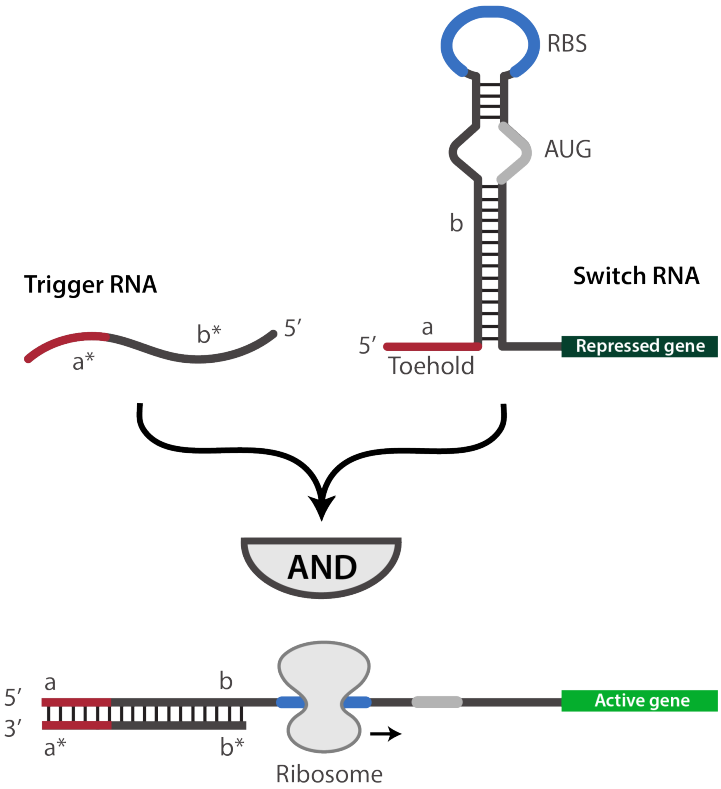

Figure 4: Schematic representation of a toehold switch. Variable domains a* and b* (both 15 nts) of the trigger RNA can bind to, respectively, complementary sequences a and b (both 15 nts) of the toehold RNA. Opening of the hairpin is initiated by binding of domain a* to the toehold domain a. Once opened, ribosomes can bind to the RBS and initiate translation of the gene. Figure adapted from [29].

Green et al. have shown that the toehold switch is an orthogonal riboregulator that controls gene activation with ON/OFF ratios up

to 250 [29]. Furthermore, domains a and b (and their complementary trigger sequences) are not restricted to one specific sequence, making it possible to design multiple orthogonal trigger and switch combinations. The specific sequence for such riboregulators can be incorporated in the linear DNA of our species. This hands us another control element for the regulation of the species within the FFL circuit.

2.1.4 *Implementation*

The sigma factors and toehold switches, the control elements described in previous sections, can be combined in order to construct the final circuit. Since the coherent feed-forward loop consists of three different nodes, the in vitro implementation will consist of three different DNA species (Figure 5).

Node X will be represented by a linear DNA strand consisting of a σ70 promoter (P70) and a trigger sequence. Because σ70 is naturally present in the IVTT reaction mixture, the trigger RNA will be produced continuously. Node Y is represented by a DNA strand consisting of P70, a toehold switch and the gene coding for the σ28 transcription factor. This DNA strand will also be continuously transcribed because of the P70. However, translation of σ28 is repressed as long as the toehold switch is in its hairpin conformation. If the correct trigger has been produced, it can bind to the switch, unwinding the hairpin and enabling translation. The produced σ28 can then subsequently bind to core RNAP, enabling the RNAP holoenzyme to bind to the sigma factor 28 promoter of the last DNA strand. As described, the DNA strand representing node Z consists of a P28, followed by a toehold switch and the gene coding for the fluorophore eGFP. The AND-gate behaviour necessary for species Z follows from the fact that both σ28 and the trigger need to be present in order to produce an eGFP output. First, the RNAP-σ28 complex can enable transcription of species Z, after which the trigger can activate the switch. This event frees the RBS, making it possible for ribosomes to translate the eGFP gene into the actual fluorophore eGFP, the measurable output of this genetic circuit.

2.2 METHODS

2.2.1 *Design and assembly of linear DNA constructs*

In order to assemble the linear DNA constructs that are used in the IVTT experiments, we use the 'In Vitro Linear DNA Assembly' protocol from Sun et al. (2014) [34]. This protocol uses Golden Gate Assembly to clone multiple DNA fragments into a pBEST plasmid [34] [40]. Each linear DNA fragment contains a sequence coding for for example the promoter region, a trigger sequence, a toehold switch, σ28

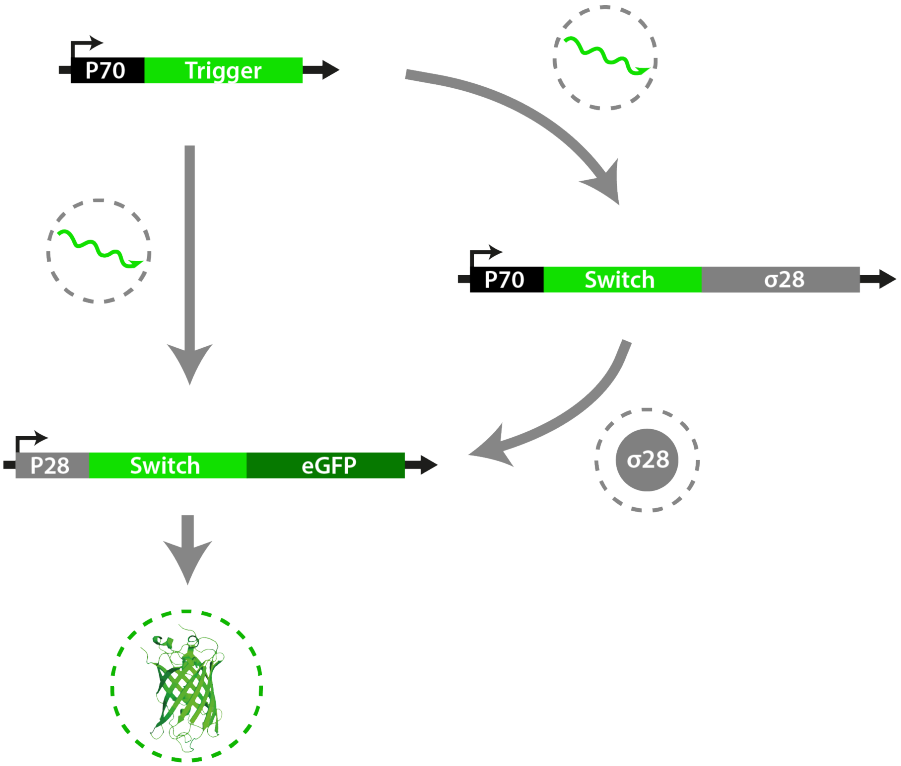

Figure 5: Schematic representation of the DNA species used to construct a coherent feed-forward loop in vitro. Species Z is only activated if both trigger RNA and σ28 have been produced, leading to the production of the fluorophore eGFP.

transcription factor, or a fluorescent protein. The fragments can be retrieved through PCR amplification from earlier constructs or bought as a gBlock from IDT. Each fragment is flanked by a digestion site for the BsaI restriction enzyme, which can create double stranded cuts outside of the recognition site, forming a four nucleotide overhang. The overhang sequences at the end of one fragment and the beginning of the second fragment are complementary and are unique between fragments. In a reaction inside a thermocycler, the DNA fragments and pBEST vector are BsaI digested and ligated by a T_4 Ligase. The newly formed plasmids are amplified using a PCR reaction and verified with agarose gel electrophorese.

The plasmids retrieved from the GGA are transformed into NovaBlue (DE3) competent cells and successfull transformation is verified using the KAPA2G PCR Kit (Kapa Biosystems) and agaraose gel electrophorese. Furthermore, successfull GGA is verified by sequencing (BaseClear). Bacteria for which transformation was successfull are cultured and stored in glycerol stocks at -80 °C for later use.

The linear DNA fragments can be retrieved from the glycerol stocks by first culturing the bacteria overnight and purifying the the plasmids using the QIAprep Spin Miniprep Kit (QIAGEN). The linear DNA fragments are then amplified from the plasmids using the NEB

Phusion PCR Kit (New England Biolabs) and purified using the QIAquick PCR Purification Kit (QIAGEN). The sequences of the DNA fragments and linear DNA constructs can be found in Appendix A.

2.2.2 *TXTL protocol*

With the linear DNA fragments produced, it is now possible to combine several of them to implement a genetic circuit and express it using a TXTL reaction [27] [34]. The TXTL mixture contains several components crucial for in vitro expression of a genetic circuit. The first and foremost component is the *E. coli* cytoplasmic extract. This cell lysate (3X) contains the necessary transcription and translation machinery for successfull expression [41] [42]. To this, we add an amino acid mixture (37.5 mM) [43], Magnesium glutamate (8 mM) and PEG-8K (2%). Furthermore, we add a 3-PGA feeding buffer (14X) to the TXTL mixture that contains nucleotides, *E. coli* tRNA and an energy mixture necessary to sustain the reaction [34] [44]. This TXTL reaction mixture is then added to the linear DNA fragments forming the genetic circuit. The ratio of TXTL reaction mixture to linear DNA fragments in a 9.5 µL reaction is 2:1. Each 9.5 µL sample is pipetted into a 384-well plate (Nunc) and the genetic circuit expression is carried out in a platereader at 29 °C.

2.2.3 *Platereader protocol*

The TXTL reaction takes place in a platereader at 29 °C for 16 hours, measuring fluorescence every 5 minutes. The following settings are used to measure the fluorescence of the eGFP and CFP fluorophores:

- eGFP - Excitation: 470 nm, Emission: 510 nm
- CFP - Excitation: 440 nm, Emission: 480 nm

Fluorescence measurements are corrected for background noise and lysate autofluorescence by substracting the fluorescence measured in a well only containing the TXTL mixture. The fluorescence measured after 16 hours is used to determine the fluorophore production shown in the results below.

2.3 RESULTS AND DISCUSSION

2.3.1 *Expression of the coherent feed-forward loop in vitro*

The first circuit that has been tested in vitro is the coherent feed-forward loop, as described in section 2.1.4. The toehold switch and trigger pair that has been used for this experiment is variant number 10. The concentration of DNA species X and Y are respectively 10 nM

and 1 nM. The concentration of DNA species Z has been varied as shown on the x-axis of Figure 6. Figure 6 shows the eGFP production of the cFFL circuit, depicted by the fluorescence intensity measured by the platereader. As can be seen in this figure, the production of eGFP increases for higher concentrations of the output DNA species. As can be observed for a linear increase in DNA concentration, the eGFP production also linearly increases. Furthermore, the grey bar shows the eGFP production of a cFFL circuit where the DNA species containing the sequence for Trigger 10 has been replaced for the sequence of an off-target trigger. An off-target trigger is a trigger with a sequence that is not complementary to the toehold switch used in the experiment. The off-target trigger is however compatible with a different toehold switch; here variant 2.1. Figure 9 shows that a cFFL circuit with an off-target trigger input produces about a 10-fold less eGFP than with an on-target trigger.

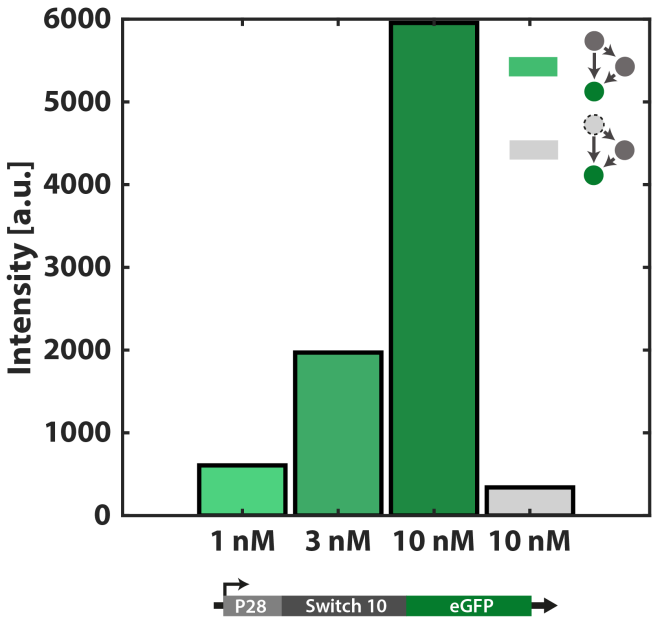

Figure 6: The trigger/switch pair used for this experiment is variant 10. The green bars represent the eGFP production of a complete cFFL circuit in vitro. eGFP production is represented by the fluorescent intensity measured on a platereader. The light grey and encircled node in the schematic overview of the genetic circuits depicts the use of an off-target trigger sequence.

2.3.2 *Additional toehold switches*

After testing the cFFL circuit with trigger/switch pair 10, the same circuit topology was tested with different trigger/switch pairs. The final goal of coupling two coherent feed-forward loops at the intermediate

node is only possible if one has control over the two different circuit inputs. The two inputs will be two distinct trigger variants, complementary to one of two toehold switches. Therefore, also the toehold switches incorporated in DNA species Y and Z will be different on both sides of the coupled feed-forward loop. In order to successfully couple two cFFLs in a later stage of the project, it is crucial that both cFFLs have been tested thoroughly. The testing of both cFFLs is crucial because the coupled feed-forward loop will consist of two separate cFFLs that share σ28 as a common node. Another necessary aspect is that the output of both cFFLs should be in the same order of magnitude and should be distinguishable from any background noise of the platereader. If this is not the case, fluorescence of one of the outputs might not be measurable or an excessive production of one output might decrease the production of the other output.

2.3.2.1 *Toehold switch 8*

The first alternative trigger/switch pair that was tested was variant 8. The corresponding sequence of both trigger and switch can also be found in Appendix A. Apart from the different trigger and switch sequences incorporated in the DNA species, the topology of the cFFL circuit remained exactly the same. Unfortunately, the initial tests with this trigger/switch pair resulted in less fluorophore production than achieved before with trigger/switch pair 10. (Figure 7a, grey bars). As can be seen in Figure 7a, the eGFP production for this particular trigger/switch pair was 15-fold smaller than with trigger/switch pair 10, for the same concentration of DNA species.

In order to increase the performance of the cFFL with trigger/switch pair 8, we took a closer look at the sequences of the DNA constructs. It was observed that the σ28 producing construct with toehold switch 8 had a slightly different sequence compared to the same construct with toehold switch 10 (apart from the difference in sequence of the actual toehold switch). A sequence of six nucleotides *(AAGCGG)* between the promoter and the toehold switch was present in variant 8, but not in variant 10. This six nucleotide sequence was a cloning scar caused by the GGA of the DNA construct. The cloning scar increased the number of nucleotides between the promoter and the toehold switch, which could influence the forming of the hairpin structure, and thus the functioning of the toehold switch. Therefore, it was tried to remove them from the sequence and perform a new experiment with the possibly improved DNA construct. The new DNA construct was constructed using GGA using a newly synthesized toehold switch 8 DNA fragment, in which the six nucleotide sequence was absent. As shown in Figure 7a, this yielded a two-fold increase in eGFP production compared to the old toehold switch 8 sequence.

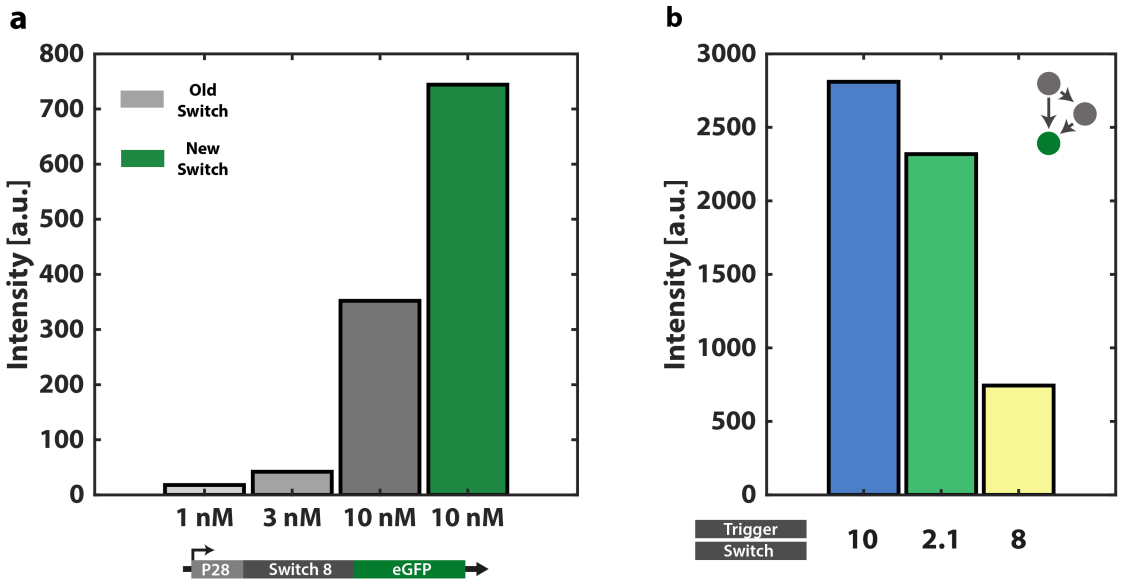

Figure 7: (a) eGFP production of the cFFL with trigger/switch pair variant 8. Shown in grey are the eGFP productions for the old σ28 producing constructs. The green bar depicts the same circuit with a newly synthesized DNA construct, where a six nucleotide sequence has been removed between the promoter and toehold switch. The DNA concentrations of DNA species X and Y are respectively 10 nM and 1 nM. The DNA concentration of species Z is shown underneath the bars in the chart.
(b) eGFP production of the cFFL circuit for different trigger/switch pairs, displayed underneath the bars in the chart. The DNA concentrations of DNA species X, Y and Z are respectively 10 nM, 1 nM and 10 nM.

2.3.2.2 *Toehold switch 2.1*

However, the performance of the cFFL with trigger/switch variant 8 was not yet sufficient compared to the performance when using trigger/switch variant 10, because the difference in fluorophore production was still a factor 5. Therefore, a third variant (2.1) trigger/switch pair was tested. This eventually yielded the results shown in Figure 7b. This Figure shows the eGFP production of three coherent feed-forward loops with different trigger/switch pairs. The trigger/switch pair is shown underneath the corresponding bar in the chart. As can be seen in Figure 7b, the intensity of the cFFL with trigger/switch pair 2.1 is more comparable to the intensity of the original trigger/switch pair 10, with a relative eGFP production of approximately 80%. Therefore, it was decided to continue with only variants 10 and 2.1.

Another aspect that had to be tested with the new trigger/switch pairs was the ideal concentration of DNA species Y, the σ28 producing construct, within the cFFL topology. This was tested to determine if the σ28 producing construct concentration would influence the pro-

duction of fluorophore in presence and absence of a trigger input. Therefore, three different concentrations, 0.6 nM, 0.8 nM, and 1.0 nM, were tested with the cFFL. The goal of this experiment was to determine the amount of 'leakage' this switch shows in both σ28 and eGFP production. Therefore, an experiment was designed which used a circuit where the toehold switch was removed from the output circuit (Figure 8a). Figure 8a shows the ON/OFF ratios of this circuit for varying σ28 producing construct concentrations. The ON state is the circuit with the matching trigger construct, the OFF state is represented by the same circuit, but with an off-target trigger. The experiment shows that for construct concentrations 0.8 nM and 1.0 nM the ON/OFF ratios are close to 1 and that there is much off-target σ28 production. For a construct concentration of 0.6 nM, the ON/OFF ratio is approximately 28, showing a clear difference in eGFP production between use of on-target and off-target trigger sequences.

Figure 8b shows the ON/OFF ratios for a full cFFL circuit with the same concentrations of σ28 producing construct as in Figure 8a. Here it can be observed that 0.6 nM construct concentration again yields the best ON/OFF ratio of approximately 10. This ON/OFF ratio is in the same order of magnitude as the ratio for trigger/switch pair 10 (Figure 6). Since a construct concentration of 0.6 nM yielded the best results, it was decided to keep using this concentration in future experiments.

2.3.3 *Additional fluorophore*

The last component needed in order to construct a coupled feed-forward loop is a second fluorescent output. For this output, the CFP fluorophore was chosen and incorporated in the output DNA construct just similar to eGFP. The production of fluorophore in a cFFL circuit was tested in vitro and the results are shown in Figure 9. One can see that for linearly increasing concentrations of the CFP producing DNA construct, the CFP production also linearly increases. Furthermore, the circuit was tested with an off-target trigger, yielding an ON/OFF ratio of approximately 6. This circuit was tested using trigger/switch pair 10 and the off-target trigger was variant 2.1.

2.3.4 *Outlook for construction of coupled feed-forward loop*

Now that all necessary components for a coupled feed-forward loop have been identified, produced and tested, the construction of this genetic circuit can be started more specifically. Since there are two available trigger/switch pairs and two output fluorophores, it is important that we determine on which side of the coupled feed-forward loop which combination will be used. Therefore, it was tested, for a cFFL topology, how each trigger/switch pair performs with each

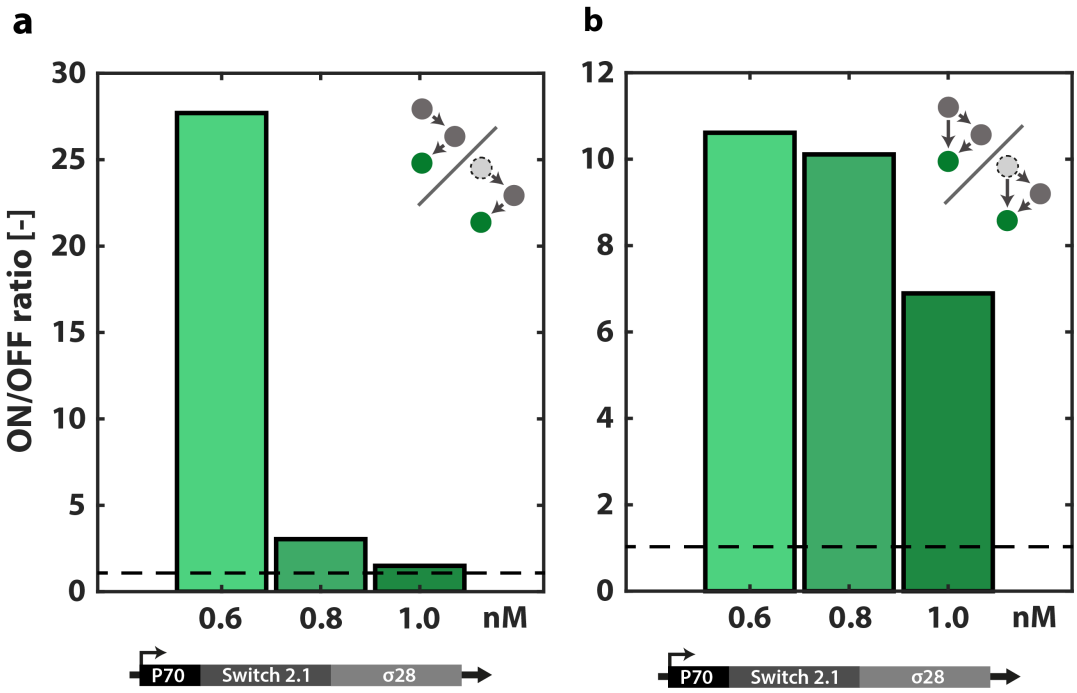

Figure 8: (a) ON/OFF ratios for eGFP production for circuit topology shown in figure with trigger/switch pair 2.1. The light grey and encircled node in the schematic overview of the genetic circuits depicts the use of an off-target trigger sequence. Concentrations of σ28 producing construct are shown underneath the bars.
(b) ON/OFF ratios for eGFP production of cFFL with trigger/switch pair 2.1. Concentrations of σ28 producing construct are shown underneath the bars.

fluorophore (Figure 10). As can be observed in Figure 10 for both fluorophores, circuits with trigger/switch pair variant 10 produce more fluorophore than with trigger/switch pair 2.1. The amount of CFP produced by variant 2.1 is quite low, and close to the detection limit of the platereader. For the eGFP production this is not the case. Therefore, it was decided that in future experiments, the one cFFL will consist of trigger/switch pair 10 with fluorescent output CFP, and the other cFFL will contain trigger/switch pair 2.1 in combination with eGFP.

2.3.5 *Behaviour of the final two coherent feed-forward loop circuits in vitro*

In the previous section it has been decided which trigger/switch pairs and fluorophores will be combined to form the two separate coherent feed-forward loops needed to eventually construct the coupled feed-forward loop. As preparation for the final construction of the coupled feed-forward loop, both coherent feed-forward loops have been tested in another in vitro experiment. The experiments have

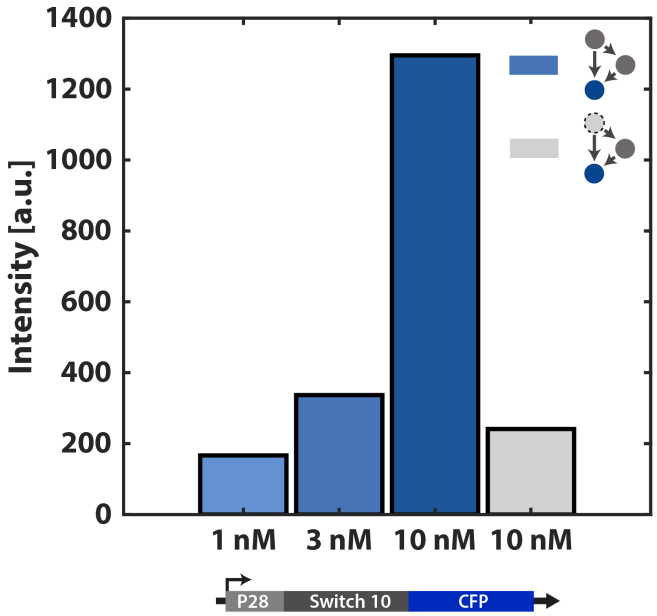

Figure 9: CFP production of the cFFL with trigger/switch pair variant 10. The light grey and encircled node in the schematic overview of the genetic circuits depicts the use of an off-target trigger sequence (variant 2.1). The concentration of output DNA construct is shown underneath the respective bar.

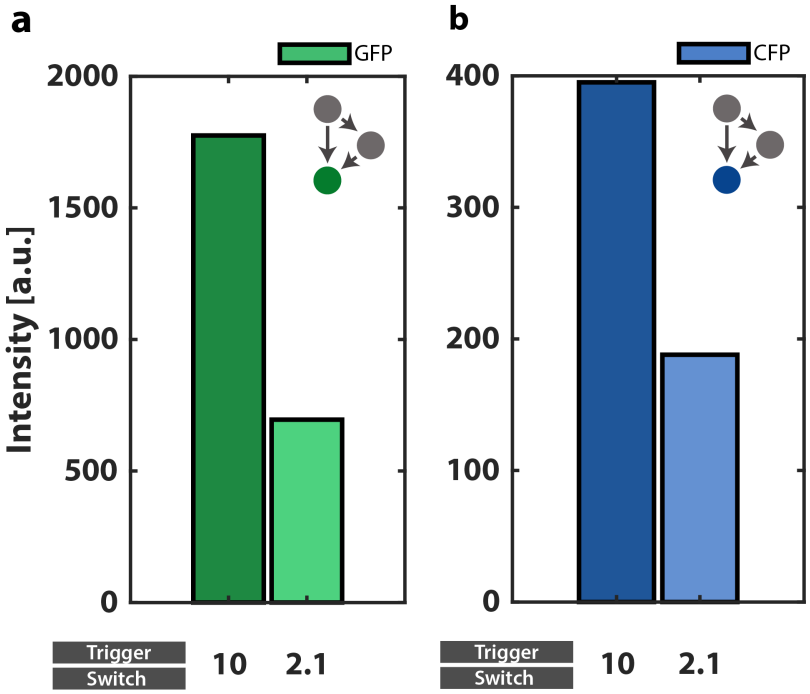

Figure 10: (a) eGFP production of cFFL for trigger/switch pairs 10 and 2.1. (b) CFP production of cFFL for trigger/switch pairs 10 and 2.1.

been performed in triplo and clearly show the quantitative properties of the coherent feed-forward loops (Figure 11). With these experiments, we want to show behaviour of the two coherent feed-forward loops that will later be used to construct the coupled feed-forward loop. It is demonstrated how these the cFFL circuits react to off-target DNA constructs and what implications this has on the construction and functioning of the coupled feed-forward loop. Furthermore, we will discuss the role of σ28 within both the cFFL and coupled FFL genetic circuit.

2.3.5.1 *cFFL with trigger/switch pair 2.1 and eGFP output*

Figure 11a shows the production of eGFP for the complete cFFL and its performance in absence of a trigger or with an off-target trigger. The coherent feed-forward loop produces on average approximately 0.75 μM of eGFP, with trigger construct, σ28 producing construct and output construct concentrations of respectively 10 nM, 0.6 nM and 10 nM. As shown before, the eGFP production in absence of a trigger and with an off-target trigger is relatively low compared to the full cFFL. The ON/OFF ratio for this situation is at least 15.

The schematics shown in Figure 11b depict a circuit where the toehold switch in front of the σ28 gene has been removed. Therefore, the mRNA strand needs no trigger activation in order to be translated. The experiment depicted here shows the influence of the toehold switch that is incorporated in the σ28 producing construct. It is demonstrated that the ON/OFF ratio of this control circuit decreased to approximately 4, a drastic decrease compared to the ON/OFF ratio of the full coherent feed-forward loop. This confirms that with each control element, in this case the toehold switch, the ON/OFF ratio of the genetic circuit increases.

Lastly, Figure 11c shows the influence of the σ28 producing construct on the cFFL. As can be seen, production of σ28 is crucial in order to start transcription of the output DNA construct. Furthermore, as can be observed that with an off-target σ28 producing construct, there is still quite some production of eGFP, about 80% of the original production. This finding shows that σ28 producing construct still shows some leakage and still produces enough σ28 in order to start transcription of the output construct. However, it should be mentioned that this off-target construct concentration is higher, with 0.8 nM instead of 0.6 nM of on-target construct. The leakage might therefore be explained by the results observed in Figure 8. Furthermore, the last bar shows the eGFP production for both off-target trigger and off-target σ28 producing construct. One should realise that the trigger sequence is complementary to the toehold switch of the intermediate construct, but not to the output construct. This experiment is conducted to determine the influence of an off-target trigger on the translation of the fluorophore gene when transcription can already be

performed due to the presence of σ28. In the coupled feed-forward loop topology, similar situations might arise where σ28 is present, but not the correct trigger RNA. Therefore, we want to know how this influences the production of fluorophore. The results here are comparable to the ones shown in Figure 11b and confirm that both correct trigger and σ28 are crucial for optimal fluorophore production.

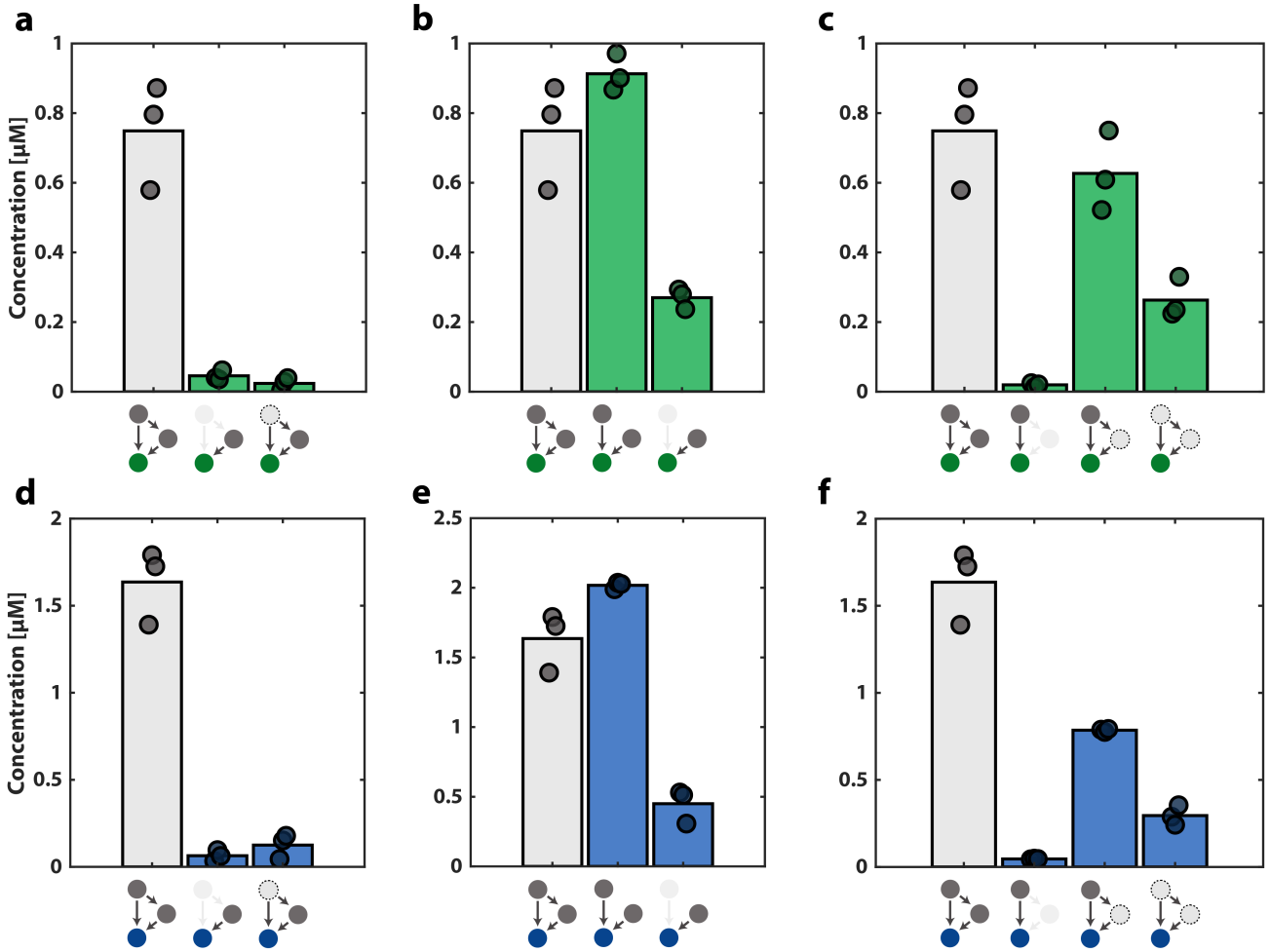

Figure 11: Fluorophore production of both coherent feed-forward loops in triplo. Figures a-c show the performance of the cFFL with trigger/switch pair 2.1 and eGFP output. Figures d-f show the performance of the cFFL with trigger/switch pair 10 and CFP output
(a, d) Performance of cFFL in absence of trigger and with an off-target trigger.
(b, e) Shows a control circuit where the toehold switch in front of the σ28 gene has been removed.
(c, f) Influence of σ28 producing constructs on circuit behaviour. Shows performance in absence of this construct and with off-target variant.

2.3.5.2 *cFFL with trigger/switch pair 10 and CFP output*

As can be seen in Figure 11d-f, this cFFL, and the control circuits tested, shows very similar behaviour as the cFFL with trigger/switch pair 2.1 and eGFP output. However, the absolute concentration of CFP produced is approximately two times bigger than the absolute concentration eGFP produced by the cFFL shown before. Furthermore, it can be seen in Figure 11f that the relative production of CFP in presence of an off-target σ28 producing DNA construct is lower than for the eGFP cFFL circuit. This difference might be caused by the use of a lower concentration of σ28 producing construct for the CFP circuit; 0.6 nM of the off-target construct as opposed to 0.8 nM for the on-target construct.

3

IN SILICO CHARACTERISATION OF THE COHERENT FEED-FORWARD LOOP

Since the in vitro experiments with the coherent feed-forward loop were only done in batch, we also wanted to run simulations on the coherent feed-forward loop in silico. Performing in batch experiments does not give the possibility to add DNA constructs during the process, making it difficult to determine temporal behaviour of the genetic circuit. Therefore, it was decided to also construct a computer model for the coherent feed-forward loop discussed in Chapter 2.

3.1 ORDINARY DIFFERENTIAL EQUATION MODELS

Two ordinary differential equation (ODE) models were created to predict temporal behaviour of the coherent feed-forward loop. The first model is based on the cFFL model from Mangan and Alon [4]. This model consists of two differential equations, representing nodes Y and Z of the cFFL. The model is slightly adjusted to also take into account possible leakage in the production of node Z when no input is given to the system. The complete model will be discussed in Section 3.2.

The second model is based on the in vitro implementation of the coherent feed-forward loop. This model also consists of multiple ODEs and the production of the different species is represented by mass action kinetics [45][46][47]. This model will describe the transcription from DNA to RNA, the translation from RNA to protein and the interactions between the several species forming the characteristic cFFL behaviour. Using this expanded model we can better describe the implications of the coherent feed-forward loop. Also this model will be further discussed in Section 3.2.

In order to characterise temporal behaviour of the cFFL, we quantify kinetic filtering of the circuits and determine certain circuit metrics describing this. These are the trigger time (τ_{50}) and the temporal ultrasensitivity (TU) of the circuit. Trigger time is described as the length of an input needed in order to produce 50% of the maximum circuit output [48]. In order to determine this trigger time in the simulation, the circuit is excited with multiple input pulses varying in length. The maximum outputs for these input pulses are determined and plotted against input duration. From this analysis, the input duration needed to produce 10% (τ_{10}), 50% (τ_{50}), and 90% (τ_{90}) of the maximum output is determined and used to represent the circuit met-

rics. The temporal ultrasensitivity score is calculated by dividing the input duration needed to reach 10% by the time needed to reach 90% of maximal output (τ_{10}/τ_{90}). This metric describes the steepness in production of output over time and represents the kinetic filtering of the circuit; the duration of the stimulation of the circuit in order to fully activate the production of the network output [48]. The circuit metrics are visualised in Figure 12.

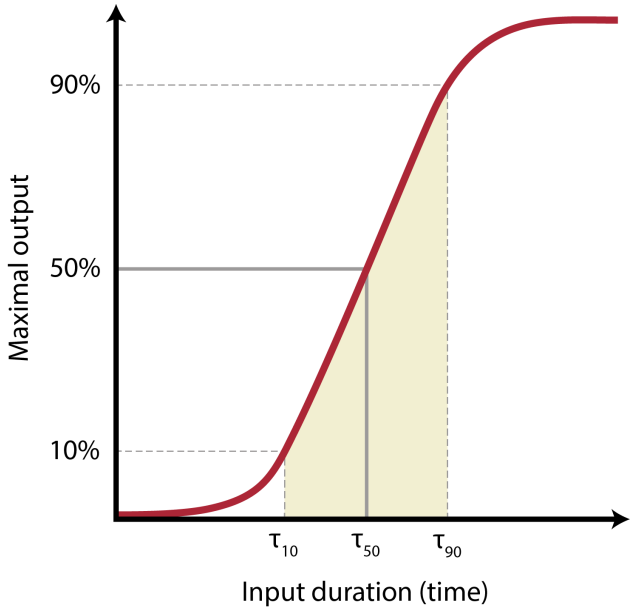

Figure 12: Quantification of temporal behaviour. The circuit is stimulated with input pulses of varying amounts of time and the maximal output for that pulse is determined. These outputs are compared to the maximal output of the circuit for an infinite amount of time. τ_{10}, τ_{50}, τ_{90} represent the input duration needed to reach an output of respectively 10%, 50%, and 90% compared to the maximum output. The trigger time of the system is τ_{50} and the TU score is defined as τ_{10}/τ_{90}.

3.2 METHODS AND EQUATIONS

3.2.1 *Coherent feed-forward loop model from Mangan et al.*

The simple version of the coherent feed-forward loop model is adapted from a model by Mangan and Alon and is constructed as follows [4].

$$dY/dt = B_y + \beta_y f(X, K_{xy}) - \delta_y Y$$
$$dZ/dt = B_z + \beta_z (f(X, K_{xz}) + \epsilon_{xz})(f(Y, K_{yz}) + \epsilon_{yz}) - \delta_z Z$$

The model consists of two differential equations, for species Y and Z each one. Parameters B_y and B_z represent the basal expression of the species and are set to zero in the model. Parameters β_y and

β_z are the production rates of the species and are multiplied with either one or two regulation function $f(u, K)$. Lastly, parameters δ_y and δ_z represent the degradation of species Y and Z. Function $f(u, K)$ is the function for an activator of the species with input parameters u, the concentration of an interacting species, and K, the activation coefficient. This function is also known as the Hill-Langmuir equation [30]. The AND-gate consists of two activator functions multiplied with each other. Furthermore, a parameter ϵ is added to the equation to simulate the leakage of the AND-gate of species Z.

$$\begin{aligned} f(u, K) &= \frac{(u/K)^H}{1 + (u/K)^H} \\ &= \frac{u^H}{K^H + u^H} \end{aligned}$$

The parameter values from Mangan and Alon are also used to run this model. Therefore, $H = 2$, $\beta_y = \beta_z = 1$, $\delta_y = \delta_z = 1$, $K_{XY} = K_{XZ} = 0.1$ and $K_{YZ} = 0.5$. Furthermore, it was chosen that $\epsilon_{XZ} = \epsilon_{YZ} = 0.1$.

One of the inputs of the activator function, species X, is either 1 or 0, meaning it is either present, thereby activating species Y and Z, or absent.

The reference circuit model is the same as the cFFL model, except that the interaction between species X and Y has been removed. This means that the activator function is always equal to 1.

3.2.2 *Expanded coherent feed-forward loop model*

The second ODE model of the coherent feed-forward loop is an expanded version and represents the DNA, RNA and proteins that are also present in the in vitro experiment. The trigger DNA is used as input of the system and when present, can activate the production of eGFP, which is the output of the system. The other DNA concentrations are, like in the in vitro experiments, constant and have the same concentrations as in the experiments. Furthermore, the model consists of 7 differential equations that represent the RNA and protein species. The model is constructed using mass-action kinetics.

$$\frac{d}{dt}Tr_1 = k_{ts,Tr} * Tr_{1;DNA} - k_{on,Tr_1,Sw_{1,1}} * Tr_1 * Sw_{1,1} + k_{off,Tr_1,Sw_{1,1}} * Tr_1 \cdot Sw_{1,1} - k_{on,Tr_1,Sw_{1,2}} * Tr_1 * Sw_{1,2} + k_{off,Tr_1,Sw_{1,2}} * Tr_1 \cdot Sw_{1,2} - \delta_{RNA} * Tr_1$$

$$\frac{d}{dt}Sw_{1,1} = k_{ts,Sw} * Sw_{1,1}\_S_{28;DNA} - k_{on,Tr_1,Sw_{1,1}} * Tr_1 * Sw_{1,1} + k_{off,Tr_1,Sw_{1,1}} * Tr_1 \cdot Sw_{1,1} - \delta_{RNA} * Sw_{1,1}$$

$$\frac{d}{dt}Tr_1 \cdot Sw_{1,1} = k_{on,Tr_1,Sw_{1,1}} * Tr_1 * Sw_{1,1} - k_{off,Tr_1,Sw_{1,1}} * Tr_1 \cdot Sw_{1,1} - \delta_{RNA} * Tr_1 \cdot Sw_{1,1}$$

$$\frac{d}{dt}S_{28} = k_{tl,S_{28}} * Tr_1 \cdot Sw_{1,1} + \epsilon_{S_{28}} * Sw_{1,1} - \delta_P * S_{28}$$

$$\frac{d}{dt}Sw_{1,2} = k_{ts,Sw} * P_{28}\_Sw_{1,2}\_GFP_{;DNA} * \frac{S_{28}^H}{K_{S_{28}}^H + S_{28}^H} + \epsilon_{Sw_{1,2}} * P_{28}\_Sw_{1,2}\_GFP_{;DNA} - k_{on,Tr_1,Sw_{1,2}} * Tr_1 * Sw_{1,2} + k_{off,Tr_1,Sw_{1,2}} * Tr_1 \cdot Sw_{1,2} - \delta_{RNA} * Sw_{1,2}$$

$$\frac{d}{dt}Tr_1 \cdot Sw_{1,2} = k_{on,Tr_1,Sw_{1,2}} * Tr_1 * Sw_{1,2} - k_{off,Tr_1,Sw_{1,2}} * Tr_1 \cdot Sw_{1,2} - \delta_{RNA} * Tr_1 \cdot Sw_{1,2}$$

$$\frac{d}{dt}GFP = k_{tl,GFP} * Tr_1 \cdot Sw_{1,2} + \epsilon_{GFP} * Sw_{1,2} - \delta_P * GFP$$

Species $Sw_{1,1}$ and $Sw_{1,2}$ represent the inactive, hairpinned, forms of the toehold switch. The active, and bound to trigger, forms of the toehold switch are represented by species $Tr_1 \cdot Sw_{1,1}$ and $Tr_1 \cdot Sw_{1,2}$. Furthermore, the interaction between transcription factor σ28 and its promoter is modelled with a Hill-Langmuir equation [30]. The parameters k_{ts} and k_{tl} are respectively the transcription and translation rates of DNA and RNA. The binding kinetics of the trigger and switch RNA strands are represented with parameters k_{on} and k_{off}. Furthermore, a leakage term ϵ has been added to the equations covering σ28 and GFP production to simulate the leakage also observed in in vitro experiments. The parameter values can be found in Appendix B. These values are retrieved from literature and some are slightly adapted to match observations from the in vitro experiment on fluorophore concentration and time-scale.

The reference circuit model is the same model as the expanded cFFL model, however, the interaction between trigger and switch(1,1) has been removed. This means that there has to be no trigger present in order to start translation of σ28.

3.2.3 *Simulation*

The models are simulated using MATLAB and the differential equations are solved with MATLAB's ODE solver *ode15s*. The initial values

of all species (variables) are zero at the beginning of the simulation, except for the DNA concentrations (constants). The model is run several times with the final values of the previous run as intitial values of the next run. In this way, the trigger DNA concentration can be altered during a run to simulate pulse input. Before an input pulse is given to the model, each model is run for some time to ensure that the RNA and protein species that need no further activation, can already be produced. This means that when the input is fed to the model, production of the output can start directly (with a possible time delay).

Furthermore, to determine the kinetic filtering metrics discussed before, the model is also run multiple times, but then with varying input duration. For each different input duration, the maximal output is determined. Thereafter, τ_{10}, τ_{50} and τ_{90} can be determined, and the temporal ultrasensitivity calculated.

3.3 RESULTS AND DISCUSSION

3.3.1 *Coherent feed-forward loop model from Mangan et al.*

First, the cFFL model adapted from the work by Mangan and Alon was run in MATLAB and the results are shown in Figure 13. Panel a shows a pulse input of 8 a.u. of time for the cFFL and reference model. As can be observed in this figure, the increase in output happens quicker and is steeper for the reference circuit than for the cFFL circuit. This finding is completely in line with expectations and literature [4]. Panel b shows the quantification of kinetic filtering of both circuits. As can be seen in panel b and c, the reference model has smaller τ_{10}, τ_{50} and τ_{90} compared to the cFFL model. The trigger time is more than doubled for the cFFL compared to the reference circuit. These differences are caused by the inherent properties of the coherent feed-forward loop as described before. Because in the cFFL an input is first needed in order to activate species Y, the production of species Z is delayed. The reference model does not have this interaction between species X and Y, thereby being able to produce an output at the same instant that the input is fed to the circuit.

The degradation of output the product looks similar for both circuits. This similarity is because the degradation rate for both circuits is the same and the interaction between species X and Y does not influence this process. As shown in literature, this finding is true for the coherent feed-forward loop type 1 that is described in this report [4].

Furthermore, we see that the temporal ultrasensitivity does not seem a good metric in this situation. The paper from Gerardin et al. describes that a steeper increase in output would give a higher tem-

poral ultrasensitivity score [48]. However, in Figure 13c it can be seen that the TU is higher for cFFL despite having a less steep increase in output than the reference circuit. This illogical difference is probably caused by the very small τ_{10} of the reference model.

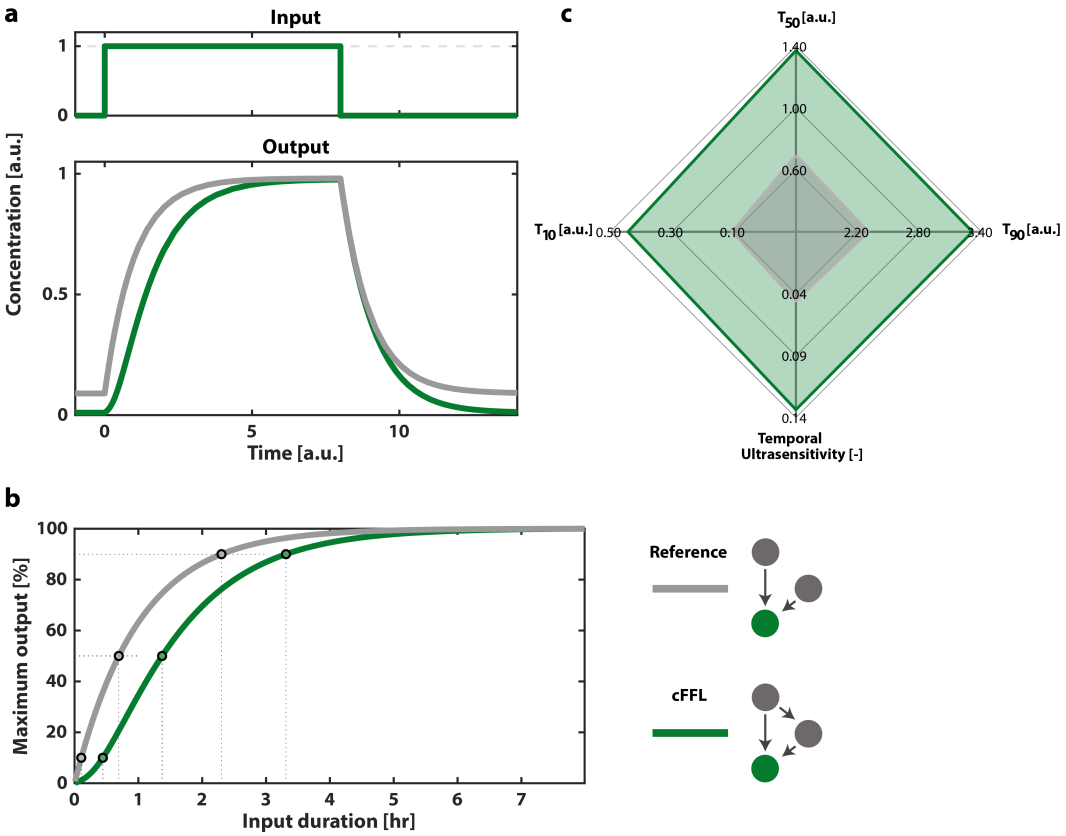

Figure 13: (a) Output production for the input pulse shown in the upper panel.
(b) Quantification of kinetic filtering. The figure shows the maximal output value for an input duration described on the x-axis.
(c) Radar chart showing the kinetic filtering metrics.

3.3.2 *Expanded coherent feed-forward loop model*

3.3.2.1 *Pulse input*

The following section shows the results of the simulations of the expanded coherent feed-forward loop model (Figure 14). This model shows similar results as the cFFL model from Mangan et al., but can better describe the observed behaviour by looking at the separate components. First, the response to a trigger input pulse is shown in Figure 14a and it can be seen that the shape of the response is very similar to the one in Figure 13a. An input pulse in this situation means that 10 nM trigger DNA is fed to the system for the time duration shown in the figure. Furthermore, before giving an input pulse,

the model is run for several hours to ensure that all species independent of trigger input can already be produced. Since the reference circuit has one control element less (toehold switch at intermediate node), the background fluorophore production is higher than for the cFFL circuit.

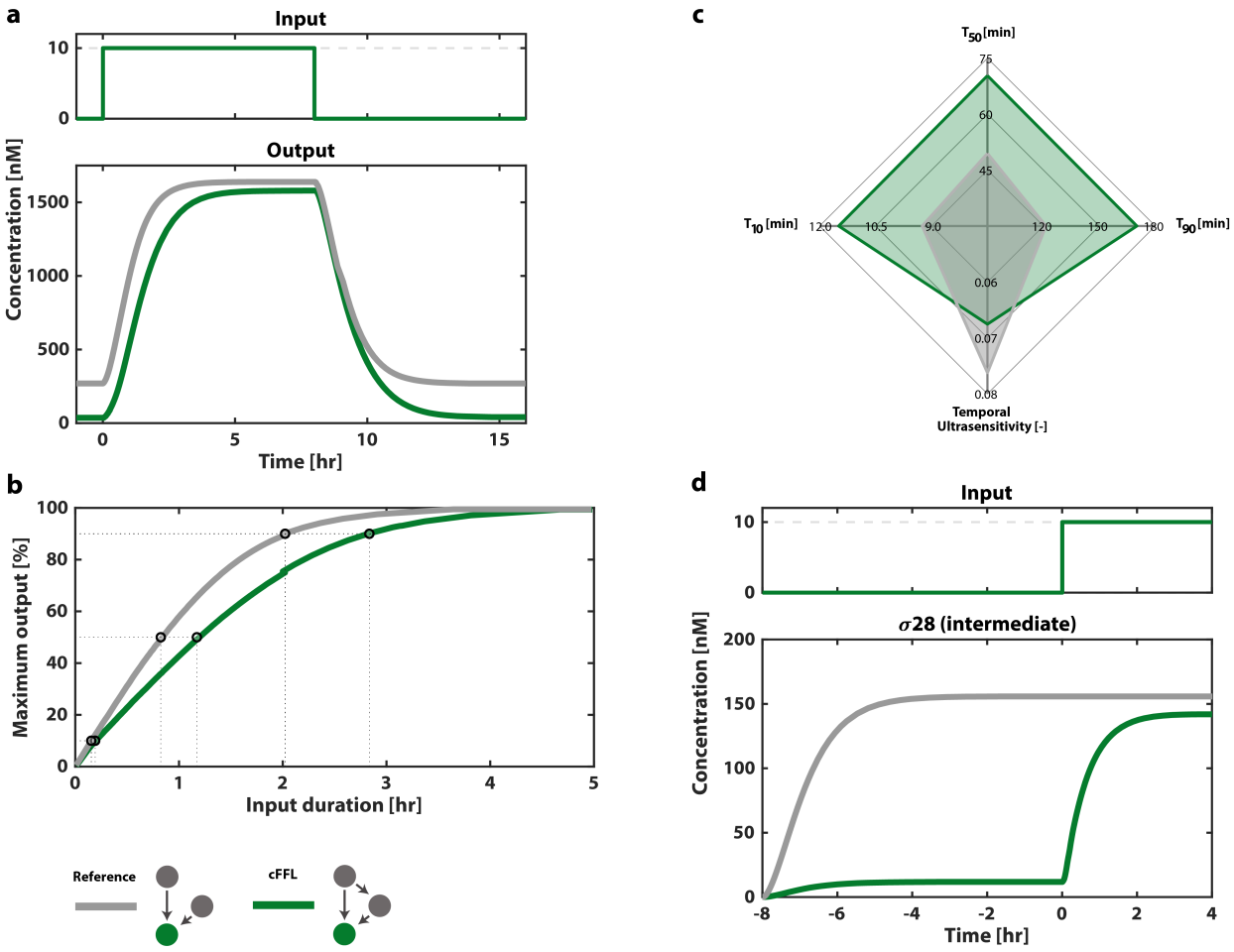

Figure 14: (a) GFP production for the trigger DNA input pulse shown in the upper panel.
(b) Quantification of kinetic filtering. The figure shows the relative maximal GFP production for a trigger input pulse duration described on the x-axis.
(c) Radar chart showing the kinetic filtering metrics of the cFFL and reference circuit.
(d) σ28 concentrations of both circuits prior to trigger input pulse.

As expected, this model also shows that the time to reach 10%, 50% and 90% of maximal output is shorter for the reference system than for the cFFL system, although difference in τ_{10} is minimal (Figure 14b and c). Furthermore, the TU score for the reference model is higher because the increase in fluorophore production is steeper. The results observed can be further explained by looking at the σ28 concentrations throughout the simulation (Figure 14d). As explained

before, production of RNA and protein species that are not regulated by trigger input can already be started before trigger input is fed to the system. Since σ28 production of the reference circuit is not regulated by trigger input, it can be seen that concentration levels of σ28 already rise to their maximum level before trigger input is fed to the circuit. In comparison, the increase of σ28 levels only minimally occurs in the cFFL, since σ28 can only be produced if the trigger is present in this circuit. Therefore, for the cFFL circuit, the σ28 concentration only increases strongly if the trigger impulse is started and that it takes about 2 hours to reach its maximum concentration. These results show that the difference in σ28 concentration between the two systems at the start of an input pulse might cause the difference in trigger times and temporal ultrasensitivity. For the reference system with higher σ28 concentrations, transcription of the output gene can already be started. Whenever the trigger input is fed to the system and the trigger DNA is transcribed, the trigger RNA can immediately bind to the toehold switch of the output gene and translation is initiated. However, this process could take longer for the cFFL model, since the transcription of the σ28 gene has to be initiated first.

3.3.2.2 *Batch circumstances*

The ODE model was also used to simulate an experiment in batch circumstances in order to show that an in vitro experiment in batch is not the ideal way to uncover the temporal behaviour of the feed-forward loop. The batch circumstances were simulated by neglecting the time prior to an input pulse that has been used in previous simulations. This alteration is similar to circumstances in batch experiments, because in these experiments all DNA species are also added at once to the IVTT mixture. The results in Figure 15 show that in these circumstances, the production of fluorophore over time looks very similar for both the reference and cFFL circuits. The trigger times are nearly the same and the rest of the kinetic filtering behaviour looks comparable. This confirms that model simulations or different experimental circumstances are necessary in order to discuss temporal behaviour of the coherent and coupled feed-forward loop. Therefore, the following chapter will use in vitro experiments in batch to discuss the possibility of in vitro coupled feed-forward loop construction and computer simulations are used to discuss temporal behaviour of the circuits at hand.

3.3.3 *Alternative experimental methods*

In vitro experiments in batch with the coherent/coupled feed-forward loop are not ideal to determine temporal behaviour of these circuits. In order to determine this behaviour more successfully, one would need a system with a steady expression of all components, which

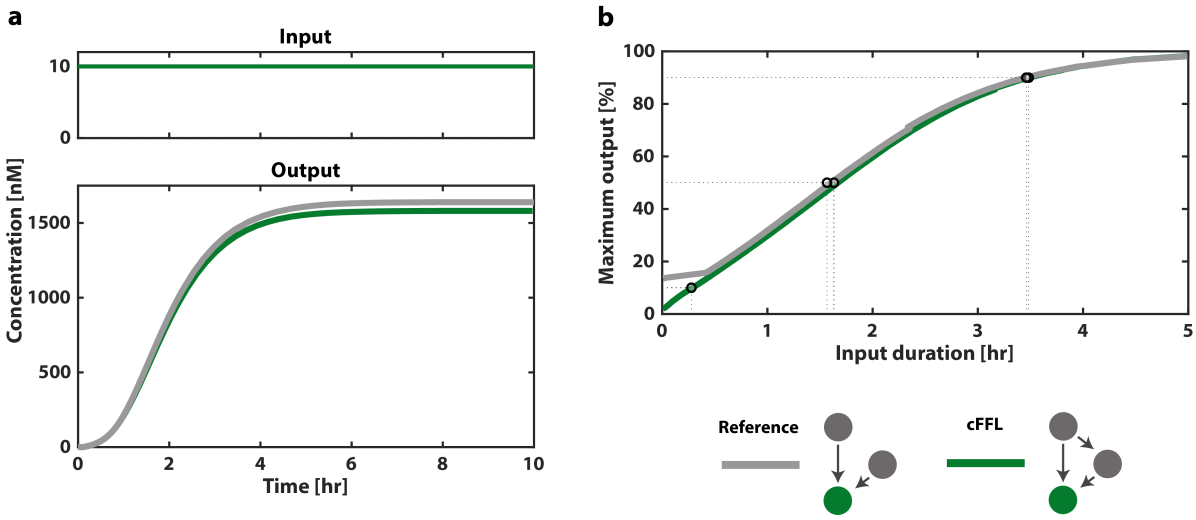

Figure 15: (a) GFP production for under in batch experiment circumstances. There has been no maturation of the reaction mixture prior to trigger DNA input.
(b) Quantification of kinetic filtering. The figure shows the relative maximal GFP production for a trigger input pulse duration described on the x-axis.

would show a direct perturbation in fluorophore production once an input (e.g. trigger DNA) is added to the system. As showed before, temporal behaviour could be simulated using ODE models, but in vitro testing would be preferred. One way to achieve these circumstances is by performing the experiments in a microfluidic device for TXTL expression designed by Niederholtmeyer et al. This microfluidic device consists of a ring-shaped reaction chamber in which in vitro reactions can be sustained for up to at least 24 hours [49]. The microfluidic flow reactor is connected to multiple inlets through which different components of the reaction mixture can be added to the system. The flow in the device and the mixing of the components in the reaction chamber can be controlled by pressure valves connected to a peristaltic pump [50]. Using this system, one can prepare and mature reaction mixtures inside the reaction chamber, and add an input to the system when desired. The platform can sustain reactions for longer periods of time. Moreover, since one can add input DNA strands at any moment, one can also observe temporal behaviour of the genetic circuits under investigation [49] [51] [50]. This platform would be very suitable to further test the temporal behaviour of the coherent feed-forward loop in vitro. However, it is still difficult to fully control and sustain IVTT reactions inside the microfluidic device. Due to time restrictions, it was not possible to include this method in this master thesis project.

Part II

COUPLED FEED-FORWARD LOOP

4

IN VITRO CHARACTERISATION OF THE COUPLED FEED-FORWARD LOOP

As has been demonstrated in the paper from Gorochowski et al., it is possible to couple two coherent feed-forward loops in 12 different ways. Possible couplings show circuits with one common input, one common output, or situations where the output of one cFFL acts as the input for the following cFFL. All circuits might possibly exhibit interesting behaviour when it comes to either time delay or noise cancellation, but due to time restrictions it is not possible to investigate all of them. As discussed before, it was decided to further investigate the fourth coupled feed-forward loop variant described in the paper from Gorochowski et al. (Figure 16). This circuit consists of two distinct inputs (X1 and X2) and two outputs (Z1 and Z2), sharing one common intermediate node (Y). This shared intermediate node couples the two coherent feed-forward loops concerned. One can imagine that because of this shared intermediate node, interesting temporal behaviour might occur for either one or both sides of the coupled FFL.

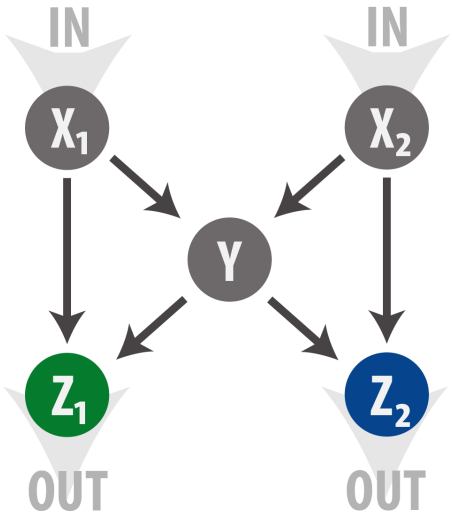

Figure 16: Schematic representation of coupled feed-forward loop topology. The coupled feed-forward loop consists of five nodes, of which two act as input (X1 and X2) and two act as output (Z1 and Z2). The middle node (Y) acts as the connection between the two separate coherent feed-forward loops.

When either one of the inputs is given to the circuit, production of the intermediate node transcription factor is activated. For the cFFL, it takes time to produce this transcription factor and therefore,

production of the output of the circuit is delayed. However, when the intermediate node in the coupled feed-forward loop has already been stimulated, its product is already present for later instants. Now, when the second input is fed into the system, it is hypothesised that it will eventually take less time to generate the second output. This would mean that time delay in the production of the second output is diminished in comparison to the first output.

Since the in vitro experiments with the coupled feed-forward loop are done in batch, it is unfortunately not possible to feed different inputs to the system at different time instances. Therefore, it will not be possible to learn about specific and changing time delays from the in vitro implementation of this system. However, this behaviour could possibly be examined by using computer simulations, which will be further investigated in Chapter 5.

Although temporal behaviour cannot be investigated using the IVTT system, it is interesting to explore whether it is possible to construct a coupled feed-forward loop system in vitro. The following chapter will further discuss the topology of the circuit and its implementation in vitro using the DNA strands considered in Chapter 2.

4.1 COUPLED FEED-FORWARD LOOP TOPOLOGY

The coupled feed-forward loop topology that will be investigated in this chapter is shown in Figure 16. Chapter 2 described the characteristics of the coherent feed-forward loop and showed how it can be implemented in vitro. Furthermore, it was discussed how one can construct two different cFFLs with distinct inputs and outputs. The distinct circuits discussed in Chapter 2 will be build upon in this chapter and will be coupled to form one genetic circuit. The coupled feed-forward loop circuit will consist of two different trigger/switch pairs (variant 2.1 and 10) and two different fluorescent outputs (eGFP and CFP).

4.1.1 *Implementation*

The final implementation of the coupled feed-forward loop in vitro is displayed in Figure 17. This coupled feed-forward loop consists of six different linear DNA constructs and eventually produces two distinct outputs. Furthermore, σ28 is used as the shared intermediate product in order to couple the two coherent feed-forward loops. The intermediate node is represented by two DNA constructs, containing both a different toehold switch, but with a common σ28 gene.

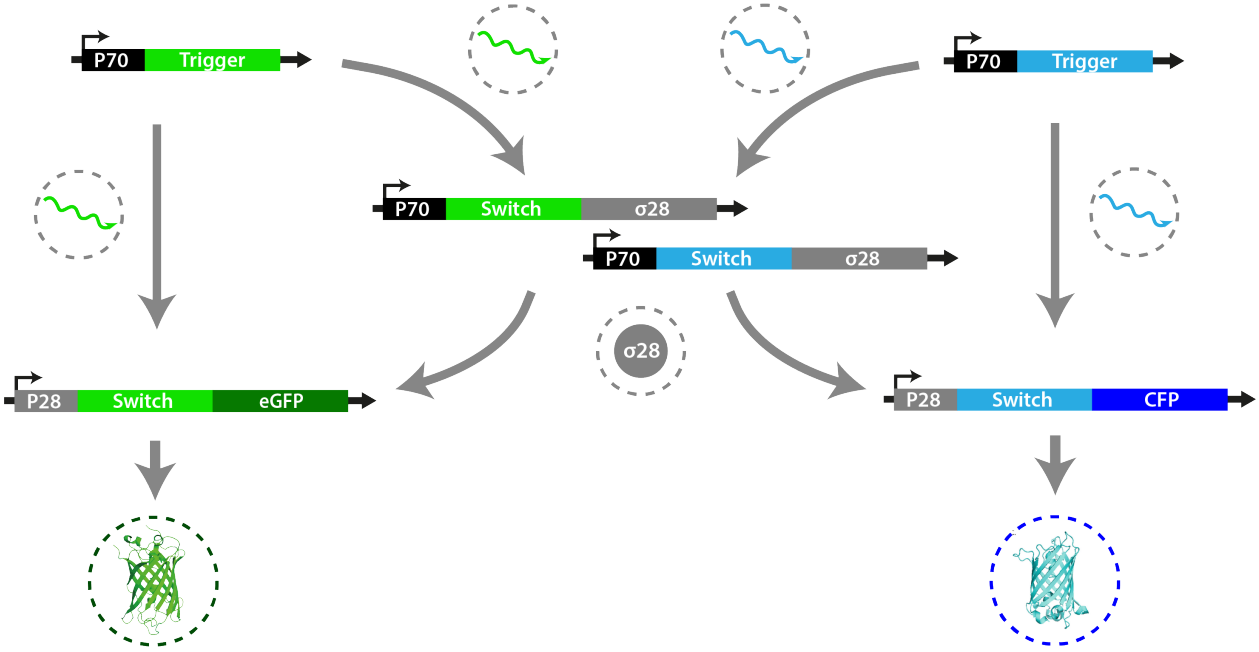

Figure 17: Schematic representation of the implementation of a coupled feed-forward loop in vitro. This genetic circuit is a combination of the two coherent feed-forward loops described in Section 4.3.3. The coupled feed-forward loop genetic circuit makes use of two distinct trigger/switch pairs (variants 2.1 and 10) and produces two different outputs (eGFP and CFP). The intermediate node of the circuit is represented by two DNA strands, both responsible for producing the σ28 transcription factor.

4.2 METHODS

The methods for the coupled feed-forward loop in vitro experiments are the same as for the coherent feed-forward loop experiments. All experiments with the coupled feed-forward loop are executed in triplo. For the platereader experiments, we use the following DNA construct concentrations: 10 nM for both trigger constructs and 10 nM for both output constructs. The left-side σ28 producing construct has a concentration of 0.6 nM and the right-side construct of 0.8 nM.

Since we need to measure the emission of two fluorophores at the same time, we use a platereader that can excite and detect fluorophores at two different wavelengths. The excitation and emission wavelengths used for the detection of eGFP and CFP are the following:

- eGFP - Excitation: 485 nm, Emission: 530 nm
- CFP - Excitation: 433 nm, Emission: 488 nm

Experiments are run for 16 hours and fluorescence is measured every 5 minutes.

4.2.1 *Calibration and correction*

Normally, the excitation and emission spectra of eGFP and CFP show overlap. Therefore, the excitation and emission wavelengths of the platereader were chosen as to minimize the effect of measuring fluorescence from the other fluorophore. However, it is not possible to reduce this effect completely. Therefore, it was decided to create a 3D calibration curve which can convert the arbitrary units measured by the platereader into fluorophore concentration, and correct for spectral overlap and background noise of the platereader. We created a dilution range of pure samples of eGFP and CFP fluorophore and measured these on the platereader. Thereafter, the intensities measured were plotted against the known concentrations of eGFP and CFP. In order to convert and correct the measured intensities, the data was fitted through the following equations:

$$I_{eGFP} = a_1 * C_{eGFP} + b_1 * C_{CFP} + d_1$$

$$I_{CFP} = a_2 * C_{CFP} + b_2 * C_{eGFP} + d_2$$

Variable I stands for the measured intensity (in a.u.) for either the eGFP or CFP channel. Variable C stands for the known absolute concentration (in μM) of fluorophores eGFP and CFP.

The system of equations is solved for the concentrations eGFP and CFP to retrieve a converted and corrected measurement.

4.3 RESULTS AND DISCUSSION

The coupled feed-forward loop has been tested in vitro and its performance been analysed for multiple different situations. The experiments below will show the necessity of certain components of the genetic circuit and it will be discussed how these components influence the behaviour of the system.

4.3.1 *Comparison between coupled feed-forward loop and coherent feed-forward loop*

The absolute fluorophore production of the coupled feed-forward loop in vitro had to be determined first, in order to check whether this performance was still similar to the performance of the separate coherent feed-forward loops described in 2. The first thing we had to check when constructing and testing the coupled feed-forward loop, was whether the performance of the genetic circuit in vitro is similar to the performances of the separate coherent feed-forward loops. This comparison had to be performed, because it might have occured that increasing the absolute concentration of DNA constructs added

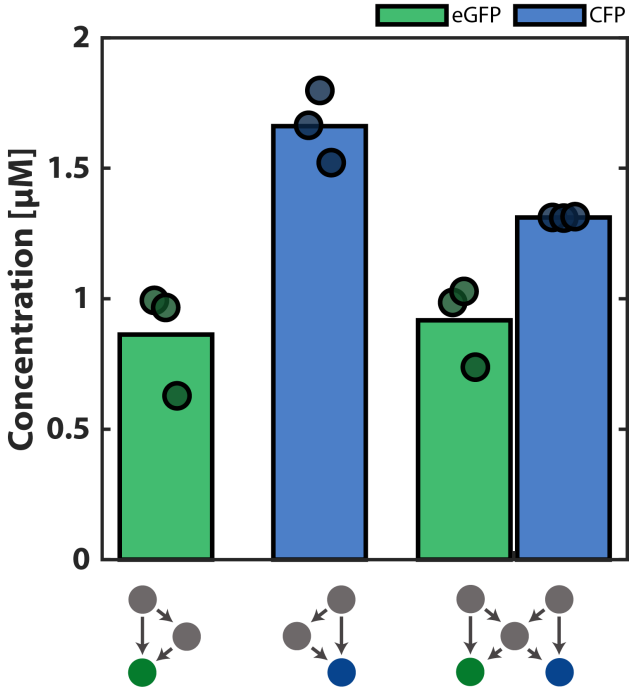

Figure 18: Performance of the coupled feed-forward loop compared to two separate coherent feed-forward loops. The total DNA construct concentration increased from 20.6 - 20.8 nM for a single cFFL to 41.4 nM for the coupled feed-forward loop.

to the IVTT mixture could have influenced the production of fluorophores. Fortunately, Figure 18 shows that this was not the case. In the experiments from Chapter 2, a single cFFL genetic circuit consisted of 20.6 - 20.8 nM of DNA constructs. Subsequently, a full coupled feed-forward loop in vitro consists of the doubled amount, 41.4 nM per circuit. Figure 18 shows that the production of fluorophores stays approximately the same for a single cFFL as for the coupled FFL. The production of CFP slightly decreases in the coupled feed-forward loop structure. This decrease might be caused by the increase of total DNA construct concentration.

It was observed in different experiments that increasing the total DNA construct concentration further actually does influence the production of fluorophore (data not shown). For cases where the output construct concentration was increased to 12 nM or higher, the total fluorophore production decreased. This implies that the TXTL mixture has a production limit and that resources (like nucleotides and amino acids) are depleted more for higher DNA concentrations [27].

4.3.2 *Influence of trigger inputs on fluorophore production*

Next, the influence of the presence and absence of the input trigger constructs on the production of both fluorophores was investigated. The findings are shown in Figure 19, where panel a shows the absolute fluorophore production and panel b describes the relative production compared to the full coupled FFL.

As can be seen in Figure 19, the production of fluorophores drastically decreases when the corresponding trigger is removed from the circuit. This event is observed when the eGFP trigger is absent, showing a decrease of the eGFP production with a factor of 4. The same is true for the CFP trigger, where the CFP production decreases with a factor of approximately 3. Furthermore, when one of two triggers is removed, the fluorophore production of the opposing side slightly increases. This increase might happen because when the trigger of one side is absent, the mRNA and protein production of this side are also omitted. This omission leads to a surplus of resources of the IVTT mixture, now possibly used by the activated side of the coupled FFL. When both trigger inputs are absent, approximately the same ON/OFF ratios are achieved. The still remaining fluorophore production might be caused by the leakage of the σ28 producing construct and toehold switches discussed in Sections 2.3.2.2 and 4.3.3, leading to fluorophore production even without a trigger input.

4.3.3 *Influence of σ28 on fluorophore production*

The following objective was to discover whether the production of one σ28 producing construct can completely replace the function of the other construct when absent. It is hypothesised that this replacement occurs because both sides of the coupled FFL use σ28 as transcription factor. However, it was unknown whether there would be enough transcription factor for transcription at both sides of the genetic circuit. Figure 20 shows that one σ28 producing construct can take over the function of the other construct when absent. As can be observed in this figure, the fluorophore production remains approximately the same for all three situations. Furthermore, as also discussed in Section , fluorophore production is completely diminished when there is no σ28 present, proving the necessity of this transcription factor for transcription of the output DNA strands.

Another aspect tested was whether the total concentration of σ28 producing constructs influenced the performance of the coupled FFL. Situations were tested in which one of the intermediate constructs was removed and the concentration of the other intermediate construct was doubled. The figure in Appendix C.1 shows that the in-

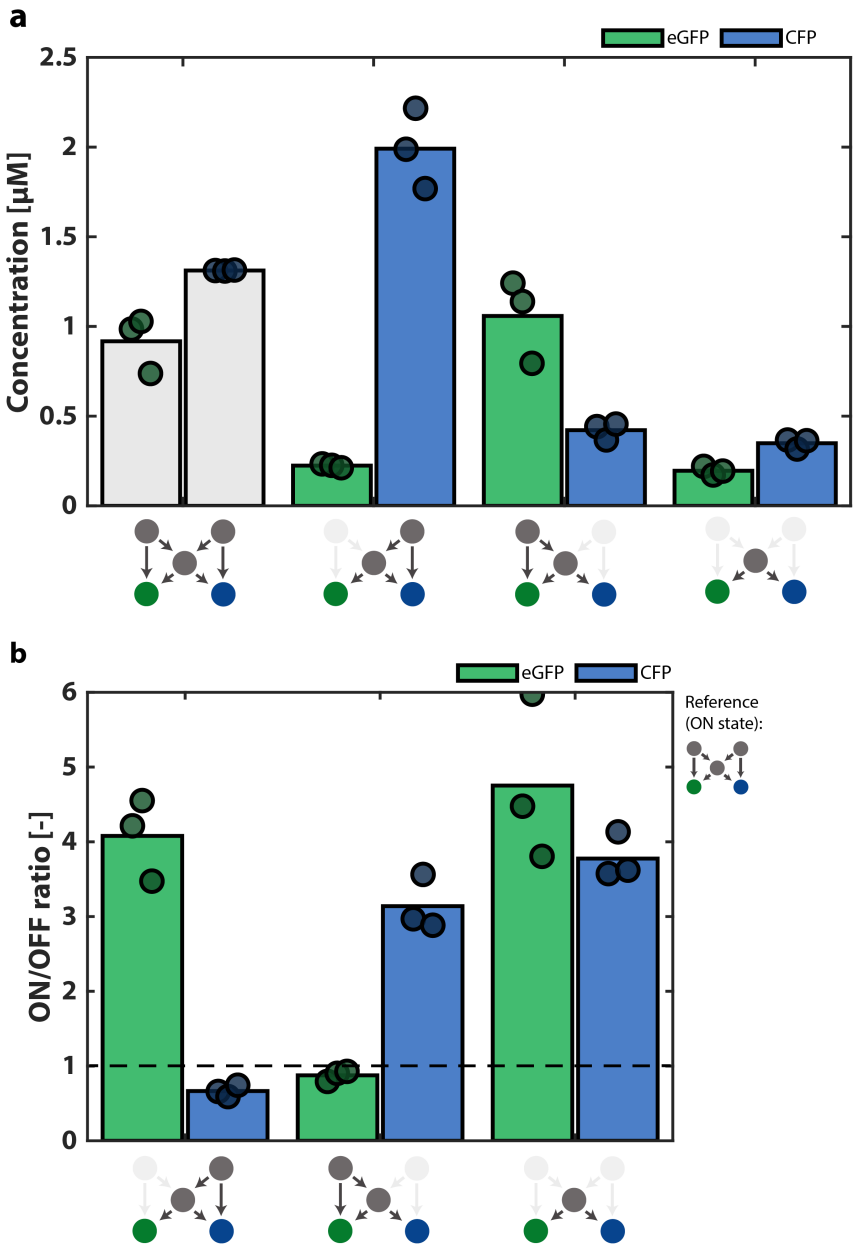

Figure 19: (a) eGFP and CFP production (in μM) of the coupled feed-forward loop in presence and absence of the trigger inputs.
(b) ON/OFF ratios for the coupled feed-forward loop. The ON state is the complete coupled FFL. The OFF-state is a structure where one or both of the trigger inputs are absent, as shown in the schematics underneath the bars.

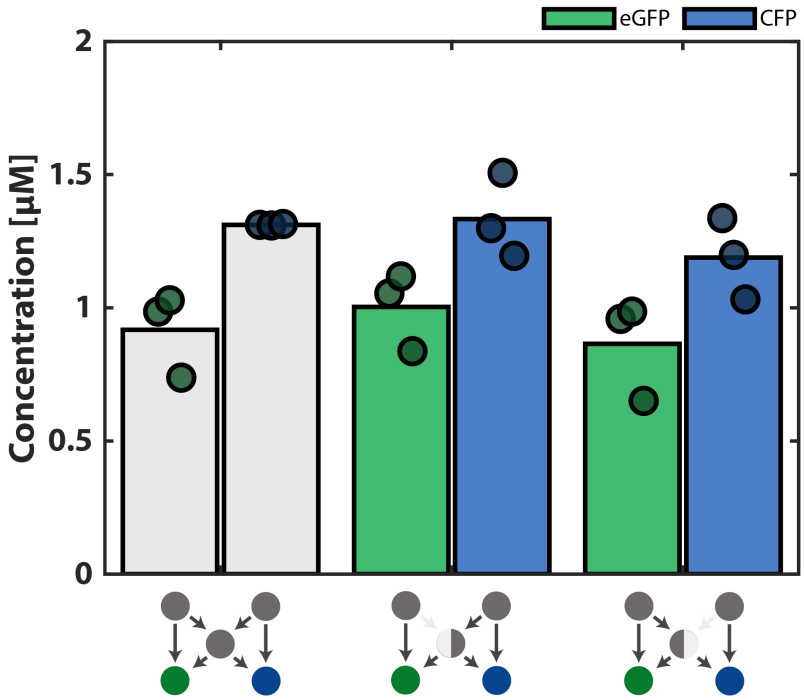

Figure 20: eGFP and CFP production (in μM) of the coupled feed-forward loop in presence and absence of σ28 producing constructs. A half intermediate node means that the DNA construct of that side is absent.

crease in DNA construct concentration has no considerable influence on the production of both fluorophores.

4.3.4 *Absence of both trigger and σ28*

The following in vitro experiment on the coupled feed-forward loop was done to confirm the functions of the triggers and σ28 transcription factor within the coupled FFL (Figure 21). Two of the entries can be recognised from Figure 20, where it was shown that the production of σ28 of one of the intermediate constructs can take over the function of the second absent construct, leading to full performance of the circuit. In Figure 21 it is shown that trigger input is the most crucial element for fluorophore production of its corresponding side. As can be observed in this figure, even when there is still σ28 present in the system, the inactive toehold switch will mostly halt the translation of the fluorophore gene. The ON/OFF ratio for these situations is on average 4.5 and the fluorophore production of the second half of the circuit is only slightly influenced. Again, increase in fluorophore production might be caused by an abundance in IVTT resources that are normally not available.

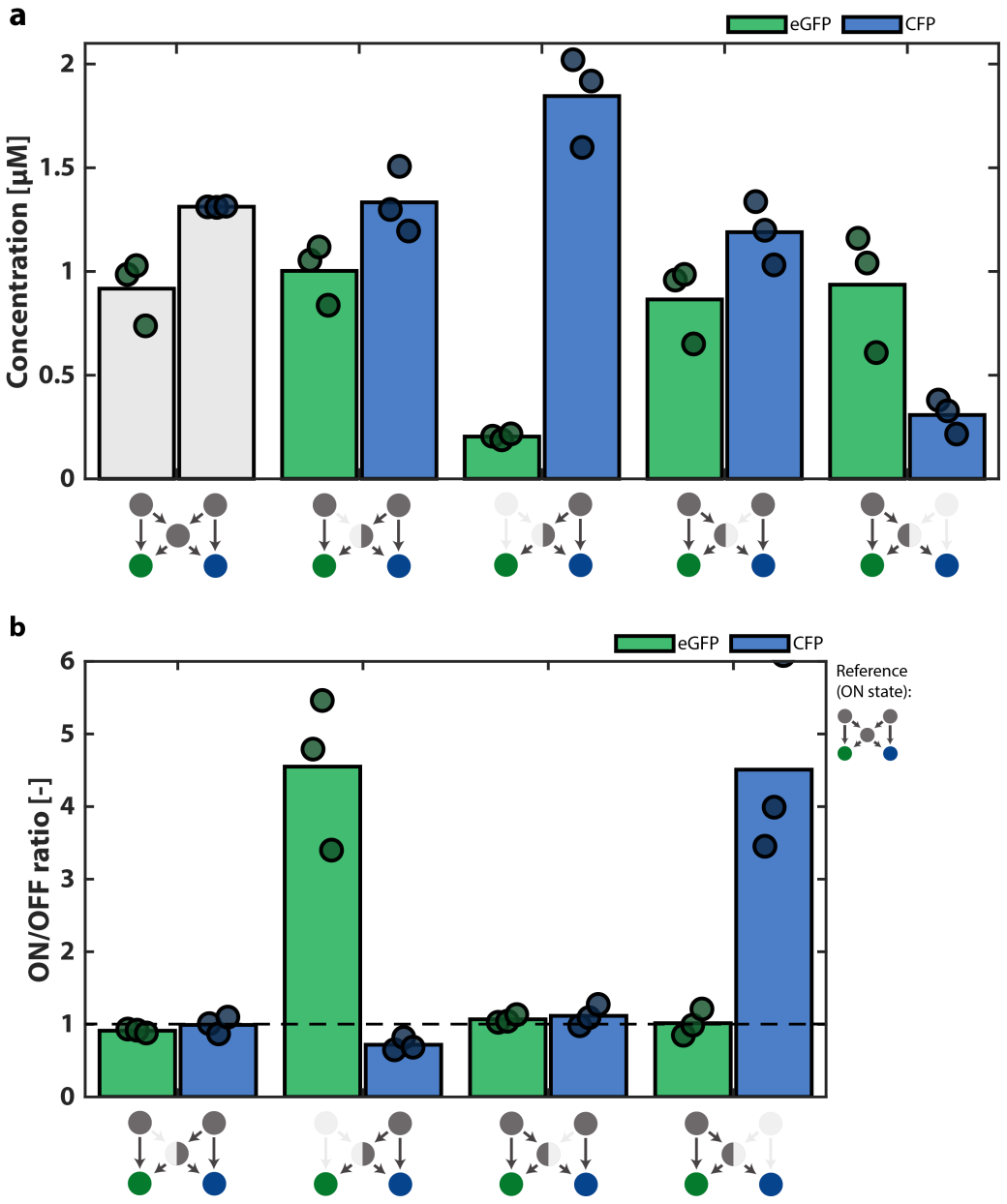

Figure 21: (a) eGFP and CFP production (in µM) of the coupled feed-forward loop in presence and absence of the trigger inputs and σ28 producing constructs.
(b) ON/OFF ratios for the coupled feed-forward loop. The ON state is the complete coupled FFL. The OFF-state is a structure where one or more of the DNA constructs are absent, as shown in the schematics underneath the bars.

4.3.5 *Incomplete coupled feed-forward loops still produce fluorophore*

The last in vitro experiment on the coupled feed-forward loop was done to demonstrate that correct trigger/switch pairing is crucial for the functioning of the circuit. Furthermore, it confirms that the σ28 transcription factor is universal for both sides of the circuit (Figure 22). This figure shows that the circuit can still produce fluorophore when the trigger and fluorophore construct of one side of the circuit are combined with the trigger and σ28 producing construct of the other side of the circuit. The performance of the circuit is even comparable to the full coupled feed-forward loop. The decrease in CFP production might again be caused by the decrease in σ28 producing DNA construct concentration (here 0.6 nM as opposed to 0.8 nM in other situations).

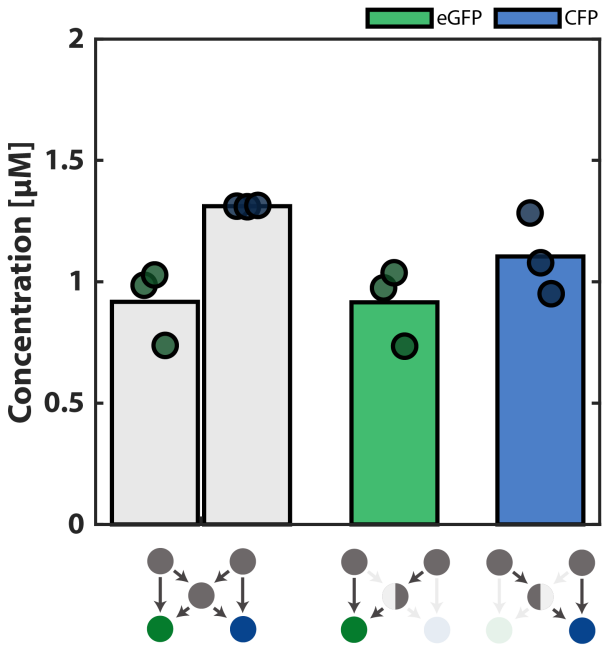

Figure 22: eGFP and CFP production for cases where trigger and fluorophore construct of one side, and trigger and σ28 construct of the other side are combined.

5

IN SILICO CHARACTERISATION OF THE COUPLED FEED-FORWARD LOOP

5.1 ORDINARY DIFFERENTIAL EQUATION MODEL FOR COUPLED FEED-FORWARD LOOP

The last objective of this project was to construct an ODE model for the coupled feed-forward loop. The experiments from Chapter 4 have shown that it is indeed possible to construct this genetic circuit in vitro, but it is difficult to determine the temporal behaviour of the circuit. To further explore this temporal behaviour, one could make use of a microfluidic device described by Niederholtmeyer et al., or construct a mathematical model. It was chosen to do the latter and the results generated by this mathematical motdel are discussed in this chapter. In order to quantify temporal behaviour and kinetic filtering of the coupled feed-forward loop, the methods discussed in Section 3.1 will also be used for the coupled FFL model.

5.2 METHODS AND EQUATIONS

5.2.1 *Coupled feed-forward loop model*

The ODE model of the coupled feed-forward loop is also a model that represents the DNA, RNA and proteins that are present in the in vitro experiments from Chapter 4. The trigger DNA is used as input of the system and when present, can activate the production of eGFP and CFP, the output of the system. The other DNA concentrations are constant and have the same values as in the in vitro experiments. Furthermore, the model consists of 13 ordinary differential equations that represent the RNA and protein species. The model is constructed in the exact same way as the expanded coherent feed-forward loop model, except that the coupled FFL model describes more different DNA, RNA and protein species.

$$\frac{d}{dt}Tr_1 = k_{ts,Tr} * Tr_{1;DNA} - k_{on,Tr_1,Sw_{1,1}} * Tr_1 * Sw_{1,1} + k_{off,Tr_1,Sw_{1,1}} * Tr_1 \cdot Sw_{1,1} - k_{on,Tr_1,Sw_{1,2}} * Tr_1 * Sw_{1,2} + k_{off,Tr_1,Sw_{1,2}} * Tr_1 \cdot Sw_{1,2} - \delta_{RNA} * Tr_1$$

$$\frac{d}{dt}Tr_2 = k_{ts,Tr} * Tr_{2;DNA} - k_{on,Tr_2,Sw_{2,1}} * Tr_2 * Sw_{2,1} + k_{off,Tr_2,Sw_{2,1}} * Tr_2 \cdot Sw_{2,1} - k_{on,Tr_2,Sw_{2,2}} * Tr_2 * Sw_{2,2} + k_{off,Tr_2,Sw_{2,2}} * Tr_2 \cdot Sw_{2,2} - \delta_{RNA} * Tr_2$$

$$\frac{d}{dt}Sw_{1,1} = k_{ts,Sw} * Sw_{1,1}\_S_{28;DNA} - k_{on,Tr_1,Sw_{1,1}} * Tr_1 * Sw_{1,1} + k_{off,Tr_1,Sw_{1,1}} * Tr_1 \cdot Sw_{1,1} - \delta_{RNA} * Sw_{1,1}$$

$$\frac{d}{dt}Sw_{2,1} = k_{ts,Sw} * Sw_{2,1}\_S_{28;DNA} - k_{on,Tr_2,Sw_{2,1}} * Tr_2 * Sw_{2,1} + k_{off,Tr_2,Sw_{2,1}} * Tr_2 \cdot Sw_{2,1} - \delta_{RNA} * Sw_{2,1}$$

$$\frac{d}{dt}Tr_1 \cdot Sw_{1,1} = k_{on,Tr_1,Sw_{1,1}} * Tr_1 * Sw_{1,1} - k_{off,Tr_1,Sw_{1,1}} * Tr_1 \cdot Sw_{1,1} - \delta_{RNA} * Tr_1 \cdot Sw_{1,1}$$

$$\frac{d}{dt}Tr_2 \cdot Sw_{2,1} = k_{on,Tr_2,Sw_{2,1}} * Tr_2 * Sw_{2,1} - k_{off,Tr_2,Sw_{2,1}} * Tr_2 \cdot Sw_{2,1} - \delta_{RNA} * Tr_2 \cdot Sw_{2,1}$$

$$\frac{d}{dt}S_{28} = k_{tl,S_{28}} * (Tr_1 \cdot Sw_{1,1} + Tr_2 \cdot Sw_{2,1}) + \epsilon_{S_{28}} * (Sw_{1,1} + Sw_{2,1}) - \delta_P * S_{28}$$

$$\frac{d}{dt}Sw_{1,2} = k_{ts,Sw} * P_{28}\_Sw_{1,2}\_GFP_{;DNA} * \frac{S_{28}^H}{K_{S_{28}}^H + S_{28}^H} + \epsilon_{Sw_{1,2}} * P_{28}\_Sw_{1,2}\_GFP_{;DNA} - k_{on,Tr_1,Sw_{1,2}} * Tr_1 * Sw_{1,2} + k_{off,Tr_1,Sw_{1,2}} * Tr_1 \cdot Sw_{1,2} - \delta_{RNA} * Sw_{1,2}$$

$$\frac{d}{dt}Sw_{2,2} = k_{ts,Sw} * P_{28}\_Sw_{2,2}\_GFP_{;DNA} * \frac{S_{28}^H}{K_{S_{28}}^H + S_{28}^H} + \epsilon_{Sw_{2,2}} * P_{28}\_Sw_{2,2}\_GFP_{;DNA} - k_{on,Tr_2,Sw_{2,2}} * Tr_2 * Sw_{2,2} + k_{off,Tr_2,Sw_{2,2}} * Tr_2 \cdot Sw_{2,2} - \delta_{RNA} * Sw_{2,2}$$

$$\frac{d}{dt}Tr_1 \cdot Sw_{1,2} = k_{on,Tr_1,Sw_{1,2}} * Tr_1 * Sw_{1,2} - k_{off,Tr_1,Sw_{1,2}} * Tr_1 \cdot Sw_{1,2} - \delta_{RNA} * Tr_1 \cdot Sw_{1,2}$$

$$\frac{d}{dt}Tr_2 \cdot Sw_{2,2} = k_{on,Tr_2,Sw_{2,2}} * Tr_2 * Sw_{2,2} - k_{off,Tr_2,Sw_{2,2}} * Tr_2 \cdot Sw_{2,2} - \delta_{RNA} * Tr_2 \cdot Sw_{2,2}$$

$$\frac{d}{dt}GFP = k_{tl,GFP} * Tr_1 \cdot Sw_{1,2} + \epsilon_{GFP} * Sw_{1,2} - \delta_P * GFP$$

$$\frac{d}{dt}CFP = k_{tl,CFP} * Tr_2 \cdot Sw_{2,2} + \epsilon_{CFP} * Sw_{2,2} - \delta_P * CFP$$

The use of species and parameter names is the same as in Chapter 3 and is expanded further for the coupled feed-forward loop model. The parameter values can be found in Appendix B. These values are retrieved from literature and some are slightly adapted to match observations from the in vitro experiment on fluorophore concentration and time-scale.

5.2.2 *Simulation*

Again, the models are simulated and solved using MATLAB, in the same way as the models discussed in Chapter 3. Furthermore, the kinetic filtering metrics are also determined in the same way as described before. The difference between the coherent feed-forward loop models and the coupled feed-forward loop model is that the latter has two inputs and two outputs. Therefore, it is also possible to feed inputs to model at the same time or at different time instances. The model here is also run several times, where each time the final concentrations of the previous run are used as initial values of the next run. This way, it is possible to add multiple inputs to the model at different times. The DNA concentrations used in the simulation are the same as in the in vitro experiments from Chapter 4. Similar to the in vitro experiments, in some situations one or a few DNA constructs are removed from the system by setting their initial DNA concentrations to zero. Lastly, in order to create the trigger time heatmaps of this chapter, the model is run 900 times for 30 different σ28 producing construct concentrations.

5.3 RESULTS AND DISCUSSION

5.3.1 *Full coupled feed-forward loop*

The first simulation done with the coupled feed-forward loop model is one where both trigger inputs are fed to the system. Also this model is run for 8 hours prior to the first impulse to ensure that any species that do not need trigger activation can be transcribed or translated. We can model the production of eGFP and CFP by the coupled feed forward loop upon introduction of a trigger DNA construct. Furthermore, it can be determined how long an input pulse should be present in order to activate one of the two sides of the circuit for 10%, 50% (trigger time), and 90%. Figure 23 shows the results from these simulations. As can be seen in this figure, kinetic filtering metrics are very similar for eGFP and CFP and the trigger time is approximately 1 hour.

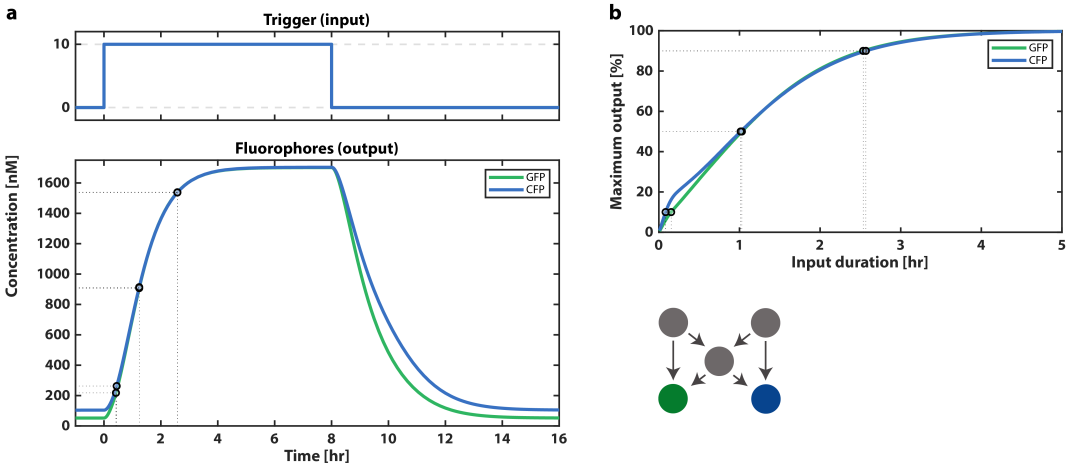

Figure 23: (a) Production of eGFP and CFP upon circuit activation by both trigger DNA inputs. Circles on the trajectory mark the moment that the fluorophore concentration reaches 10%, 50% and 90% of its maximum.
(b) Relative maximal production of eGFP and CFP for multiple trigger DNA input durations. Inputs are given to the system simultaneously.

5.3.2 *Coupled feed-forward loop with one trigger input*

Similar to the in vitro experiments, the model was also tested for situations where only one trigger is present. The results for these simulations are shown in Figure 24. The parameters ϵ_{GFP} and ϵ_{CFP} have been altered to achieve similar ON/OFF ratios as in the in vitro experiments. Therefore, it can be observed that the ON/OFF ratio for eGFP is approximately 5 and the ON/OFF ratio of CFP is slightly smaller, approximately 3. Furthermore, as can be seen in Figure 24, the maximum concentrations of both eGFP and CFP are lower when only one trigger is present, compared to the situation with two triggers. With one trigger input, only one of the intermediate RNA species can be translated, causing a decrease in the total σ28 concentration. This probably causes the overall decrease in fluorophore production, showing a larger effect on eGFP than on CFP.

5.3.3 *Alternating inputs under different circumstances*

As was discussed in the introduction of this project, it would be interesting to test how giving two inputs at different moments would effect the fluorophore production and temporal behaviour of the genetic circuit. The first insights in this matter are shown in Figure 25. Panel a shows a simulation for a full coupled FFL in which the eGFP trigger is given to the system first. Once the eGFP concentration reaches its maximum, the second impulse with the CFP trigger

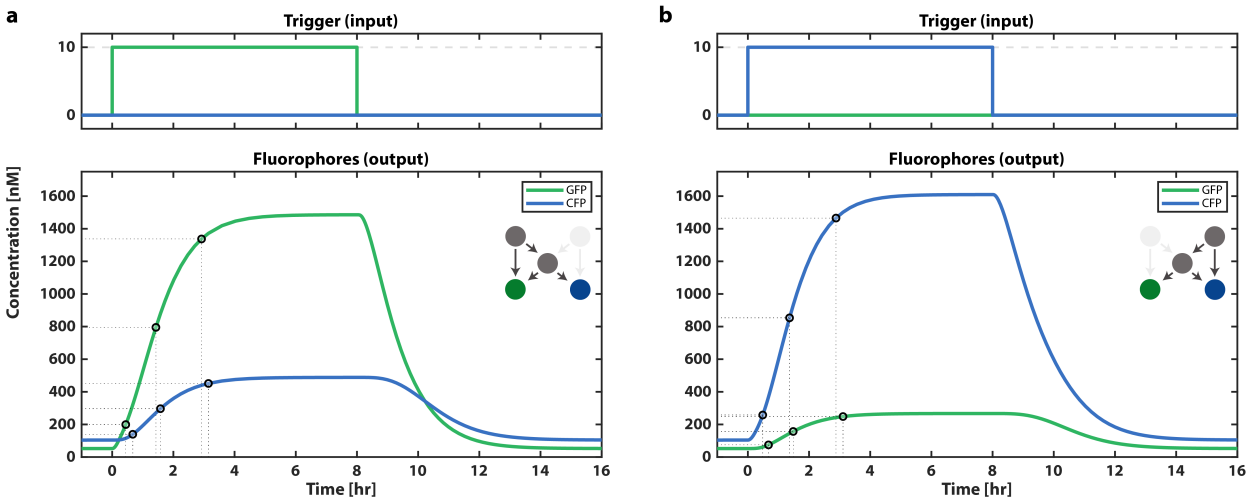

Figure 24: (a) Production of eGFP and CFP upon addition of the left-side trigger DNA to the circuit.
(b) Production of eGFP and CFP upon addition of the right-side trigger DNA to the circuit.

is given to the system. Upon the addition of the second trigger, also the production of CFP makes a sharp increase. Furthermore, it can be observed that when one of the two triggers is given to the system, the fluorophore production of the opposing side of the circuit also increases. This off-target production is due to the simulated leakage in the translation of the eGFP and CFP genes. Moreover, τ_{50} and τ_{90} are smaller for the CFP production than for the eGFP production. The decrease in trigger time is probably caused by the fact that σ28 is already present in the system once the second trigger input is given.

Furthermore, a situation was tested in which the right-side σ28 producing construct is left out of the coupled FFL circuit. Figure 25b shows that in this situation, the difference in trigger times between eGFP and CFP become larger and the CFP τ_{50} and τ_{90} have decreased. First of all, the shorter CFP trigger times (compared to eGFP) are again caused by the fact that the eGFP trigger input is added to the circuit first. The σ28 transcription factor is already present and no additional time is needed to produce this transcription factor once the second trigger is added. Secondly, an absolute decrease in CFP trigger time is observed in Figure 25b, which is caused by the removal of the right-side intermediate construct. Since this construct also has a toehold switch incorporated, it normally binds a large portion of the trigger available to open the switch. However, now that the construct is removed, all available trigger RNA can bind to the toehold switch in front of the CFP gene. Because a higher concentration of CFP trigger is present for this task, it is thought that this causes the decrease in trigger times shown in Figure 24. The same phenomenon is observed for situations where the CFP trigger is added to the system

first and where the left-side intermediate construct is removed from the circuit. The results of this simulation can be found in Appendix C.2.

In the following section it will be discussed further what influence the intermediate constructs and the order of input pulses have on the trigger times and temporal ultrasensitivity of the circuit.

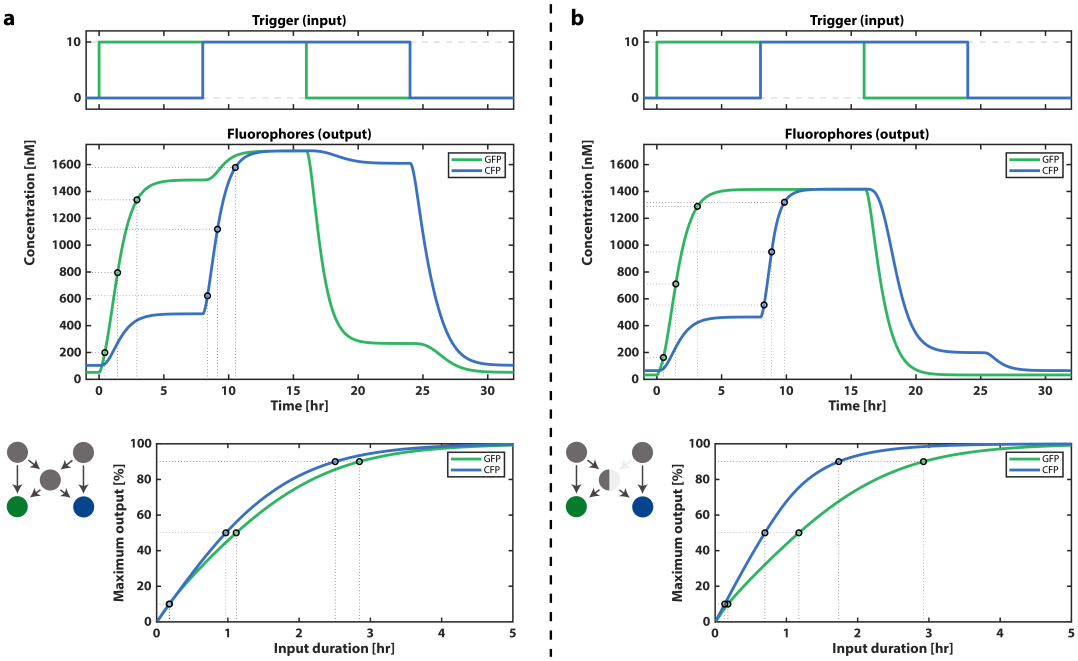

Figure 25: (a) Production of eGFP and CFP upon addition of first the left-side trigger DNA and subsequently the right-side trigger DNA to the full coupled FFL circuit.
(b) Production of eGFP and CFP upon addition of first the left-side trigger DNA and subsequently the right-side trigger DNA to a version of the coupled FFL circuit where the right-side σ28 producing construct is removed.

5.3.4 *The influence of the intermediate node and input order on time delay*

In the previous section we saw that the order of trigger inputs and the presence (or absence) of intermediate DNA constructs influences the trigger times and temporal ultrasensitivity of the production of both fluorophores. In order to test this more thoroughly, multiple combinations of input order and DNA construct removal have been simulated. The results of these simulations can be found in Figure 26. Each radar chart shows three planes, each representing an order in which the inputs are given to the system. The grey plane shows the situation where both DNA triggers are added at the same moment. Green represents a situation in which the eGFP trigger is given prior to the CFP trigger and the blue plane represents the opposite. The radar charts show four metrics of the fluorophore production; trigger

times of eGFP and CFP production, and the temporal ultrasensitivity of both activations.

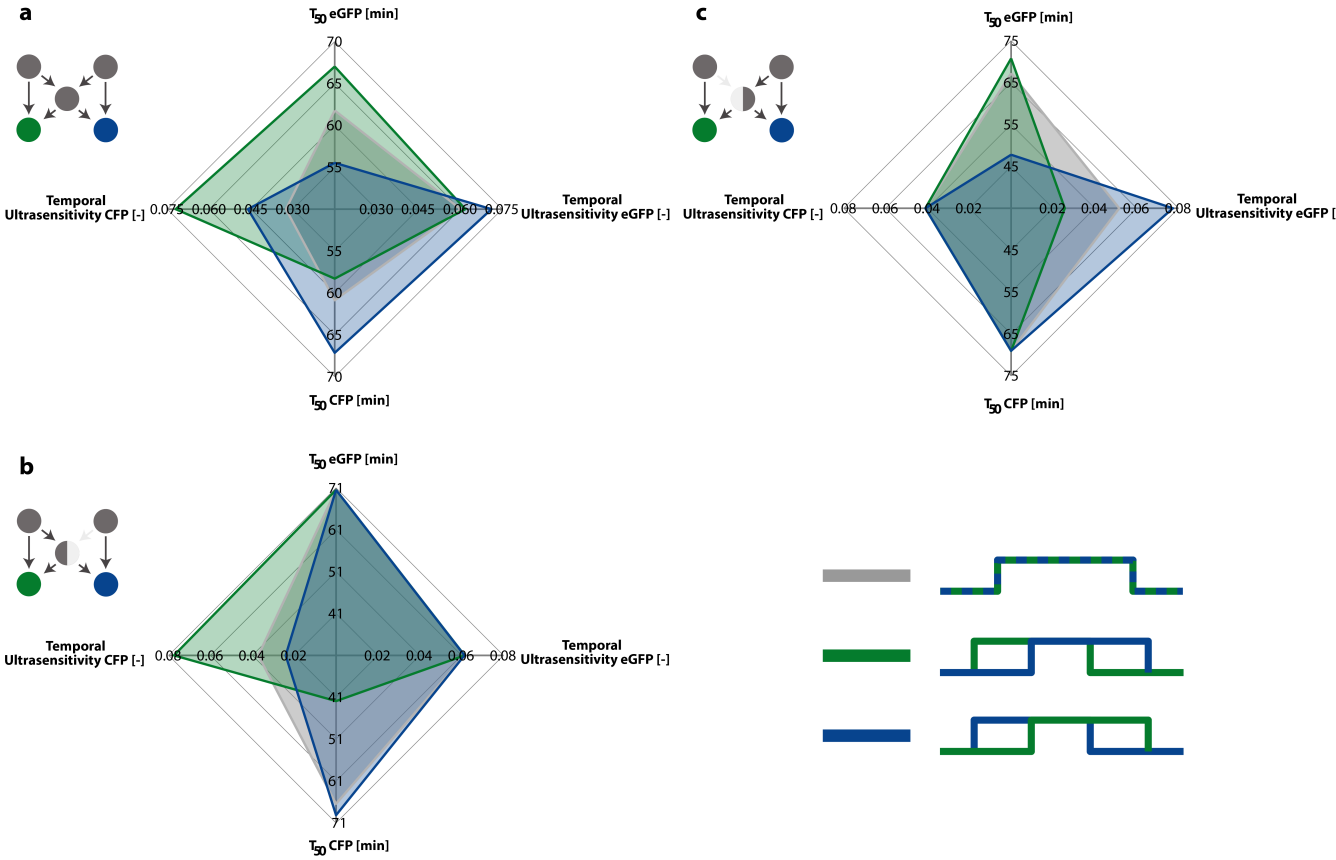

Figure 26: Radar charts showing eGFP and CFP trigger times and temporal ultrasensitivity for three different orders of trigger input. (a) Full coupled FFL circuit. (b) Coupled FFL circuit without right-side intermediate construct. (c) Coupled FFL circuit without left-side intermediate construct.

We have shown that the order in which trigger inputs are given to the system, influences the trigger times of both eGFP and CFP production. For the situation that the eGFP trigger is given to the system first, the eGFP trigger time is larger than the CFP trigger time (Figure 26a). These trigger times are also, respectively, longer and shorter than the trigger times for a simultaneous addition of triggers. The same is true for the situation where first the CFP trigger and then the eGFP trigger are added, but there the CFP trigger time gets longer and the eGFP trigger time gets shorter.

Removal of one of two intermediate DNA constructs selectively influences trigger times and temporal ultrasensitivty, which is shown in Figure 26b and c. First, the results for the situation where the right-side σ28 producing construct has been removed will be discussed

(Figure 26b). As can be seen in Figure 26b, the trigger time of the eGFP production is not influenced by the order in which the inputs are fed to the circuit. This lack of influence can be explained by the fact that σ28 production can be only be initiated if the eGFP trigger is present. Therefore, the order of inputs does not seem to matter and eGFP trigger times are the same in each situation. Furthermore, trigger times are larger compared to the situation with a complete coupled feed-forward loop because with two intermediate DNA constructs, more σ28 is produced.

On the other hand, CFP trigger times are influenced by the order of inputs when the right-side intermediate DNA construct is missing. As can be seen in Figure 26a and b, the CFP trigger times are similar in the case where both inputs are given at the same moment and the case where the CFP input is given first. However, when the eGFP input is given to the system first, CFP trigger time becomes shorter and is almost halved. This decrease in trigger time is caused by the fact that σ28 is already present when the CFP trigger input is added and no trigger can be used for σ28 production. Furthermore, temporal ultrasensitivity of the CFP production also increases (double compared to simultaneous inputs), meaning that the increase in CFP concentration is steeper and the system reacts quicker to an activation on that side of the circuit.

Similar results can be seen in Figure 26c, where the influence of removing the left-side intermediate DNA construct from the circuit is presented. The radar chart looks to be inverted, compared to Figure 26b, showing decreased eGFP trigger time in cases where the CFP trigger is given to the system first. Furthermore, the temporal ultrasensitivity of the eGFP production also increases in this situation in the same way the CFP production did when the right-side intermediate construct was removed. Moreover, CFP trigger time and temporal ultrasensitivity stay the same for the three different input situations for this circuit.

5.3.5 *The influence of σ28 on time delay*

Simulations have shown that the absence of σ28 producing constructs, in combination with trigger input order, influences the trigger times of eGFP and CFP production. However, it is unknown how larger or smaller amounts of σ28 influences the trigger times of the coupled FFL circuit. This situation, in which the amounts of σ28 producing construct have been varied, has again been simulated for three different cases in which trigger input order is changed. The heatmaps in Figure 27 show the trigger time of eGFP and CFP as a function of σ28 producing construct concentrations. It should be noted that in previous simulations and in vitro experiments, the DNA construct

concentrations used were 0.6 nM and 0.8 nM of respectively the left-side and right-side intermediate constructs.

As observed before, trigger times of eGFP and CFP are very similar in situations where both inputs are given to the system at the same time (Figure 27a). Furthermore, a decrease in trigger times can be observed for higher DNA construct concentrations. This effect is probably seen because with higher DNA construct concentrations, more σ28 can be produced and more transcription can be initiated from P28, increasing the rate of fluorophore production.

CFP trigger times are shorter than eGFP trigger times in cases where the eGFP trigger input is given to the system first (Figure 27b). Furthermore, lower concentrations of the CFP-side intermediate construct concentrations, close to 0 nM, show again that this shortens CFP trigger times. eGFP trigger times are short for low concentrations of eGFP-side intermediate construct. Moreover, in can be seen in Figure 27 that a higher total concentrations of intermediate DNA construct decreases trigger times of both fluorophores. Especially in cases where CFP-side construct concentration is high and eGFP-side construct concentration is low, an area of higher CFP trigger times is observed. σ28 cannot be produced in great amounts when the left-side trigger is added and can only be produced when also the right-side trigger is introduced. This addition causes much trigger to be used for σ28 production and less on CFP production, increasing CFP trigger times.

A similar pattern in the heatmaps occurs for the situation where the eGFP trigger is added after the CFP trigger, except that the lower trigger times are now observed for eGFP production (Figure 27c). Moreover, the heatmaps seem to be reflected through x=y because the influences of the intermediate DNA constructs on trigger times are switched when the order of input addition is changed.

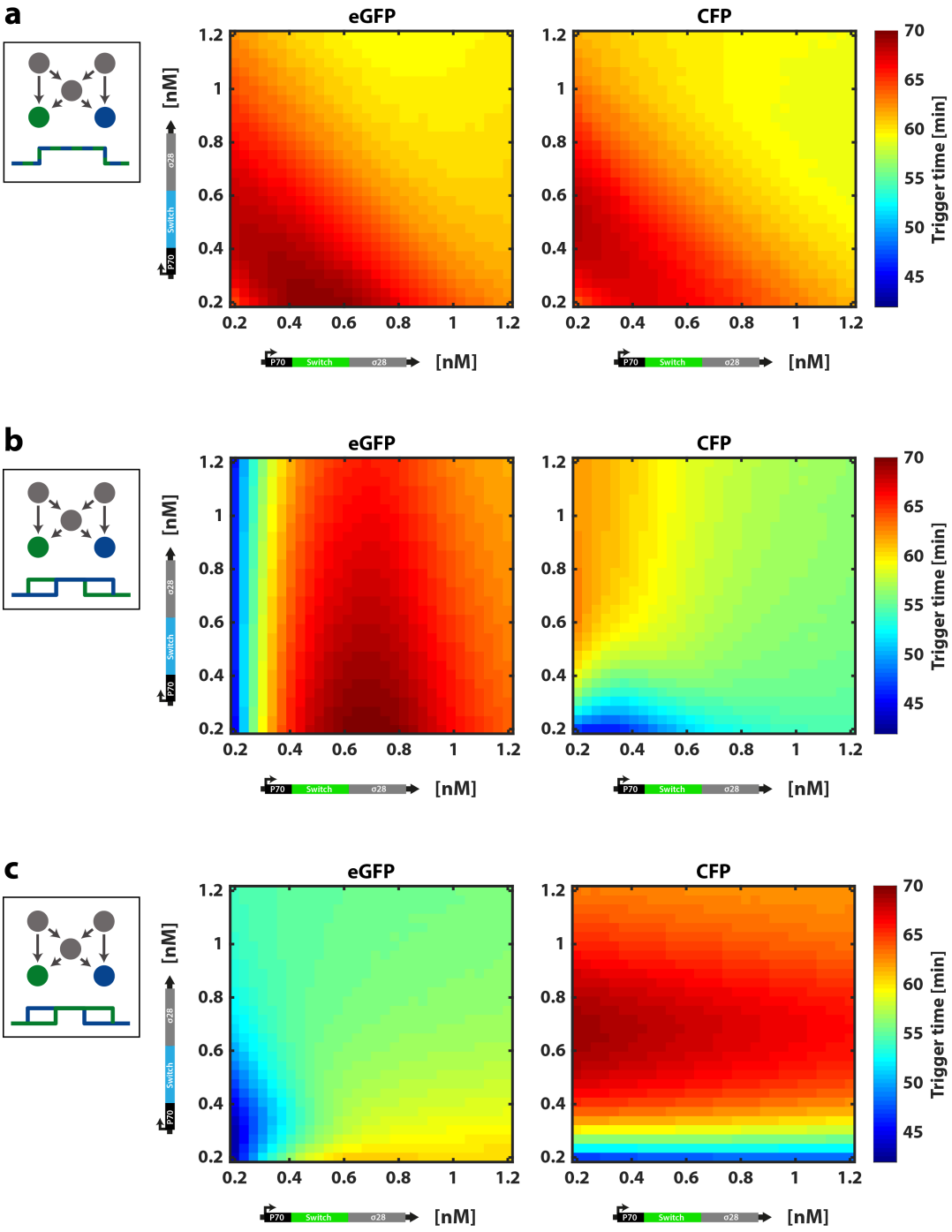

Figure 27: Heatmaps showing the influence of DNA construct concentrations on the trigger times of eGFP and CFP production.
(a) Both inputs are given at the same time. (b) The eGFP trigger input is given first, followed by the CFP trigger input. (c) The CFP trigger input is given first, followed by the eGFP trigger input.

6

CONCLUSION AND OUTLOOK

In this work, an in vitro implementation of a coupled feed-forward was presented and the process of constructing this genetic circuit was thoroughly described. The coupled feed-forward loop described in this project consisted of two separate coherent feed-forward loops that shared the σ28 transcription factor to form one coupled system. Therefore, two separate inputs were needed, provided in the form of different trigger RNA sequences, that could control the translation of species Y and Z. Two different coherent feed-forward loops which consisted of different toehold switches with matching trigger sequences were successfully constructed. Furthermore, the importance of trigger RNA input and the presence of the σ28 transcription factor for the expression of fluorophore was shown. In this way, it would be possible to control translation on both sides of the coupled feed-forward loop. Furthermore, in order to be able to distinguish the two outputs of the coupled feed-forward loop, two separate fluorescent output proteins were needed. Therefore, another coherent feed-forward loop was constructed with a CFP gene incorporated in the output DNA construct and the circuit was successfully expressed in vitro. Overlap between the eGFP and CFP emission spectra were corrected for by using a 3D calibration curve.

With two separate and distinguishable coherent feed-forward loops it was possible to construct the coupled feed-forward loop by adding both cFFLs to the same IVTT reaction mixture. Fortunately, the final implementation of the coupled feed-forward loop retrieved similar fluorophore expression levels as the two separate coherent feed-forward loops. Removing a trigger DNA input from the circuit resulted in a decrease of fluorophore production on that side of the circuit. It was shown that for these situations, ON/OFF ratios of 3 to 5 could be achieved. It would be interesting to further experiment with the coupled feed-forward loop circuit and explore whether it is possible to increase the ON/OFF ratios in presence and absence of the trigger input. This could for example be tried by using a different set of σ factors that show less crosstalk [27]. Another possibility would be to use a different set of toehold switches or introduce a second toehold switch in front of the σ28 or fluorophore gene [29].

The in vitro implementation of the coupled FFL also demonstrated that σ28 producing construct of one side could take over the function of the construct of the other side of the circuit. Further experiments with this situation showed again the crucial role of trigger inputs in

this circuit.

Future research on the coupled feed-forward loop could also focus on the implementation of the genetic circuit inside the TXTL microfluidic device from Niederholtmeyer et al. [49]. By using the microfluidic device for in vitro experiments, one can sustain reactions for longer periods of time. More importantly, it is possible to add DNA constructs to the reaction mixture at any given moment. This way, one could already load certain parts of the coupled feed-forward loop into the device, so that RNA sequences and proteins that need no trigger activation can already be produced before adding trigger input. Once the trigger input is added to the reaction mixture, fluorophore production is initiated and one can accurately observe differences in trigger time and temporal ultrasensitivity of the genetic circuits in different circumstances.

Since it was not possible to conduct experiments in the microfluidic device, an ODE model was created in order to simulate temporal behaviour of the coherent and coupled feed-forward loops. These simulations showed that the reference circuit for a cFFL shows less delay in the production of the output compared to the actual cFFL. Furthermore, a model for the coupled FFL showed under which circumstances temporal behaviour of the circuit can be influenced. It was shown that higher concentrations of σ28 decrease trigger times for both outputs. Furthermore, the order in which the trigger inputs are given to the system influence the trigger times and temporal ultrasensitivity of the output productions. The output activated by the second input impulse shows shorter time delay and an increase in temporal ultrasensitivity. Moreover, the absence of an intermediate DNA construct, in combination with a specific order in trigger input does also influence kinetic filtering of the circuit.

Unfortunately, this work could only focus on one of the twelve possible coupled feed-forward loops described by Gorochowski et al.. For future research, it would be interesting to also explore the behaviour of the other coupled feed-forward loops. As was illustrated in this report, the described coupled feed-forward loop can show interesting temporal behaviour due to its shared intermediate node. Other coupled feed-forward loops consist of shared outputs or shared inputs, which have also been found in for example *E. coli* metabolism and transcription networks [26]. Other coupled feed-forward loops that would be interesting to study are coupled FFLs where, for example, the output node of one FFL serves as the input or intermediate node of the second FFL. One could study whether these circuits also exhibit time delay or input persistence detection in ON steps or OFF steps of the circuit or that they show other temporal behaviour not

discussed in this report.

In conclusion, this study showed the successful construction and implementation of a coupled feed-forward loop in vitro and the exploration of its temporal behaviour in silico. These methods have provided us more insight in the functioning of this genetic circuit. However, in the future its behaviour could be explored even more using alternative methods. Nevertheless, this coupled feed-forward loop circuit could be implemented in a larger synthetic genetic circuit in the future to regulate the timing and sensitivity of the production of different protein outputs.

APPENDICES

A

DNA SEQUENCES

A.1 GENERAL PARTS

1. **P70 promoter**
   TGAGCTAACACCGTGCGTGTTGACAATTTTACCTCTGGC
   GGTGATAATGGTTGCA

2. **PR2 promoter**
   TGAGCTAACACCGTGCGTGTTGACAATTTTACCTCTGGC
   GGTGATAATGGTTGCA

3. **P28 promoter**
   CAAGCTTCAATAAAGTTTCCCCCCTCCTTGCCGATAACG
   AGATCAA

4. **Toehold switch 10**
   GATTGAATATGATAGAAGTTTAGTAGTAGACAATAGAA
   CAGAGGAGATATTGATGACTACTAAACTA

5. **Trigger 10**
   GATACACATAGAATCATGTGTATAACACTACTAAACTTC
   TATCATATTCAATCAC

6. **Toehold switch 8**
   GCTTATGAGTGTAATACGTTCTATGTCAGATTCAAGAAC
   AGAGGAGATTGAAATGGACATAGAACGA

7. **Trigger 8**
   GAGTCTTCAAGATAATGAAGACTCTGGACATAGAACGT
   ATTACACTCATAAGATA

8. **Toehold switch 2.1**
   GTCTTATCTTATCTATCTCGTTTATCCCTGCATACAGAAA
   CAGAGGAGATATGCAATGATAAACGAGA

9. **Trigger 2.1**
   ACCGCAATGCGGAAATTGCGGTAATGAAATAGAAACAG
   AACAGCAGGGATAAACGAGATAGATAAGATAAGAATG
   AAATGAATAGAGGCGAATAGCATAACCCCTT

10. **σ28**
    TGAATTCACTCTATACCGCTGAAGGTGTAATGGATAAAC
    ACTCGCTGTGGCAGCGTTATGTCCCGCTGGTGCGTCACG
    AAGCATTGCGCCTGCAGGTTCGACTGCCCGCGAGCGTGG
    AACTTGACGATCTGCTACAGGCGGGCGGCATTGGGTTAC

TTAATGCCGTCGAACGCTATGACGCCCTACAAGGAACG
GCATTTACAACTTACGCAGTGCAGCGTATCCGTGGCGCT
ATGCTGGATGAACTTCGCAGCCGTGACTGGGTGCCGCGC
AGCGTGCGACGCAACGCGCGTGAAGTGGCACAGGCAAT
AGGGCAACTGGAGCAGGAACTTGGCCGCAACGCCACGG
AAACTGAGGTAGCGGAACGTTTAGGGATCGATATTGCC
GATTATCGCCAAATGTTGCTCGACACCAATAACAGCCAG
CTCTTCTCCTACGATGAGTGGCGCGAAGAGCACGGCGAT
AGCATCGAACTGGTTACTGATGATCATCAGCGAGAAAA
CCCGCTACAACAACTACTGGACAGTAATCTGCGCCAGC
GGGTGATGGAAGCCATCGAAACGTTGCCGGAGCGCGAA
AAACTGGTATTAACCCTCTATTACCAGGAAGAGCTGAAT
CTCAAAGAGATTGGCGCGGTGCTGGAGGTCGGGGAATC
GCGGGTCAGTCAGTTACACAGCCAGGCTATTAAACGGTT
ACGCACTAAACTGGGTAAGTTATGA

11. **eGFP**

GTTGGAGCTTTTCACTGGCGTTGTTCCCATCCTGGTCGAG
CTGGACGGCGACGTAAACGGCCACAAGTTCAGCGTGTC
CGGCGAGGGCGAGGGCGATGCCACCTACGGCAAGCTGA
CCCTGAAGTTCATCTGCACCACCGGCAAGCTGCCCGTGC
CCTGGCCCACCCTCGTGACCACCCTGACCTACGGCGTGC
AGTGCTTCAGCCGCTACCCCGACCACATGAAGCAGCAC
GACTTCTTCAAGTCCGCCATGCCCGAAGGCTACGTCCAG
GAGCGCACCATCTTCTTCAAGGACGACGGCAACTACAA
GACCCGCGCCGAGGTGAAGTTCGAGGGCGACACCCTGG
TGAACCGCATCGAGCTGAAGGGCATCGACTTCAAGGAG
GACGGCAACATCCTGGGGCACAAGCTGGAGTACAACTA
CAACAGCCACAACGTCTATATCATGGCCGACAAGCAGA
AGAACGGCATCAAGGTGAACTTCAAGATCCGCCACAAC
ATCGAGGACGGCAGCGTGCAGCTCGCCGACCACTACCA
GCAGAACACCCCCATCGGCGACGGCCCCGTGCTGCTGC
CCGACAACCACTACCTGAGCACCCAGTCCGCCCTGAGC
AAAGACCCCAACGAGAAGCGCGATCACATGGTCCTGCT
GGAGTTCGTGACCGCCGCCGGGATCTAA

12. **CFP**

GTTGGAGCTTTTCACTGGCGTTGTTCCCATCCTGGTCGAG
CTGGACGGCGACGTAAACGGCCACAAGTTCAGCGTGTC
CGGCGAGGGCGAGGGCGATGCCACCTACGGCAAGCTGA
CCCTGAAGTTCATCTGCACCACCGGCAAGCTGCCCGTGC
CCTGGCCCACCCTCGTGACCACCCTGACCTGGGGCGTGC
AGTGCTTCAGCCGCTACCCCGACCACATGAAGCAGCAC
GACTTCTTCAAGTCCGCCATGCCCGAAGGCTACGTCCAG
GAGCGCACCATCTTCTTCAAGGACGACGGCAACTACAA
GACCCGCGCCGAGGTGAAGTTCGAGGGCGACACCCTGG
TGAACCGCATCGAGCTGAAGGGCATCGACTTCAAGGAG

GACGGCAACATCCTGGGGCACAAGCTGGAGTACAACTA
CATCAGCCACAACGTCTATATCACCGCCGACAAGCAGA
AGAACGGCATCAAGGCCAACTTCAAGATCCGCCACAAC
ATCGAGGACGGCAGCGTGCAGCTCGCCGACCACTACCA
GCAGAACACCCCCATCGGCGACGGCCCCGTGCTGCTGC
CCGACAACCACTACCTGAGCACCCAGTCCGCCCTGAGC
AAAGACCCCAACGAGAAGCGCGATCACATGGTCCTGCT
GGAGTTCGTGACCGCCGCCGGGATCTAA

13. **pBEST vector**
AAGGATCTTACCGCTGTTGAGATCCAGTTCGATGTAACC
CACTCGTGCACCCAACTGATCTTCAGCATCTTTTACTTTC
ACCAGCGTTTCTGGGTGAGCAAAAACAGGAAGGCAAAA
TGCCGCAAAAAAGGGAATAAGGGCGACACGGAAATGT
TGAATACTCATACTCTTCCTTTTTCAATATTATTGAAGCA
TTTATCAGGGTTATTGTCTCATGAGCGGATACATATTTGA
ATGTATTTAGAAAAATAAACAAATAGGGGTTCCGCGCA
CATTTCCCCGAAAAGTGCCACCTGACGTCTAAGAAACC
ATTATTATCATGACATTAACCTATAAAAATAGGCGTATC
ACGAGGCCCTTTCGTCTTCAAGAATTCTGGCGAATCCTCT
GACCAGCCAGAAAACGACCTTTCTGTGGTGAAACCGGA
TGCTGCAATTCAGAGCGGCAGCAAGTGGGGGACAGCAG
AAGACCTGACCGCCGCAGAGTGGATGTTTGACATGGTG
AAGACTATCGCACCATCAGCCAGAAAACCGAATTTTGC
TGGGTGGGCTAACGATATCCGCCTGATGCGTGAACGTGA
CGGACGTAACCACCGCGACATGTGTGTGCTGTTCCGCTG
GGCATGCCAGGACAACTTCTGGTCCGGTAACGCCTCAGG
TAGGATGTAGGCCCTCAAAGAGATTGGCGCGGTGCTGG
AGGTCGGGGAATCGCGGGTCAGTCAGTTACACAGCCAG
GCTATTAAACGGTTACGCACTAAACTGGGTAAGTTATAA
TCTAGAGGCGCCACTCGAGAGTCGACCAAAGCCCGCCG
AAAGGCGGGCTTTTCTGTGCCGGCATGATAAGCTGTCAA
ACATGAGAATTACAACTTATATCGTATGGGGCTGACTTC
AGGTGCTACATTTGAAGAGATAAATTGCACTGAAATCTA
GAAATATTTTATCTGATTAATAAGATGATCTTCTTGAGAT
CGTTTTGGTCTGCGCGTAATCTCTTGCTCTGAAAACGAAA
AAACCGCCTTGCAGGGCGGTTTTTCGAAGGTTCTCTGAG
CTACCAACTCTTTGAACCGAGGTAACTGGCTTGGAGGAG
CGCAGTCACCAAAACTTGTCCTTTCAGTTTAGCCTTAACC
GGCGCATGACTTCAAGACTAACTCCTCTAAATCAATTAC
CAGTGGCTGCTGCCAGTGGTGCTTTTGCATGTCTTTCCGG
GTTGGACTCAAGACGATAGTTACCGGATAAGGCGCAGC
GGTCGGACTGAACGGGGGGTTCGTGCATACAGTCCAGC
TTGGAGCGAACTGCCTACCCGGAACTGAGTGTCAGGCGT
GGAATGAGACAAACGCGGCCATAACAGCGGAATGACA
CCGGTAAACCGAAAGGCAGGAACAGGAGAGCGCACGA
GGGAGCCGCCAGGGGAAACGCCTGGTATCTTTATAGTCC

TGTCGGGTTTCGCCACCACTGATTTGAGCGTCAGATTTCG
TGATGCTTGTCAGGGGGGCGGAGCCTATGGAAAAACGG
CTTTGCCGCGGCCCTCTCACTTCCCTGTTAAGTATCTTCC
TGGCATCTTCCAGGAAATCTCCGCCCCGTTCGTAAGCCA
TTTCCGCTCGCCGCAGTCGAACGACCGAGCGTAGCGAGT
CAGTGAGCGAGGAAGCGGAATATATCCTGTATCACATA
TTCTGCTGACGCACCGGTGCAGCCTTTTTTCTCCTGCCAC
ATGAAGCACTTCACTGACACCCTCATCAGTGCCAACATA
GTAAGCCAGTATACACTCCGCTAGGGTCATGAGATTATC
AAAAAGGATCTTCACCTAGATCCTTTTAAATTAAAAATG
AAGTTTTAAATCAATCTAAAGTATATATGAGTAAACTTG
GTCTGACAGTTACCAATGCTTAATCAGTGAGGCACCTAT
CTCAGCGATCTGTCTATTTCGTTCATCCATAGTTGCCTGA
CTCCCCGTCGTGTAGATAACTACGATACGGGAGGGCTTA
CCATCTGGCCCCAGTGCTGCAATGATACCGCGCGACCCA
CGCTCACCGGCTCCAGATTTATCAGCAATAAACCAGCCA
GCCGGAAGGGCCGAGCGCAGAAGTGGTCCTGCAACTTT
ATCCGCCTCCATCCAGTCTATTAATTGTTGCCGGGAAGCT
AGAGTAAGTAGTTCGCCAGTTAATAGTTTGCGCAACGTT
GTTGCCATTGCTACAGGCATCGTGGTGTCACGCTCGTCG
TTTGGTATGGCTTCATTCAGCTCCGGTTCCCAACGATCAA
GGCGAGTTACATGATCCCCCATGTTGTGCAAAAAAGCG
GTTAGCTCCTTCGGTCCTCCGATCGTTGTCAGAAGTAAGT
TGGCCGCAGTGTTATCACTCATGGTTATGGCAGCACTGC
ATAATTCTCTTACTGTCATGCCATCCGTAAGATGCTTTTC
TGTGACTGGTGAGTACTCAACCAAGTCATTCTGAGAATA
GTGTATGCGGCGACCGAGTTGCTCTTGCCCGGCGTCAAT
ACGGGATAATACCGCGCCACATAGCAGAACTTTAAAAG
TGCTCATCATTGGAAAACGTTCTTCGGGGCGAAAACTCT
C

A.2 LINEAR DNA CONSTRUCTS

1. **P70_Tr10**
   GGCGAATCCTCTGACCAGCCAGAAAACGACCTTTCTGTG
   GTGAAACCGGATGCTGCAATTCAGAGCGGCAGCAAGTG
   GGGGACAGCAGAAGACCTGACCGCCGCAGAGTGGATGT
   TTGACATGGTGAAGACTATCGCACCATCAGCCAGAAAA
   CCGAATTTTGCTGGGTGGGCTAACGATATCCGCCTGATG
   CGTGAACGTGACGGACGTAACCACCGCGACATGTGTGT
   GCTGTTCCGCTGGGCATGCCAGGACAACTTCTGGTCCGG
   TAACGCATGATGTCTGAGCTAACACCGTGCGTGTTGACA
   ATTTTACCTCTGGCGGTGATAATGGTTGCAAAGCGGGAT
   ACACATAGAATCATGTGTATAACACTACTAAACTTCTAT
   CATATTCAATCACTAGCTGAACAAAGCCCGCCGAAAGG
   CGGGCTTTTCTGTGATGTCGTCGCGGCATGATAAGCTGTC

AAACATGAGAATTGCAACTTATATCGTATGGGGCTGACT
TCAGGTGCTACATTTGAAGAGATAAATTGCACTGAAATC
TAGAAATATTTTATCTGATTAATAAGATGATCTTCTTGAG
ATCGTTTTGGTCTGCGCGTAATCTCTTGCTCTGAAAACGA
AAAAACCGCCTTGCAGGGCGGTTTTTCGAAGGTTCTCTG
AGCTACCAACTCTTCGAACCGAGGTAACTGGCTTGGAGG
AGCGCAGTCACCAAAACTTGTCCTTTCAGTTTAGCCTTA
ACCGGCGCATGACTTCAAGACTAACTCCTCTAAATCAAT
TACCAGTGGCTGCTGCCAGAGGTGCTTTTGCATGTCTTTC
CGGGTTGGACTCAAGACGATAGTTACCGGATAAGGCGC
AGCGGTCGGACTGAACGGGGGGTTcgtgcatacagtccagcttgg

2. **P70_Tr8**
GGCGAATCCTCTGACCAGCCAGAAAACGACCTTTCTGTG
GTGAAACCGGATGCTGCAATTCAGAGCGGCAGCAAGTG
GGGGACAGCAGAAGACCTGACCGCCGCAGAGTGGATGT
TTGACATGGTGAAGACTATCGCACCATCAGCCAGAAAA
CCGAATTTTGCTGGGTGGGCTAACGATATCCGCCTGATG
CGTGAACGTGACGGACGTAACCACCGCGACATGTGTGT
GCTGTTCCGCTGGGCATGCCAGGACAACTTCTGGTCCGG
TAACGCATGATGTCTGAGCTAACACCGTGCGTGTTGACA
ATTTTACCTCTGGCGGTGATAATGGTTGCAAAGCGGGAG
TCTTCAAGATAATGAAGACTCTGGACATAGAACGTATTA
CACTCATAAGATATGAACAAAGCCCGCCGAAAGGCGGG
CTTTTCTGTGATGTCGTCGCGGCATGATAAGCTGTCAAA
CATGAGAATTGCAACTTATATCGTATGGGGCTGACTTCA
GGTGCTACATTTGAAGAGATAAATTGCACTGAAATCTAG
AAATATTTTATCTGATTAATAAGATGATCTTCTTGAGATC
GTTTTGGTCTGCGCGTAATCTCTTGCTCTGAAAACGAAA
AAACCGCCTTGCAGGGCGGTTTTTCGAAGGTTCTCTGAG
CTACCAACTCTTCGAACCGAGGTAACTGGCTTGGAGGAG
CGCAGTCACCAAAACTTGTCCTTTCAGTTTAGCCTTAACC
GGCGCATGACTTCAAGACTAACTCCTCTAAATCAATTAC
CAGTGGCTGCTGCCAGAGGTGCTTTTGCATGTCTTTCCGG
GTTGGACTCAAGACGATAGTTACCGGATAAGGCGCAGC
GGTCGGACTGAACGGGGGGTTcgtgcatacagtccagcttgg

3. **P70_Tr2.1**
GGCGAATCCTCTGACCAGCCAGAAAACGACCTTTCTGTG
GTGAAACCGGATGCTGCAATTCAGAGCGGCAGCAAGTG
GGGGACAGCAGAAGACCTGACCGCCGCAGAGTGGATGT
TTGACATGGTGAAGACTATCGCACCATCAGCCAGAAAA
CCGAATTTTGCTGGGTGGGCTAACGATATCCGCCTGATG
CGTGAACGTGACGGACGTAACCACCGCGACATGTGTGT
GCTGTTCCGCTGGGCATGCCAGGACAACTTCTGGTCCGG
TAACGCATGATGTCTGAGCTAACACCGTGCGTGTTGACA
ATTTTACCTCTGGCGGTGATAATGGTTGCAAAGCGGGAC

CGCAATGCGGAAATTGCGGTAATGAAATAGAAACAGAA
CAGCAGGGATAAACGAGATAGATAAGATAAGAATGAA
ATGAATAGAGGCGAATAGCATAACCCCTTGTGAACGCC
ACTCGAGAGTCGACCAAAGCCCGCCGAAAGGCGGGCTT
TTCTGTGCCGGCATGATAAGCTGTCAAACATGAGAATTA
CAACTTATATCGTATGGGGCTGACTTCAGGTGCTACATTT
GAAGAGATAAATTGCACTGAAATCTAGAAATATTTTATC
TGATTAATAAGATGATCTTCTTGAGATCGTTTTGGTCTGC
GCGTAATCTCTTGCTCTGAAAACGAAAAAACCGCCTTGC
AGGGCGGTTTTTCGAAGGTTCTCTGAGCTACCAACTCTTT
GAACCGAGGTAACTGGCTTGGAGGAGCGCAGTCACCAA
AACTTGTCCTTTCAGTTTAGCCTTAACCGGCGCATGACTT
CAAGACTAACTCCTCTAAATCAATTACCAGTGGCTGCTG
CCAGTGGTGCTTTTGCATGTCTTTCCGGGTTGGACTCAAG
ACGATAGTTACCGGATAAGGCGCAGCGGTCGGACTGAA
CGGGGGGTTcgtgcatacagtccagcttgg

4. **P70_Sw10_S28**
GGCGAATCCTCTGACCAGCCAGAAAACGACCTTTCTGTG
GTGAAACCGGATGCTGCAATTCAGAGCGGCAGCAAGTG
GGGGACAGCAGAAGACCTGACCGCCGCAGAGTGGATGT
TTGACATGGTGAAGACTATCGCACCATCAGCCAGAAAA
CCGAATTTTGCTGGGTGGGCTAACGATATCCGCCTGATG
CGTGAACGTGACGGACGTAACCACCGCGACATGTGTGT
GCTGTTCCGCTGGGCATGCCAGGACAACTTCTGGTCCGG
TAACGCATTGAGCTAACACCGTGCGTGTTGACAATTTTA
CCTCTGGCGGTGATAATGGTTGCAGATTGAATATGATAG
AAGTTTAGTAGTAGACAATAGAACAGAGGAGATATTGA
TGACTACTAAACTAAACCTGGCGGCAGCGCAAAAGTTG
AATTCACTCTATACCGCTGAAGGTGTAATGGATAAACAC
TCGCTGTGGCAGCGTTATGTCCCGCTGGTGCGTCACGAA
GCATTGCGCCTGCAGGTTCGACTGCCCGCGAGCGTGGAA
CTTGACGATCTGCTACAGGCGGGCGGCATTGGGTTACTT
AATGCCGTCGAACGCTATGACGCCCTACAAGGAACGGC
ATTTACAACTTACGCAGTGCAGCGTATCCGTGGCGCTAT
GCTGGATGAACTTCGCAGCCGTGACTGGGTGCCGCGCA
GCGTGCGACGCAACGCGCGTGAAGTGGCACAGGCAATA
GGGCAACTGGAGCAGGAACTTGGCCGCAACGCCACGGA
AACTGAGGTAGCGGAACGTTTAGGGATCGATATTGCCGA
TTATCGCCAAATGTTGCTCGACACCAATAACAGCCAGCT
CTTCTCCTACGATGAGTGGCGCGAAGAGCACGGCGATA
GCATCGAACTGGTTACTGATGATCATCAGCGAGAAAAC
CCGCTACAACAACTACTGGACAGTAATCTGCGCCAGCG
GGTGATGGAAGCCATCGAAACGTTGCCGGAGCGCGAAA
AACTGGTATTAACCCTCTATTACCAGGAAGAGCTGAATC
TCAAAGAGATTGGCGCGGTGCTGGAGGTCGGGGAATCG
CGGGTCAGTCAGTTACACAGCCAGGCTATTAAACGGTTA

CGCACTAAACTGGGTAAGTTATGAACGCCACTCGAGAG
TCGACCAAAGCCCGCCGAAAGGCGGGCTTTTCTGTGCCG
GCATGATAAGCTGTCAAACATGAGAATTACAACTTATAT
CGTATGGGGCTGACTTCAGGTGCTACATTTGAAGAGATA
AATTGCACTGAAATCTAGAAATATTTTATCTGATTAATA
AGATGATCTTCTTGAGATCGTTTTGGTCTGCGCGTAATCT
CTTGCTCTGAAAACGAAAAAACCGCCTTGCAGGGCGGT
TTTTCGAAGGTTCTCTGAGCTACCAACTCTTTGAACCGAG
GTAACTGGCTTGGAGGAGCGCAGTCACCAAAACTTGTCC
TTTCAGTTTAGCCTTAACCGGCGCATGACTTCAAGACTA
ACTCCTCTAAATCAATTACCAGTGGCTGCTGCCAGTGGT
GCTTTTGCATGTCTTTCCGGGTTGGACTCAAGACGATAGT
TACCGGATAAGGCGCAGCGGTCGGACTGAACGGGGGGT
Tcgtgcatacagtccagcttgg

5. **P70_Sw8_S28**
GGCGAATCCTCTGACCAGCCAGAAAACGACCTTTCTGTG
GTGAAACCGGATGCTGCAATTCAGAGCGGCAGCAAGTG
GGGGACAGCAGAAGACCTGACCGCCGCAGAGTGGATGT
TTGACATGGTGAAGACTATCGCACCATCAGCCAGAAAA
CCGAATTTTGCTGGGTGGGCTAACGATATCCGCCTGATG
CGTGAACGTGACGGACGTAACCACCGCGACATGTGTGT
GCTGTTCCGCTGGGCATGCCAGGACAACTTCTGGTCCGG
TAACGCATGATGTCTGAGCTAACACCGTGCGTGTTGACA
ATTTTACCTCTGGCGGTGATAATGGTTGCAAAGCGGGCT
TATGAGTGTAATACGTTCTATGTCAGATTCAAGAACAGA
GGAGATTGAAATGGACATAGAACGAAACCTGGCGGCAG
CGCAAAAGTTGAATTCACTCTATACCGCTGAAGGTGTAA
TGGATAAACACTCGCTGTGGCAGCGTTATGTCCCGCTGG
TGCGTCACGAAGCATTGCGCCTGCAGGTTCGACTGCCCG
CGAGCGTGGAACTTGACGATCTGCTACAGGCGGGCGGC
ATTGGGTTACTTAATGCCGTCGAACGCTATGACGCCCTA
CAAGGAACGGCATTTACAACTTACGCAGTGCAGCGTAT
CCGTGGCGCTATGCTGGATGAACTTCGCAGCCGTGACTG
GGTGCCGCGCAGCGTGCGACGCAACGCGCGTGAAGTGG
CACAGGCAATAGGGCAACTGGAGCAGGAACTTGGCCGC
AACGCCACGGAAACTGAGGTAGCGGAACGTTTAGGGAT
CGATATTGCCGATTATCGCCAAATGTTGCTCGACACCAA
TAACAGCCAGCTCTTCTCCTACGATGAGTGGCGCGAAGA
GCACGGCGATAGCATCGAACTGGTTACTGATGATCATCA
GCGAGAAAACCCGCTACAACAACTACTGGACAGTAATC
TGCGCCAGCGGGTGATGGAAGCCATCGAAACGTTGCCG
GAGCGCGAAAAACTGGTATTAACCCTCTATTACCAGGA
AGAGCTGAATCTCAAAGAGATTGGCGCGGTGCTGGAGG
TCGGGGAATCGCGGGTCAGTCAGTTACACAGCCAGGCT
ATTAAACGGTTACGCACTAAACTGGGTAAGTTATGAACG
CCACTCGAGAGTCGACCAAAGCCCGCCGAAAGGCGGGC

TTTTCTGTGCCGGCATGATAAGCTGTCAAACATGAGAAT
TACAACTTATATCGTATGGGGCTGACTTCAGGTGCTACA
TTTGAAGAGATAAATTGCACTGAAATCTAGAAATATTTT
ATCTGATTAATAAGATGATCTTCTTGAGATCGTTTTGGTC
TGCGCGTAATCTCTTGCTCTGAAAACGAAAAAACCGCCT
TGCAGGGCGGTTTTTCGAAGGTTCTCTGAGCTACCAACT
CTTTGAACCGAGGTAACTGGCTTGGAGGAGCGCAGTCA
CCAAAACTTGTCCTTTCAGTTTAGCCTTAACCGGCGCAT
GACTTCAAGACTAACTCCTCTAAATCAATTACCAGTGGC
TGCTGCCAGTGGTGCTTTTGCATGTCTTTCCGGGTTGGAC
TCAAGACGATAGTTACCGGATAAGGCGCAGCGGTCGGA
CTGAACGGGGGGTTcgtgcatacagtccagcttgg

6. **P70_Sw8_S28 (improved)**
GGCGAATCCTCTGACCAGCCAGAAAACGACCTTTCTGTG
GTGAAACCGGATGCTGCAATTCAGAGCGGCAGCAAGTG
GGGGACAGCAGAAGACCTGACCGCCGCAGAGTGGATGT
TTGACATGGTGAAGACTATCGCACCATCAGCCAGAAAA
CCGAATTTTGCTGGGTGGGCTAACGATATCCGCCTGATG
CGTGAACGTGACGGACGTAACCACCGCGACATGTGTGT
GCTGTTCCGCTGGGCATGCCAGGACAACTTCTGGTCCGG
TAACGCATTGAGCTAACACCGTGCGTGTTGACAATTTTA
CCTCTGGCGGTGATAATGGTTGCAGCTTATGAGTGTAAT
ACGTTCTATGTCAGATTCAAGAACAGAGGAGATTGAAAT
GGACATAGAACGAAACCTGGCGGCAGCGCAAAAGTTGA
ATTCACTCTATACCGCTGAAGGTGTAATGGATAAACACT
CGCTGTGGCAGCGTTATGTCCCGCTGGTGCGTCACGAAG
CATTGCGCCTGCAGGTTCGACTGCCCGCGAGCGTGGAAC
TTGACGATCTGCTACAGGCGGGCGGCATTGGGTTACTTA
ATGCCGTCGAACGCTATGACGCCCTACAAGGAACGGCA
TTTACAACTTACGCAGTGCAGCGTATCCGTGGCGCTATG
CTGGATGAACTTCGCAGCCGTGACTGGGTGCCGCGCAGC
GTGCGACGCAACGCGCGTGAAGTGGCACAGGCAATAGG
GCAACTGGAGCAGGAACTTGGCCGCAACGCCACGGAAA
CTGAGGTAGCGGAACGTTTAGGGATCGATATTGCCGATT
ATCGCCAAATGTTGCTCGACACCAATAACAGCCAGCTCT
TCTCCTACGATGAGTGGCGCGAAGAGCACGGCGATAGC
ATCGAACTGGTTACTGATGATCATCAGCGAGAAAACCC
GCTACAACAACTACTGGACAGTAATCTGCGCCAGCGGG
TGATGGAAGCCATCGAAACGTTGCCGGAGCGCGAAAAA
CTGGTATTAACCCTCTATTACCAGGAAGAGCTGAATCTC
AAAGAGATTGGCGCGGTGCTGGAGGTCGGGGAATCGCG
GGTCAGTCAGTTACACAGCCAGGCTATTAAACGGTTACG
CACTAAACTGGGTAAGTTATGAACGCCACTCGAGAGTC
GACCAAAGCCCGCCGAAAGGCGGGCTTTTCTGTGCCGG
CATGATAAGCTGTCAAACATGAGAATTACAACTTATATC
GTATGGGGCTGACTTCAGGTGCTACATTTGAAGAGATAA

ATTGCACTGAAATCTAGAAATATTTTATCTGATTAATAA
GATGATCTTCTTGAGATCGTTTTGGTCTGCGCGTAATCTC
TTGCTCTGAAAACGAAAAAACCGCCTTGCAGGGCGGTTT
TTCGAAGGTTCTCTGAGCTACCAACTCTTTGAACCGAGG
TAACTGGCTTGGAGGAGCGCAGTCACCAAAACTTGTCCT
TTCAGTTTAGCCTTAACCGGCGCATGACTTCAAGACTAA
CTCCTCTAAATCAATTACCAGTGGCTGCTGCCAGTGGTG
CTTTTGCATGTCTTTCCGGGTTGGACTCAAGACGATAGTT
ACCGGATAAGGCGCAGCGGTCGGACTGAACGGGGGGTT
cgtgcatacagtccagcttgg

7. **P70_Sw2.1_S28**
GGCGAATCCTCTGACCAGCCAGAAAACGACCTTTCTGTG
GTGAAACCGGATGCTGCAATTCAGAGCGGCAGCAAGTG
GGGGACAGCAGAAGACCTGACCGCCGCAGAGTGGATGT
TTGACATGGTGAAGACTATCGCACCATCAGCCAGAAAA
CCGAATTTTGCTGGGTGGGCTAACGATATCCGCCTGATG
CGTGAACGTGACGGACGTAACCACCGCGACATGTGTGT
GCTGTTCCGCTGGGCATGCCAGGACAACTTCTGGTCCGG
TAACGCATTGAGCTAACACCGTGCGTGTTGACAATTTTA
CCTCTGGCGGTGATAATGGTTGCAGTCTTATCTTATCTAT
CTCGTTTATCCCTGCATACAGAAACAGAGGAGATATGCA
ATGATAAACGAGAACCTGGCGGCAGCGCAAAAGTTGAA
TTCACTCTATACCGCTGAAGGTGTAATGGATAAACACTC
GCTGTGGCAGCGTTATGTCCCGCTGGTGCGTCACGAAGC
ATTGCGCCTGCAGGTTCGACTGCCCGCGAGCGTGGAACT
TGACGATCTGCTACAGGCGGGCGGCATTGGGTTACTTAA
TGCCGTCGAACGCTATGACGCCCTACAAGGAACGGCATT
TACAACTTACGCAGTGCAGCGTATCCGTGGCGCTATGCT
GGATGAACTTCGCAGCCGTGACTGGGTGCCGCGCAGCGT
GCGACGCAACGCGCGTGAAGTGGCACAGGCAATAGGGC
AACTGGAGCAGGAACTTGGCCGCAACGCCACGGAAACT
GAGGTAGCGGAACGTTTAGGGATCGATATTGCCGATTAT
CGCCAAATGTTGCTCGACACCAATAACAGCCAGCTCTTC
TCCTACGATGAGTGGCGCGAAGAGCACGGCGATAGCAT
CGAACTGGTTACTGATGATCATCAGCGAGAAAACCCGCT
ACAACAACTACTGGACAGTAATCTGCGCCAGCGGGTGA
TGGAAGCCATCGAAACGTTGCCGGAGCGCGAAAAACTG
GTATTAACCCTCTATTACCAGGAAGAGCTGAATCTCAAA
GAGATTGGCGCGGTGCTGGAGGTCGGGGAATCGCGGGT
CAGTCAGTTACACAGCCAGGCTATTAAACGGTTACGCAC
TAAACTGGGTAAGTTATGAACGCCACTCGAGAGTCGAC
CAAAGCCCGCCGAAAGGCGGGCTTTTCTGTGCCGGCATG
ATAAGCTGTCAAACATGAGAATTACAACTTATATCGTAT
GGGGCTGACTTCAGGTGCTACATTTGAAGAGATAAATTG
CACTGAAATCTAGAAATATTTTATCTGATTAATAAGATG
ATCTTCTTGAGATCGTTTTGGTCTGCGCGTAATCTCTTGC

TCTGAAAACGAAAAAACCGCCTTGCAGGGCGGTTTTTCG
AAGGTTCTCTGAGCTACCAACTCTTTGAACCGAGGTAAC
TGGCTTGGAGGAGCGCAGTCACCAAAACTTGTCCTTTCA
GTTTAGCCTTAACCGGCGCATGACTTCAAGACTAACTCC
TCTAAATCAATTACCAGTGGCTGCTGCCAGTGGTGCTTTT
GCATGTCTTTCCGGGTTGGACTCAAGACGATAGTTACCG
GATAAGGCGCAGCGGTCGGACTGAACGGGGGGTTcgtgcat
acagtccagcttgg

8. **P70_S28**
GGCGAATCCTCTGACCAGCCAGAAAACGACCTTTCTGTG
GTGAAACCGGATGCTGCAATTCAGAGCGGCAGCAAGTG
GGGGACAGCAGAAGACCTGACCGCCGCAGAGTGGATGT
TTGACATGGTGAAGACTATCGCACCATCAGCCAGAAAA
CCGAATTTTGCTGGGTGGGCTAACGATATCCGCCTGATG
CGTGAACGTGACGGACGTAACCACCGCGACATGTGTGT
GCTGTTCCGCTGGGCATGCCAGGACAACTTCTGGTCCGG
TAACGCATGATGTCTGAGCTAACACCGTGCGTGTTGACA
ATTTTACCTCTGGCGGTGCTAATGGTTGCAAAGCAATAA
TTTTGTTTAACTTTAAGAAGGAGATATAGCATGAATTCA
CTCTATACCGCTGAAGGTGTAATGGATAAACACTCGCTG
TGGCAGCGTTATGTCCCGCTGGTGCGTCACGAAGCATTG
CGCCTGCAGGTTCGACTGCCCGCGAGCGTGGAACTTGAC
GATCTGCTACAGGCGGGCGGCATTGGGTTACTTAATGCC
GTCGAACGCTATGACGCCCTACAAGGAACGGCATTTAC
AACTTACGCAGTGCAGCGTATCCGTGGCGCTATGCTGGA
TGAACTTCGCAGCCGTGACTGGGTGCCGCGCAGCGTGCG
ACGCAACGCGCGTGAAGTGGCACAGGCAATAGGGCAAC
TGGAGCAGGAACTTGGCCGCAACGCCACGGAAACTGAG
GTAGCGGAACGTTTAGGGATCGATATTGCCGATTATCGC
CAAATGTTGCTCGACACCAATAACAGCCAGCTCTTCTCC
TACGATGAGTGGCGCGAAGAGCACGGCGATAGCATCGA
ACTGGTTACTGATGATCATCAGCGAGAAAACCCGCTACA
ACAACTACTGGACAGTAATCTGCGCCAGCGGGTGATGG
AAGCCATCGAAACGTTGCCGGAGCGCGAAAAACTGGTA
TTAACCCTCTATTACCAGGAAGAGCTGAATCTCAAAGAG
ATTGGCGCGGTGCTGGAGGTCGGGGAATCGCGGGTCAG
TCAGTTACACAGCCAGGCTATTAAACGGTTACGCACTAA
ACTGGGTAAGTTATGAAAAGCCCACGACCGTTCTCGTGC
GCCAATTCAAACTCTCGCCCTAAATCAACTAACCCTATG
GTTACCCGAGTCACTCAGGAAGGTGCTAAAACTCAATA
ACTAAATCTAAACTCAACTCATCCCTATCTTCAAAGCCC
GCCGAAAGGCGGGCTTTTCTGTGATGTCGTCGCGGCATG
ATAAGCTGTCAAACATGAGAATTACAACTTATATCGTAT
GGGGCTGACTTCAGGTGCTACATTTGAAGAGATAAATTG
CACTGAAATCTAGAAATATTTTATCTGATTAATAAGATG
ATCTTCTTGAGATCGTTTTGGTCTGCGCGTAATCTCTTGC

TCTGAAAACGAAAAAACCGCCTTGCAGGGCGGTTTTTCG
AAGGTTCTCTGAGCTACCAACTCTTTGAACCGAGGTAAC
TGGCTTGGAGGAGCGCAGTCACCAAAACTTGTCCTTTCA
GTTTAGCCTTAACCGGCGCATGACTTCAAGACTAACTCC
TCTAAATCAATTACCAGTGGCTGCTGCCAGTGGTGCTTTT
GCATGTCTTTCCGGGTTGGACTCAAGACGATAGTTACCG
GATAAGGCGCAGCGGTCGGACTGAACGGGGGGTTCGTG
CATACAGTCCAGCTTGG

9. **P28_Sw10_eGFP**
GGCGAATCCTCTGACCAGCCAGAAAACGACCTTTCTGTG
GTGAAACCGGATGCTGCAATTCAGAGCGGCAGCAAGTG
GGGGACAGCAGAAGACCTGACCGCCGCAGAGTGGATGT
TTGACATGGTGAAGACTATCGCACCATCAGCCAGAAAA
CCGAATTTTGCTGGGTGGGCTAACGATATCCGCCTGATG
CGTGAACGTGACGGACGTAACCACCGCGACATGTGTGT
GCTGTTCCGCTGGGCATGCCAGGACAACTTCTGGTCCGG
TAACGCATCAAGCTTCAATAAAGTTTCCCCCCTCCTTGC
CGATAACGAGATCAAGATTGAATATGATAGAAGTTTAG
TAGTAGACAATAGAACAGAGGAGATATTGATGACTACT
AAACTAAACCTGGCGGCAGCGCAAAAGGGCGAAGAGC
TTTTCACTGGCGTTGTTCCCATCCTGGTCGAGCTGGACGG
CGACGTAAACGGCCACAAGTTCAGCGTGTCCGGCGAGG
GCGAGGGCGATGCCACCTACGGCAAGCTGACCCTGAAG
TTCATCTGCACCACCGGCAAGCTGCCCGTGCCCTGGCCC
ACCCTCGTGACCACCCTGACCTACGGCGTGCAGTGCTTC
AGCCGCTACCCCGACCACATGAAGCAGCACGACTTCTTC
AAGTCCGCCATGCCCGAAGGCTACGTCCAGGAGCGCAC
CATCTTCTTCAAGGACGACGGCAACTACAAGACCCGCG
CCGAGGTGAAGTTCGAGGGCGACACCCTGGTGAACCGC
ATCGAGCTGAAGGGCATCGACTTCAAGGAGGACGGCAA
CATCCTGGGGCACAAGCTGGAGTACAACTACAACAGCC
ACAACGTCTATATCATGGCCGACAAGCAGAAGAACGGC
ATCAAGGTGAACTTCAAGATCCGCCACAACATCGAGGA
CGGCAGCGTGCAGCTCGCCGACCACTACCAGCAGAACA
CCCCCATCGGCGACGGCCCCGTGCTGCTGCCCGACAACC
ACTACCTGAGCACCCAGTCCGCCCTGAGCAAAGACCCC
AACGAGAAGCGCGATCACATGGTCCTGCTGGAGTTCGTG
ACCGCCGCCGGGATCTAATGAACAAAGCCCGCCGAAAG
GCGGGCTTTTCTGTGATGTCGTCGCGGCATGATAAGCTGT
CAAACATGAGAATTGCAACTTATATCGTATGGGGCTGAC
TTCAGGTGCTACATTTGAAGAGATAAATTGCACTGAAAT
CTAGAAATATTTTATCTGATTAATAAGATGATCTTCTTGA
GATCGTTTTGGTCTGCGCGTAATCTCTTGCTCTGAAAACG
AAAAAACCGCCTTGCAGGGCGGTTTTTCGAAGGTTCTCT
GAGCTACCAACTCTTTGAACCGAGGTAACTGGCTTGGAG
GAGCGCAGTCACCAAAACTTGTCCTTTCAGTTTAGCCTT

AACCGGCGCATGACTTCAAGACTAACTCCTCTAAATCAA
TTACCAGTGGCTGCTGCCAGTGGTGCTTTTGCATGTCTTT
CCGGGTTGGACTCAAGACGATAGTTACCGGATAAGGCG
CAGCGGTCGGACTGAACGGGGGGTTcgtgcatacagtccagcttgg

10. **P28_Sw10_CFP**

GGCGAATCCTCTGACCAGCCAGAAAACGACCTTTCTGTG
GTGAAACCGGATGCTGCAATTCAGAGCGGCAGCAAGTG
GGGGACAGCAGAAGACCTGACCGCCGCAGAGTGGATGT
TTGACATGGTGAAGACTATCGCACCATCAGCCAGAAAA
CCGAATTTTGCTGGGTGGGCTAACGATATCCGCCTGATG
CGTGAACGTGACGGACGTAACCACCGCGACATGTGTGT
GCTGTTCCGCTGGGCATGCCAGGACAACTTCTGGTCCGG
TAACGCATCAAGCTTCAATAAAGTTTCCCCCCTCCTTGC
CGATAACGAGATCAAGATTGAATATGATAGAAGTTTAGT
AGTAGACAATAGAACAGAGGAGATATTGATGACTACTA
AACTAAACCTGGCGGCAGCGCAAAAGGGCGAAGAGCTT
TTCACTGGCGTTGTTCCCATCCTGGTCGAGCTGGACGGC
GACGTAAACGGCCACAAGTTCAGCGTGTCCGGCGAGGG
CGAGGGCGATGCCACCTACGGCAAGCTGACCCTGAAGT
TCATCTGCACCACCGGCAAGCTGCCCGTGCCCTGGCCCA
CCCTCGTGACCACCCTGACCTGGGGCGTGCAGTGCTTCA
GCCGCTACCCCGACCACATGAAGCAGCACGACTTCTTCA
AGTCCGCCATGCCCGAAGGCTACGTCCAGGAGCGCACC
ATCTTCTTCAAGGACGACGGCAACTACAAGACCCGCGC
CGAGGTGAAGTTCGAGGGCGACACCCTGGTGAACCGCA
TCGAGCTGAAGGGCATCGACTTCAAGGAGGACGGCAAC
ATCCTGGGGCACAAGCTGGAGTACAACTACATCAGCCA
CAACGTCTATATCACCGCCGACAAGCAGAAGAACGGCA
TCAAGGCCAACTTCAAGATCCGCCACAACATCGAGGAC
GGCAGCGTGCAGCTCGCCGACCACTACCAGCAGAACAC
CCCCATCGGCGACGGCCCCGTGCTGCTGCCCGACAACCA
CTACCTGAGCACCCAGTCCGCCCTGAGCAAAGACCCCA
ACGAGAAGCGCGATCACATGGTCCTGCTGGAGTTCGTGA
CCGCCGCCGGGATCTAATGAACGCCACTCGAGAGTCGA
CCAAAGCCCGCCGAAAGGCGGGCTTTTCTGTGCCGGCAT
GATAAGCTGTCAAACATGAGAATTACAACTTATATCGTA
TGGGGCTGACTTCAGGTGCTACATTTGAAGAGATAAATT
GCACTGAAATCTAGAAATATTTTATCTGATTAATAAGAT
GATCTTCTTGAGATCGTTTTGGTCTGCGCGTAATCTCTTG
CTCTGAAAACGAAAAAACCGCCTTGCAGGGCGGTTTTTC
GAAGGTTCTCTGAGCTACCAACTCTTTGAACCGAGGTAA
CTGGCTTGGAGGAGCGCAGTCACCAAAACTTGTCCTTTC
AGTTTAGCCTTAACCGGCGCATGACTTCAAGACTAACTC
CTCTAAATCAATTACCAGTGGCTGCTGCCAGTGGTGCTTT
TGCATGTCTTTCCGGGTTGGACTCAAGACGATAGTTACC

GGATAAGGCGCAGCGGTCGGACTGAACGGGGGGTTcgtgc
atacagtccagcttgg

11. **P28_Sw8_eGFP**
GGCGAATCCTCTGACCAGCCAGAAAACGACCTTTCTGTG
GTGAAACCGGATGCTGCAATTCAGAGCGGCAGCAAGTG
GGGGACAGCAGAAGACCTGACCGCCGCAGAGTGGATGT
TTGACATGGTGAAGACTATCGCACCATCAGCCAGAAAA
CCGAATTTTGCTGGGTGGGCTAACGATATCCGCCTGATG
CGTGAACGTGACGGACGTAACCACCGCGACATGTGTGT
GCTGTTCCGCTGGGCATGCCAGGACAACTTCTGGTCCGG
TAACGCATCAAGCTTCAATAAAGTTTCCCCCCTCCTTGCC
GATAACGAGATCAAGCTTATGAGTGTAATACGTTCTATG
TCAGATTCAAGAACAGAGGAGATTGAAATGGACATAGA
ACGAAACCTGGCGGCAGCGCAAAAGTTGGAGCTTTTCA
CTGGCGTTGTTCCCATCCTGGTCGAGCTGGACGGCGACG
TAAACGGCCACAAGTTCAGCGTGTCCGGCGAGGGCGAG
GGCGATGCCACCTACGGCAAGCTGACCCTGAAGTTCATC
TGCACCACCGGCAAGCTGCCCGTGCCCTGGCCCACCCTC
GTGACCACCCTGACCTACGGCGTGCAGTGCTTCAGCCGC
TACCCCGACCACATGAAGCAGCACGACTTCTTCAAGTCC
GCCATGCCCGAAGGCTACGTCCAGGAGCGCACCATCTTC
TTCAAGGACGACGGCAACTACAAGACCCGCGCCGAGGT
GAAGTTCGAGGGCGACACCCTGGTGAACCGCATCGAGC
TGAAGGGCATCGACTTCAAGGAGGACGGCAACATCCTG
GGGCACAAGCTGGAGTACAACTACAACAGCCACAACGT
CTATATCATGGCCGACAAGCAGAAGAACGGCATCAAGG
TGAACTTCAAGATCCGCCACAACATCGAGGACGGCAGC
GTGCAGCTCGCCGACCACTACCAGCAGAACACCCCCAT
CGGCGACGGCCCCGTGCTGCTGCCCGACAACCACTACCT
GAGCACCCAGTCCGCCCTGAGCAAAGACCCCAACGAGA
AGCGCGATCACATGGTCCTGCTGGAGTTCGTGACCGCCG
CCGGGATCTAATGAACGCCACTCGAGAGTCGACCAAAG
CCCGCCGAAAGGCGGGCTTTTCTGTGCCGGCATGATAAG
CTGTCAAACATGAGAATTACAACTTATATCGTATGGGGC
TGACTTCAGGTGCTACATTTGAAGAGATAAATTGCACTG
AAATCTAGAAATATTTTATCTGATTAATAAGATGATCTTC
TTGAGATCGTTTTGGTCTGCGCGTAATCTCTTGCTCTGAA
AACGAAAAAACCGCCTTGCAGGGCGGTTTTTCGAAGGTT
CTCTGAGCTACCAACTCTTTGAACCGAGGTAACTGGCTT
GGAGGAGCGCAGTCACCAAAACTTGTCCTTTCAGTTTAG
CCTTAACCGGCGCATGACTTCAAGACTAACTCCTCTAAA
TCAATTACCAGTGGCTGCTGCCAGTGGTGCTTTTGCATGT
CTTTCCGGGTTGGACTCAAGACGATAGTTACCGGATAAG
GCGCAGCGGTCGGACTGAACGGGGGGTTcgtgcatacagtccag
cttgg

12. **P28_Sw2.1_eGFP**
GGCGAATCCTCTGACCAGCCAGAAAACGACCTTTCTGTG
GTGAAACCGGATGCTGCAATTCAGAGCGGCAGCAAGTG
GGGGACAGCAGAAGACCTGACCGCCGCAGAGTGGATGT
TTGACATGGTGAAGACTATCGCACCATCAGCCAGAAAA
CCGAATTTTGCTGGGTGGGCTAACGATATCCGCCTGATG
CGTGAACGTGACGGACGTAACCACCGCGACATGTGTGT
GCTGTTCCGCTGGGCATGCCAGGACAACTTCTGGTCCGG
TAACGCATCAAGCTTCAATAAAGTTTCCCCCCTCCTTGCC
GATAACGAGATCAAGTCTTATCTTATCTATCTCGTTTATC
CCTGCATACAGAAACAGAGGAGATATGCAATGATAAAC
GAGAACCTGGCGGCAGCGCAAAAGTTGGAGCTTTTCAC
TGGCGTTGTTCCCATCCTGGTCGAGCTGGACGGCGACGT
AAACGGCCACAAGTTCAGCGTGTCCGGCGAGGGCGAGG
GCGATGCCACCTACGGCAAGCTGACCCTGAAGTTCATCT
GCACCACCGGCAAGCTGCCCGTGCCCTGGCCCACCCTCG
TGACCACCCTGACCTACGGCGTGCAGTGCTTCAGCCGCT
ACCCCGACCACATGAAGCAGCACGACTTCTTCAAGTCCG
CCATGCCCGAAGGCTACGTCCAGGAGCGCACCATCTTCT
TCAAGGACGACGGCAACTACAAGACCCGCGCCGAGGTG
AAGTTCGAGGGCGACACCCTGGTGAACCGCATCGAGCT
GAAGGGCATCGACTTCAAGGAGGACGGCAACATCCTGG
GGCACAAGCTGGAGTACAACTACAACAGCCACAACGTC
TATATCATGGCCGACAAGCAGAAGAACGGCATCAAGGT
GAACTTCAAGATCCGCCACAACATCGAGGACGGCAGCG
TGCAGCTCGCCGACCACTACCAGCAGAACACCCCCATC
GGCGACGGCCCCGTGCTGCTGCCCGACAACCACTACCTG
AGCACCCAGTCCGCCCTGAGCAAAGACCCCAACGAGAA
GCGCGATCACATGGTCCTGCTGGAGTTCGTGACCGCCGC
CGGGATCTAATGAACGCCACTCGAGAGTCGACCAAAGC
CCGCCGAAAGGCGGGCTTTTCTGTGCCGGCATGATAAGC
TGTCAAACATGAGAATTACAACTTATATCGTATGGGGCT
GACTTCAGGTGCTACATTTGAAGAGATAAATTGCACTGA
AATCTAGAAATATTTTATCTGATTAATAAGATGATCTTCT
TGAGATCGTTTTGGTCTGCGCGTAATCTCTTGCTCTGAAA
ACGAAAAAACCGCCTTGCAGGGCGGTTTTTCGAAGGTTC
TCTGAGCTACCAACTCTTTGAACCGAGGTAACTGGCTTG
GAGGAGCGCAGTCACCAAAACTTGTCCTTTCAGTTTAGC
CTTAACCGGCGCATGACTTCAAGACTAACTCCTCTAAAT
CAATTACCAGTGGCTGCTGCCAGTGGTGCTTTTGCATGTC
TTTCCGGGTTGGACTCAAGACGATAGTTACCGGATAAGG
CGCAGCGGTCGGACTGAACGGGGGGTTcgtgcatacagtccagct
tgg

13. **P28_Sw2.1_CFP**
GGCGAATCCTCTGACCAGCCAGAAAACGACCTTTCTGTG
GTGAAACCGGATGCTGCAATTCAGAGCGGCAGCAAGTG

GGGGACAGCAGAAGACCTGACCGCCGCAGAGTGGATGT
TTGACATGGTGAAGACTATCGCACCATCAGCCAGAAAA
CCGAATTTTGCTGGGTGGGCTAACGATATCCGCCTGATG
CGTGAACGTGACGGACGTAACCACCGCGACATGTGTGT
GCTGTTCCGCTGGGCATGCCAGGACAACTTCTGGTCCGG
TAACGCATCAAGCTTCAATAAAGTTTCCCCCCTCCTTGCC
GATAACGAGATCAAGTCTTATCTTATCTATCTCGTTTATC
CCTGCATACAGAAACAGAGGAGATATGCAATGATAAAC
GAGAACCTGGCGGCAGCGCAAAAGTTGGAGCTTTTCAC
TGGCGTTGTTCCCATCCTGGTCGAGCTGGACGGCGACGT
AAACGGCCACAAGTTCAGCGTGTCCGGCGAGGGCGAGG
GCGATGCCACCTACGGCAAGCTGACCCTGAAGTTCATCT
GCACCACCGGCAAGCTGCCCGTGCCCTGGCCCACCCTCG
TGACCACCCTGACCTGGGGCGTGCAGTGCTTCAGCCGCT
ACCCCGACCACATGAAGCAGCACGACTTCTTCAAGTCCG
CCATGCCCGAAGGCTACGTCCAGGAGCGCACCATCTTCT
TCAAGGACGACGGCAACTACAAGACCCGCGCCGAGGTG
AAGTTCGAGGGCGACACCCTGGTGAACCGCATCGAGCT
GAAGGGCATCGACTTCAAGGAGGACGGCAACATCCTGG
GGCACAAGCTGGAGTACAACTACATCAGCCACAACGTC
TATATCACCGCCGACAAGCAGAAGAACGGCATCAAGGC
CAACTTCAAGATCCGCCACAACATCGAGGACGGCAGCG
TGCAGCTCGCCGACCACTACCAGCAGAACACCCCCATC
GGCGACGGCCCCGTGCTGCTGCCCGACAACCACTACCTG
AGCACCCAGTCCGCCCTGAGCAAAGACCCCAACGAGAA
GCGCGATCACATGGTCCTGCTGGAGTTCGTGACCGCCGC
CGGGATCTAATGAACGCCACTCGAGAGTCGACCAAAGC
CCGCCGAAAGGCGGGCTTTTCTGTGCCGGCATGATAAGC
TGTCAAACATGAGAATTACAACTTATATCGTATGGGGCT
GACTTCAGGTGCTACATTTGAAGAGATAAATTGCACTGA
AATCTAGAAATATTTTATCTGATTAATAAGATGATCTTCT
TGAGATCGTTTTGGTCTGCGCGTAATCTCTTGCTCTGAAA
ACGAAAAAACCGCCTTGCAGGGCGGTTTTTCGAAGGTTC
TCTGAGCTACCAACTCTTTGAACCGAGGTAACTGGCTTG
GAGGAGCGCAGTCACCAAAACTTGTCCTTTCAGTTTAGC
CTTAACCGGCGCATGACTTCAAGACTAACTCCTCTAAAT
CAATTACCAGTGGCTGCTGCCAGTGGTGCTTTTGCATGTC
TTTCCGGGTTGGACTCAAGACGATAGTTACCGGATAAGG
CGCAGCGGTCGGACTGAACGGGGGGTTcgtgcatacagtccagct
tgg

A.3 PRIMERS

1. **pBEST-LinL-F primer**
   GGCGAATCCTCTGACCAGC

2. **pBEST-LinL-R primer**
   CCAAGCTGGACTGTATGCACG

B

PARAMETER VALUES ODE MODELS

The following table shows the parameter values used in the ODE models of Chapter 3 and Chapter 5.

PARAMETER	VALUE	UNIT	EXPLANATION
$k_{ts,Tr}$	1.071	min^{-1}	Transcription rate trigger constructs [52]
$k_{ts,Sw}$	1.071	min^{-1}	Transcription rate switch constructs [52]
$k_{tl,S_{28}}$	0.1223	min^{-1}	Translation rate σ28 [52]
$k_{tl,GFP}$	0.1223	min^{-1}	Translation rate GFP [52]
$k_{tl,CFP}$	0.1223	min^{-1}	Translation rate CFP [52]
$\epsilon_{S_{28}}$	0.01	min^{-1}	Leak σ28 production
$\epsilon_{Sw_{1,2}}$	0.1	min^{-1}	Leak $Sw_{1,2}$ transcription
$\epsilon_{Sw_{2,2}}$	0.1	min^{-1}	Leak $Sw_{2,2}$ transcription
ϵ_{GFP}	0.02	min^{-1}	Leak GFP production
ϵ_{CFP}	0.04	min^{-1}	Leak CFP production
δ_{RNA}	0.027	min^{-1}	Degradation rate RNA [49]
δ_{P}	0.027	min^{-1}	Degradation rate proteins [49]

PARAMETER	VALUE	UNIT	EXPLANATION
$k_{on,Tr_1,Sw_{1,1}}$	1e-1	$nM^{-1} \cdot min^{-1}$	Association rate $Tr_1 \cdot Sw_{1,1}$
$k_{off,Tr_1,Sw_{1,1}}$	1e-10	min^{-1}	Dissociation rate $Tr_1 \cdot Sw_{1,1}$
$k_{on,Tr_1,Sw_{1,2}}$	1e-1	$nM^{-1} \cdot min^{-1}$	Association rate $Tr_1 \cdot Sw_{1,2}$
$k_{off,Tr_1,Sw_{1,2}}$	1e-10	min^{-1}	Dissociation rate $Tr_1 \cdot Sw_{1,2}$
$k_{on,Tr_2,Sw_{2,1}}$	1e-1	$nM^{-1} \cdot min^{-1}$	Association rate $Tr_2 \cdot Sw_{2,1}$
$k_{off,Tr_2,Sw_{2,1}}$	1e-10	min^{-1}	Dissociation rate $Tr_2 \cdot Sw_{2,1}$
$k_{on,Tr_2,Sw_{2,2}}$	1e-1	$nM^{-1} \cdot min^{-1}$	Association rate $Tr_2 \cdot Sw_{2,2}$
$k_{off,Tr_2,Sw_{2,2}}$	1e-10	min^{-1}	Dissociation rate $Tr_2 \cdot Sw_{2,2}$
$K_{S_{28}}$	70	nM	Dissociation constant σ28 to P28 [28]
H	1.95	–	Hill coefficient [28]

C

SUPPLEMENTARY RESULTS

C.1 IN VITRO EXPERIMENTS

C.1.1 *Increasing concentration of σ28 producing constructs of coupled FFL circuit*

Section 4.3.3 showed the influence of σ28 on the fluorophore production of the coupled FFL. The necessity of σ28 as transcription factor for P28 was discussed and it was shown that the σ28 producing construct of one side of the circuit could take over the function of the other DNA construct if absent. It was also tested if fluorophore production was influenced by an increase of σ28 producing construct of one side of the coupled FFL (Figure 28). It can be concluded that increasing one of the intermediate construct concentrations, when the other is absent, does not significantly influence the production of fluorophore on either side of the circuit.

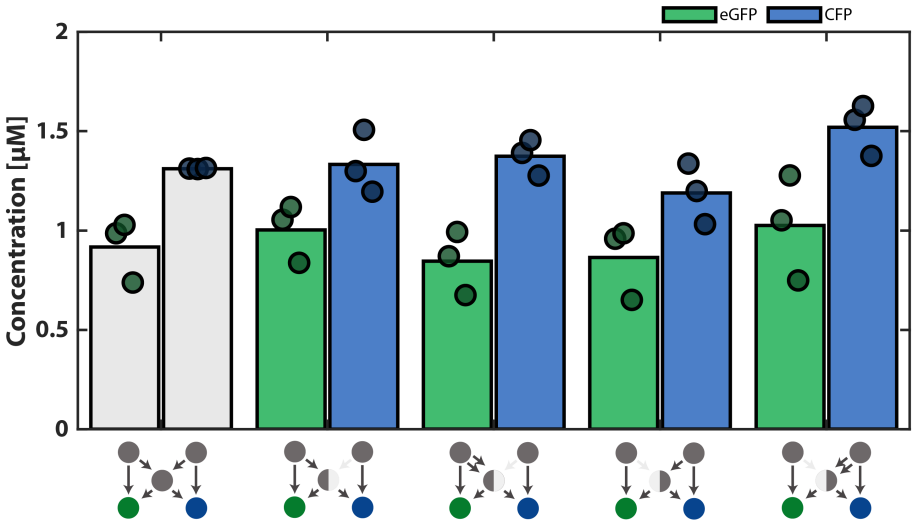

Figure 28: eGFP and CFP production (in μM) of the coupled feed-forward loop in presence and absence of σ28 producing constructs. A half intermediate node means that the DNA construct of that side is absent. Two arrows means that the DNA construct concentration of that σ28 producing construct was doubled.

C.2 IN SILICO SIMULATIONS

C.2.1 *Alternating inputs for coupled feed-forward loop*

The following figure shows the results for a situation where first the CFP trigger is added and subsequently, after CFP has reached its maximum concentration, the GFP trigger is added. Similar results can be observed for this situation compared to the one where first the GFP trigger is added. Furthermore, we see that time delay in the production of GFP is decreased more when the GFP-side intermediate DNA construct is removed from the circuit.

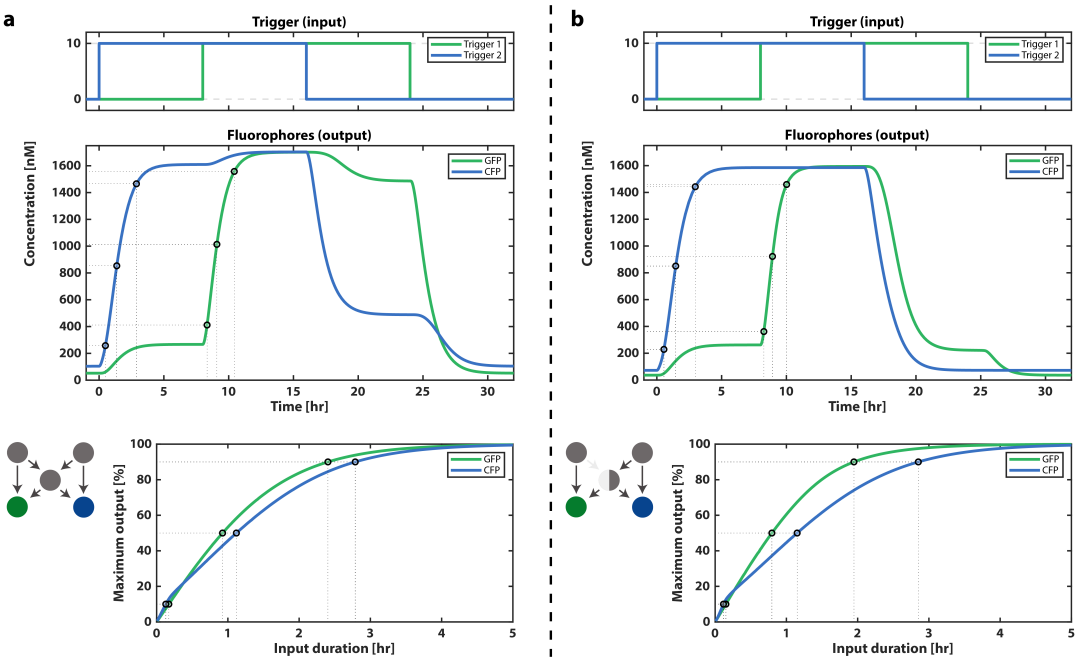

Figure 29: (a) Production of eGFP and CFP upon addition of first the right-side trigger DNA and subsequently the left-side trigger DNA to the full coupled FFL circuit.
(b) Production of eGFP and CFP upon addition of first the right-side trigger DNA and subsequently the left-side trigger DNA to a version of the coupled FFL circuit where the left-side σ28 producing construct is removed.

BIBLIOGRAPHY

[1] D Ewen Cameron, Caleb J Bashor, and James J Collins. "A brief history of synthetic biology." In: *Nature Reviews Microbiology* 12.5 (2014), pp. 381–390.

[2] Tadashi Nakano, Andrew W Eckford, and Tokuko Haraguchi. *Molecular communication*. Cambridge University Press, 2013.

[3] Clyde A Hutchison, Ray-Yuan Chuang, Vladimir N Noskov, Nacyra Assad-Garcia, Thomas J Deerinck, Mark H Ellisman, John Gill, Krishna Kannan, Bogumil J Karas, Li Ma, et al. "Design and synthesis of a minimal bacterial genome." In: *Science* 351.6280 (2016).

[4] Shmoolik Mangan and Uri Alon. "Structure and function of the feed-forward loop network motif." In: *Proceedings of the National Academy of Sciences* 100.21 (2003), pp. 11980–11985.

[5] Denis Thieffry, Araceli M Huerta, Ernesto Pérez-Rueda, and Julio Collado-Vides. "From specific gene regulation to genomic networks: a global analysis of transcriptional regulation in Escherichia coli." In: *Bioessays* 20.5 (1998), pp. 433–440.

[6] Leland H Hartwell, John J Hopfield, Stanislas Leibler, and Andrew W Murray. "From molecular to modular cell biology." In: *Nature* 402.6761 (1999), pp. C47–C52.

[7] Dennis Bray. "Protein molecules as computational elements in living cells." In: *Nature* 376.6538 (1995), pp. 307–312.

[8] Ron Milo, Shai Shen-Orr, Shalev Itzkovitz, Nadav Kashtan, Dmitri Chklovskii, and Uri Alon. "Network motifs: simple building blocks of complex networks." In: *Science* 298.5594 (2002), pp. 824–827.

[9] Ali Masoudi-Nejad, Falk Schreiber, and Zahra Razaghi Moghadam Kashani. "Building blocks of biological networks: a review on major network motif discovery algorithms." In: *IET systems biology* 6.5 (2012), pp. 164–174.

[10] Elisabeth Wong, Brittany Baur, Saad Quader, and Chun-Hsi Huang. "Biological network motif detection: principles and practice." In: *Briefings in bioinformatics* 13.2 (2012), pp. 202–215.

[11] Austin R Benson, David F Gleich, and Jure Leskovec. "Higher-order organization of complex networks." In: *Science* 353.6295 (2016), pp. 163–166.

[12] Shai S Shen-Orr, Ron Milo, Shmoolik Mangan, and Uri Alon. "Network motifs in the transcriptional regulation network of Escherichia coli." In: *Nature genetics* 31.1 (2002), pp. 64–68.

[13] Patrick Eichenberger, Masaya Fujita, Shane T Jensen, Erin M Conlon, David Z Rudner, Stephanie T Wang, Caitlin Ferguson, Koki Haga, Tsutomu Sato, Jun S Liu, et al. "The program of gene transcription for a single differentiating cell type during sporulation in Bacillus subtilis." In: *PLoS Biol* 2.10 (2004), e328.

[14] Tong Ihn Lee, Nicola J Rinaldi, François Robert, Duncan T Odom, Ziv Bar-Joseph, Georg K Gerber, Nancy M Hannett, Christopher T Harbison, Craig M Thompson, Itamar Simon, et al. "Transcriptional regulatory networks in Saccharomyces cerevisiae." In: *science* 298.5594 (2002), pp. 799–804.

[15] Duncan T Odom, Nora Zizlsperger, D Benjamin Gordon, George W Bell, Nicola J Rinaldi, Heather L Murray, Tom L Volkert, Jörg Schreiber, P Alexander Rolfe, David K Gifford, et al. "Control of pancreas and liver gene expression by HNF transcription factors." In: *Science* 303.5662 (2004), pp. 1378–1381.

[16] Laurie A Boyer, Tong Ihn Lee, Megan F Cole, Sarah E Johnstone, Stuart S Levine, Jacob P Zucker, Matthew G Guenther, Roshan M Kumar, Heather L Murray, Richard G Jenner, et al. "Core transcriptional regulatory circuitry in human embryonic stem cells." In: *cell* 122.6 (2005), pp. 947–956.

[17] Louis A Saddic, Bärbel Huvermann, Staver Bezhani, Yanhui Su, Cara M Winter, Chang Seob Kwon, Richard P Collum, and Doris Wagner. "The LEAFY target LMI1 is a meristem identity regulator and acts together with LEAFY to regulate expression of CAULIFLOWER." In: *Development* 133.9 (2006), pp. 1673–1682.

[18] Jonas Defoort, Yves Van de Peer, and Vanessa Vermeirssen. "Function, dynamics and evolution of network motif modules in integrated gene regulatory networks of worm and plant." In: *Nucleic acids research* 46.13 (2018), pp. 6480–6503.

[19] Uri Alon. "Network motifs: theory and experimental approaches." In: *Nature Reviews Genetics* 8.6 (2007), pp. 450–461.

[20] S Kalir, J McClure, K Pabbaraju, C Southward, M Ronen, S Leibler, MG Surette, and U Alon. "Ordering genes in a flagella pathway by analysis of expression kinetics from living bacteria." In: *Science* 292.5524 (2001), pp. 2080–2083.

[21] Timothy S Gardner, Charles R Cantor, and James J Collins. "Construction of a genetic toggle switch in Escherichia coli." In: *Nature* 403.6767 (2000), pp. 339–342.

[22] Lei Wang, Brandon L Walker, Stephen Iannaccone, Devang Bhatt, Patrick J Kennedy, and T Tse William. "Bistable switches control memory and plasticity in cellular differentiation." In: *Proceedings of the National Academy of Sciences* 106.16 (2009), pp. 6638–6643.

[23] Michael B Elowitz and Stanislas Leibler. "A synthetic oscillatory network of transcriptional regulators." In: *Nature* 403.6767 (2000), pp. 335–338.

[24] Bas JHM Rosier and Tom FA De Greef. "Synthetic Biology: How to make an oscillator." In: *Elife* 4 (2015), e12260.

[25] John Tsang, Jun Zhu, and Alexander van Oudenaarden. "MicroRNA-mediated feedback and feedforward loops are recurrent network motifs in mammals." In: *Molecular cell* 26.5 (2007), pp. 753–767.

[26] Thomas E Gorochowski, Claire S Grierson, and Mario di Bernardo. "Organization of feed-forward loop motifs reveals architectural principles in natural and engineered networks." In: *Science advances* 4.3 (2018), eaap9751.

[27] Jonathan Garamella, Ryan Marshall, Mark Rustad, and Vincent Noireaux. "The all E. coli TX-TL toolbox 2.0: a platform for cell-free synthetic biology." In: *ACS synthetic biology* 5.4 (2016), pp. 344–355.

[28] Maaruthy Yelleswarapu, Ardjan J van der Linden, Bob van Sluijs, Pascal A Pieters, Emilien Dubuc, Tom FA de Greef, and Wilhelm TS Huck. "Sigma factor-mediated tuning of bacterial cell-free synthetic genetic oscillators." In: *ACS synthetic biology* 7.12 (2018), pp. 2879–2887.

[29] Alexander A Green, Pamela A Silver, James J Collins, and Peng Yin. "Toehold switches: de-novo-designed regulators of gene expression." In: *Cell* 159.4 (2014), pp. 925–939.

[30] Uri Alon. *An introduction to systems biology: design principles of biological circuits*. CRC press, 2019.

[31] Vikram Singh and Pawan K Dhar. *Systems and synthetic biology*. Springer, 2015.

[32] David Garenne and Vincent Noireaux. "Cell-free transcription–translation: engineering biology from the nanometer to the millimeter scale." In: *Current opinion in biotechnology* 58 (2019), pp. 19–27.

[33] Jonghyeon Shin and Vincent Noireaux. "An E. coli cell-free expression toolbox: application to synthetic gene circuits and artificial cells." In: *ACS synthetic biology* 1.1 (2012), pp. 29–41.

[34] Zachary Z Sun, Enoch Yeung, Clarmyra A Hayes, Vincent Noireaux, and Richard M Murray. "Linear DNA for rapid prototyping of synthetic biological circuits in an Escherichia coli based TX-TL cell-free system." In: *ACS synthetic biology* 3.6 (2014), pp. 387–397.

[35] Kenan C Murphy. "Lambda Gam protein inhibits the helicase and chi-stimulated recombination activities of Escherichia coli RecBCD enzyme." In: *Journal of bacteriology* 173.18 (1991), pp. 5808–5821.

[36] Kalavathy Sitaraman, Dominic Esposito, George Klarmann, Stuart F Le Grice, James L Hartley, and Deb K Chatterjee. "A novel cell-free protein synthesis system." In: *Journal of biotechnology* 110.3 (2004), pp. 257–263.

[37] Richard Losick and Janice Pero. "Cascades of sigma factors." In: *Cell* 25.3 (1981), pp. 582–584.

[38] Maria C Davis, Christopher A Kesthely, Emily A Franklin, and Shawn R MacLellan. "The essential activities of the bacterial sigma factor." In: *Canadian Journal of Microbiology* 63.2 (2017), pp. 89–99.

[39] Mark SB Paget and John D Helmann. "The σ 70 family of sigma factors." In: *Genome biology* 4.1 (2003), pp. 1–6.

[40] Svein Valla and Rahmi Lale. *DNA cloning and assembly methods*. Springer, 2014.

[41] Jonghyeon Shin and Vincent Noireaux. "Efficient cell-free expression with the endogenous E. Coli RNA polymerase and sigma factor 70." In: *Journal of biological engineering* 4.1 (2010), pp. 1–9.

[42] OpenWetWare. *Biomolecular Breadboards:Protocols:Crude Extract Prep — OpenWetWare,* [Online; accessed 13-August-2020]. 2012. URL: https://openwetware.org/mediawiki/index.php?title=Biomolecular_Breadboards:Protocols:Crude_Extract_Prep&oldid=606996.

[43] OpenWetWare. *Biomolecular Breadboards:Protocols:Amino Acids Prep — OpenWetWare,* [Online; accessed 13-August-2020]. 2015. URL: \url{https://openwetware.org/mediawiki/index.php?title=Biomolecular_Breadboards:Protocols:Amino_Acids_Prep&oldid=881392}.

[44] OpenWetWare. *Biomolecular Breadboards:Protocols:3-PGA Buffer Prep — OpenWetWare,* [Online; accessed 13-August-2020]. 2012. URL: \url{https://openwetware.org/mediawiki/index.php?title=Biomolecular_Breadboards:Protocols:3-PGA_Buffer_Prep&oldid=607001}.

[45] Fritz Horn and Roy Jackson. "General mass action kinetics." In: *Archive for rational mechanics and analysis* 47.2 (1972), pp. 81–116.

[46] Harley H McAdams and Lucy Shapiro. "Circuit simulation of genetic networks." In: *Science* 269.5224 (1995), pp. 650–656.

[47] Hamid Bolouri and Eric H Davidson. "Modeling transcriptional regulatory networks." In: *BioEssays* 24.12 (2002), pp. 1118–1129.

[48] Jaline Gerardin, Nishith R Reddy, and Wendell A Lim. "The design principles of biochemical timers: circuits that discriminate between transient and sustained stimulation." In: *Cell systems* 9.3 (2019), pp. 297–308.

[49] Henrike Niederholtmeyer, Viktoria Stepanova, and Sebastian J Maerkl. "Implementation of cell-free biological networks at steady state." In: *Proceedings of the National Academy of Sciences* 110.40 (2013), pp. 15985–15990.

[50] Ardjan J van der Linden, Maaruthy Yelleswarapu, Pascal A Pieters, Zoe Swank, Wilhelm TS Huck, Sebastian J Maerkl, and Tom FA de Greef. "A multilayer microfluidic platform for the conduction of prolonged cell-free gene expression." In: *JoVE (Journal of Visualized Experiments)* 152 (2019), e59655.

[51] Emilien Dubuc, Pascal A Pieters, Ardjan J van der Linden, Jan CM van Hest, Wilhelm TS Huck, and Tom FA de Greef. "Cell-free microcompartmentalised transcription–translation for the prototyping of synthetic communication networks." In: *Current opinion in biotechnology* 58 (2019), pp. 72–80.

[52] Tobias Stögbauer, Lukas Windhager, Ralf Zimmer, and Joachim O Rädler. "Experiment and mathematical modeling of gene expression dynamics in a cell-free system." In: *Integrative Biology* 4.5 (2012), pp. 494–501.